Job Shop Scheduling based on Hierarchical/Multi-agent Reinforcement Learning

① Collaborative Agent FJSP

② MARL JSP for Dynamic multi-agent manufacturing systems

③ HRL for Dynamic Distributed JSP With Job Arrivals

④ Real-Time Scheduling for FJSP with AGVs Using MARL and Efficient Action Decoding

⑤ MARL Scheduling for Dynamic FJSP

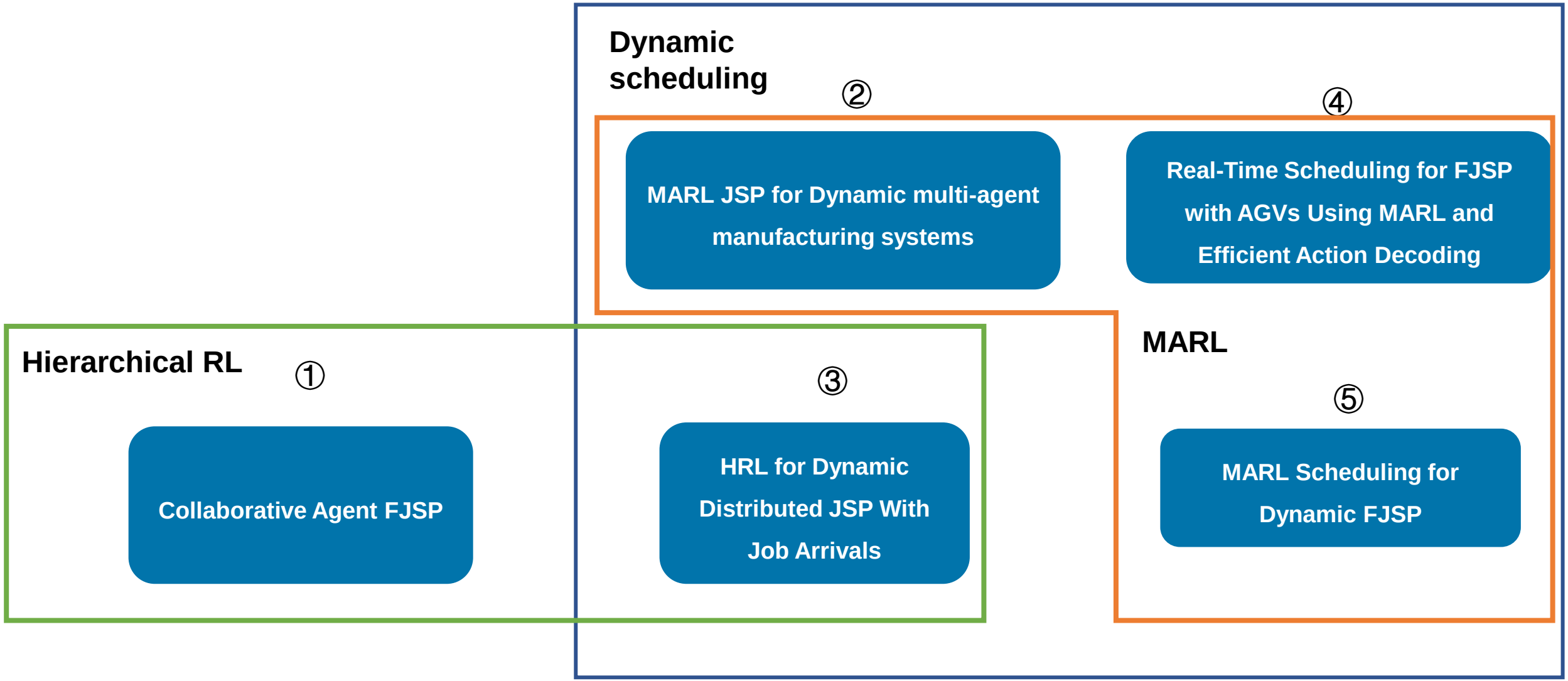
Dynamic scheduling
②
④
MARL JSP for Dynamic multi-agent manufacturing systems
Real-Time Scheduling for FJSP with AGVs Using MARL and Efficient Action Decoding
MARL
Hierarchical RL
①
③
⑤
Collaborative Agent FJSP
HRL for Dynamic Distributed JSP With Job Arrivals
MARL Scheduling for Dynamic FJSP

Paper 1

北京工業大學
BEIJING UNIVERSITY OF TECHNOLOGY

A novel collaborative agent reinforcement learning framework based on an attention mechanism and disjunctive graph embedding for flexible job shop scheduling problem

Wen quan Zhang, Fei Zhao, Yong Li, Chao Du, Xiaobing Feng, Xuesong Mei

Publish Journal: Journal of Manufacturing Systems(2024)

Contents

Contents

Problem Description

- A collaborative agent reinforcement learning (CARL) architecture was proposed, leveraging Graph Attention Network (GAT) and Transformer encoder for state representation, and trained with SAC and D5QN to optimize the Flexible Job Shop Scheduling Problem (FJSP).
- **Challenge:** Traditional state and action representations often lead to suboptimal solutions due to complexity and variability.
- **Method:** GAT was used to extract global state information, while the Transformer captured competitive relationships among machines, with SAC and D5QN optimizing the decision networks of agents.

Contents

Method Design

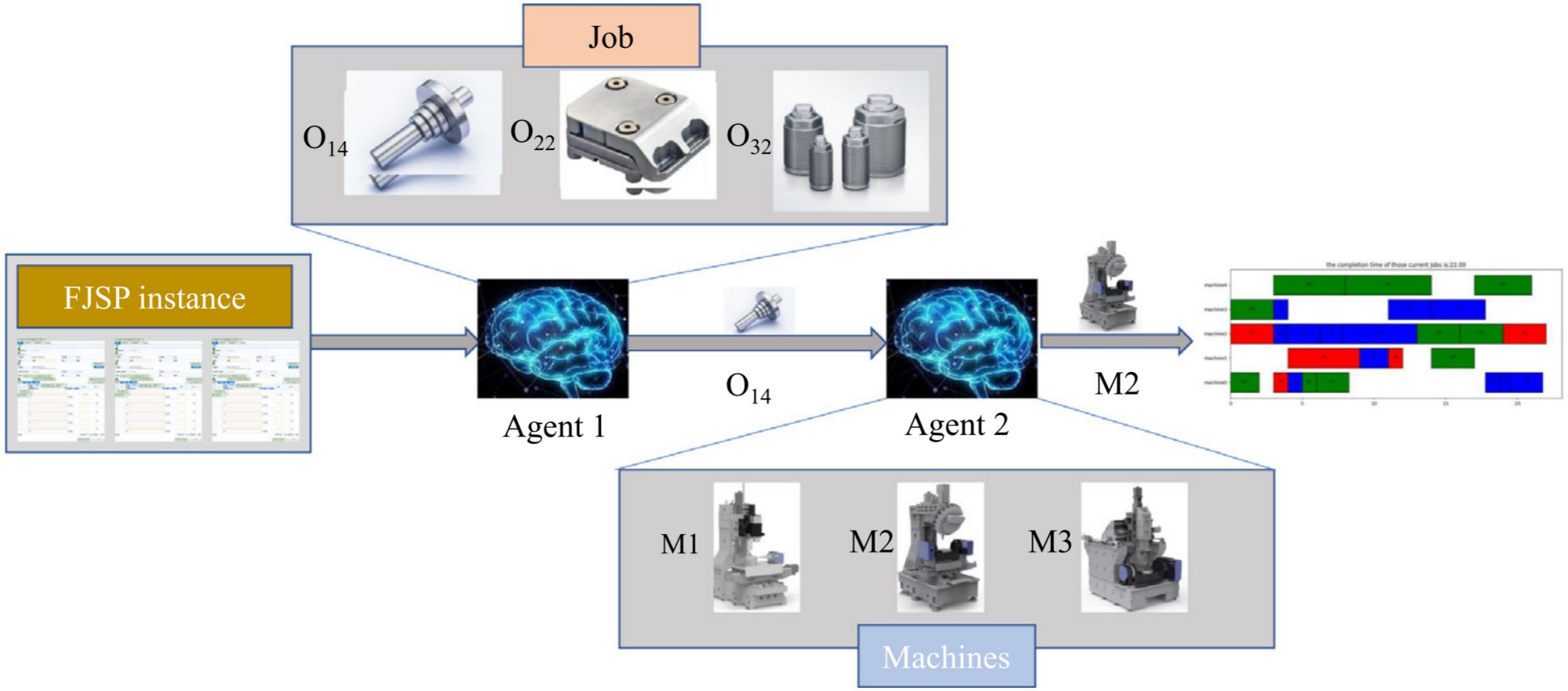

Fig. 1. CARL scheduling optimization model.

Method Design

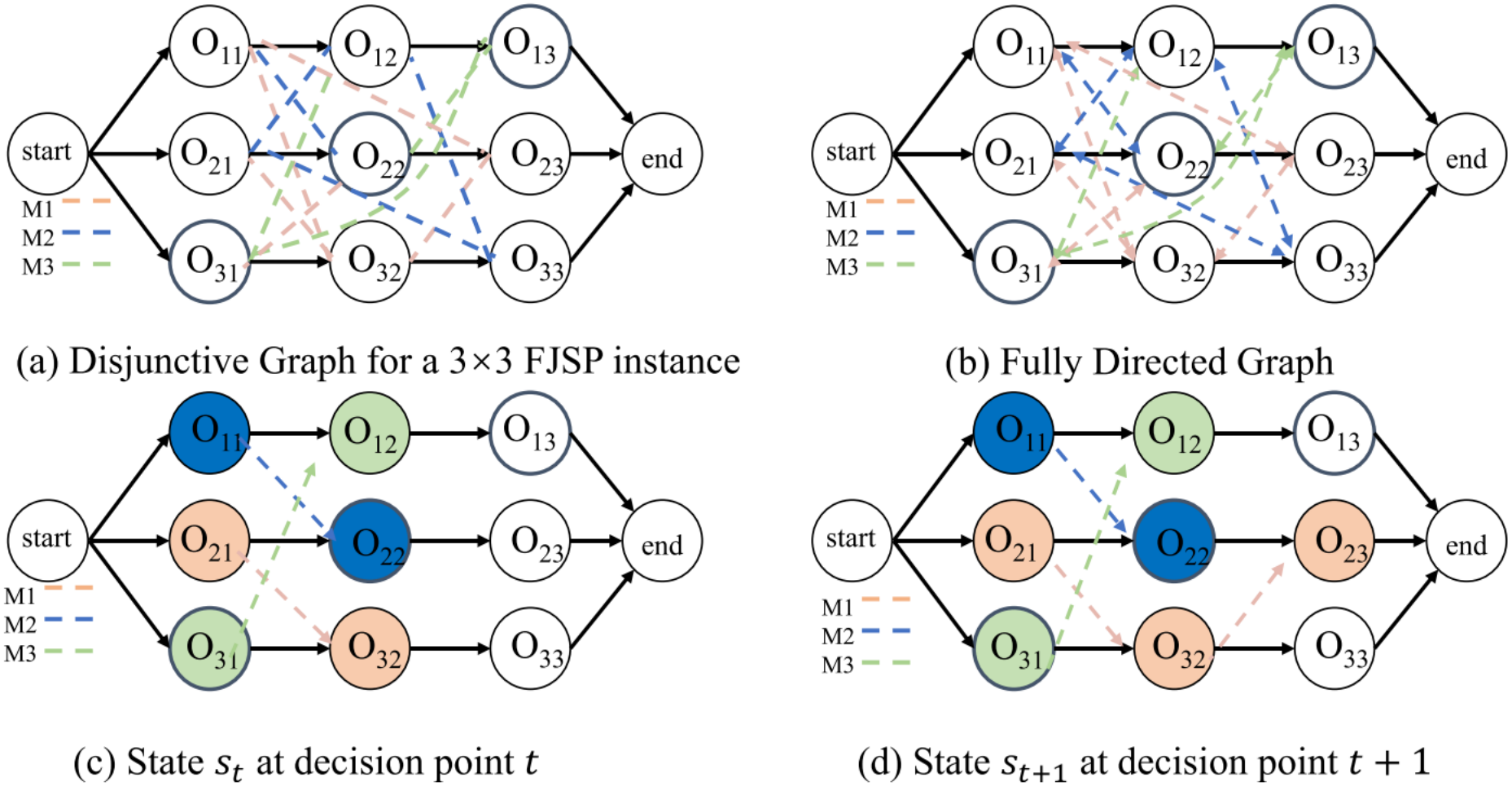

(a) Disjunctive Graph for a 3×3 FJSP instance

(b) Fully Directed Graph

(c) State s_t at decision point t

(d) State s_{t+1} at decision point $t+1$

Fig. 2. Disjunctive graph model.

Method Design

DQN

$$y_t = r_{t+1} + \gamma \max_{a'} Q^{-}\left(s_{t+1}, a'; \theta^{-}\right) \tag{5}$$

Double Deep Reinforcement Learning (DDQN)

$$y_t = r_{t+1} + \gamma Q'\left(s_{t+1}, \arg\max Q\left(s_{t+1}, a'; \theta\right); \theta'\right) \tag{6}$$

Noisy DQN (NDQN)

$$a_t = \arg\max_{a \in A} \tilde{Q}\ (s, a, \xi; \mu, \sigma)$$

Dueling DQN

$$Q(s, a) = V(s) + A(s, a)$$

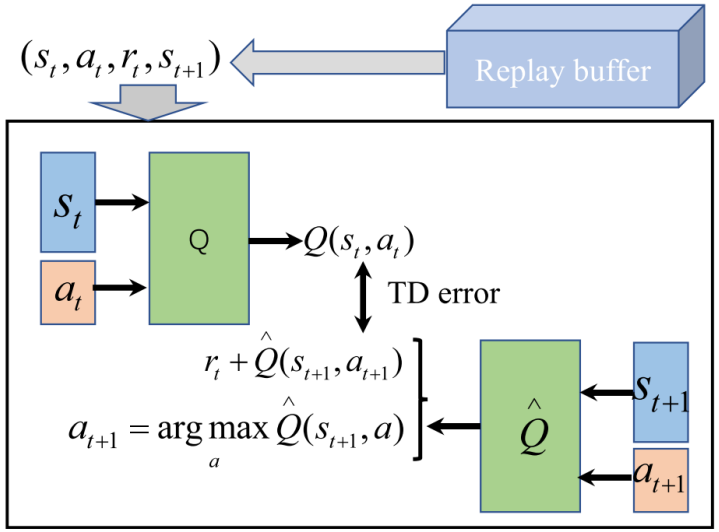

Fig. 3. Priority experience replay mechanism.

Method Design

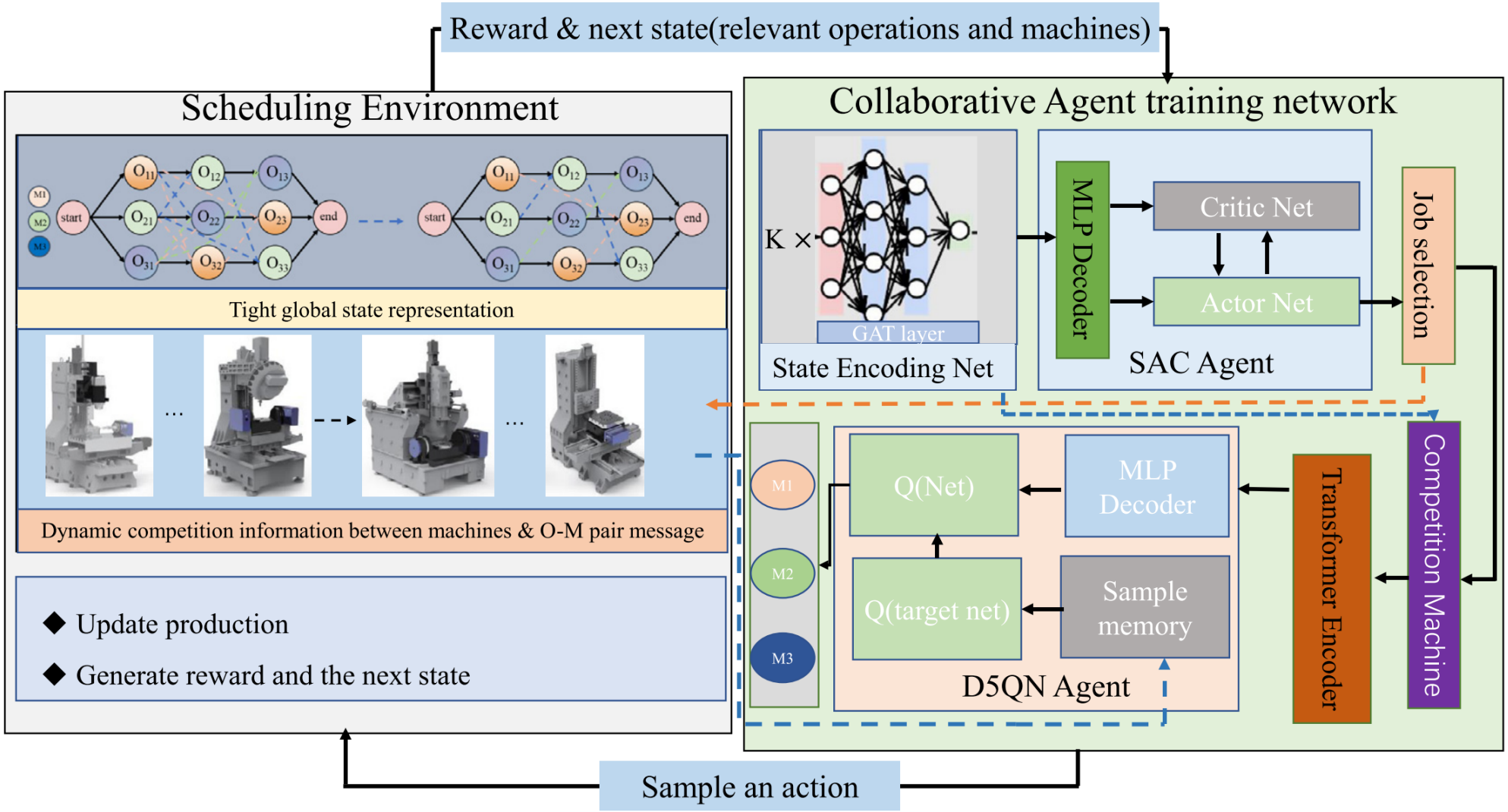

Fig. 4. Structural framework of the CARL algorithm for solving FJSP.

Method Design

MDP Formulation

- FJSP is formulated as a sequential decision-making problem requiring $|O|$ decisions. The SAC agent selects an operation using sampling or greedy decoding, while the D5QN agent assigns it to a machine. This cooperative reinforcement learning problem is modeled as a Cooperative Markov Decision Process (coMDP) (S, A, P, r, γ) with a dual-layer action space $A = A_o \times A_m$.

- The state representation integrates global and local scheduling features. The global state s_o^t is derived from the disjunctive graph $G(t) = (O, C \cup Du(t), D(t))$ classifying operations into completed, ongoing, and unplanned. The local state s_m^t represents machine statuses relevant to scheduling.

- At time t, an action $a_t = (a_o^t, a_m^t)$ is selected, and the disjunctive arcs are updated, yielding new states s_o^{t+1} and s_m^{t+1}. The reward is defined as the makespan reduction between consecutive states. With a discount factor $\gamma = 1$, the cumulative reward is computed as the sum of rewards across all decision steps. Minimizing C_{max} is equivalent to maximizing the cumulative reward, making makespan reduction the agents' objective.

- The scheduling policy $\pi(a_o, a_m \mid s)$ with parameters $\theta = [\theta_o, \theta_m]$ guides decision-making, where $\pi_{\theta_m}(a_o \mid s_t)$ and $\pi_{\theta_m}(a_m \mid s_t, a_o)$ sample actions from operation and machine spaces A_o^t and A_m^t, respectively.

Method Design

Job operation encoder

$$e_{i,j,p} = \text{LeakyReLU}\left(\vec{\mathbf{a}}^{\top}\left[\left(\mathbf{W}h_{O_{ij}}\right) \| \left(\mathbf{W}h_{O_{\text{ip}}}\right)\right]\right) \tag{15}$$

$$\alpha_{ijp} = Softmax(mask(e_{ijk})) \tag{16}$$

$$h'_{O_{ij}} = \sigma\left(\sum_{p=j-1}^{j+1} \alpha_{i,j,p}\mathbf{W}h_{O_{ip}}\right) \tag{17}$$

$$h^t_{O_{ij}} = \sigma\left(\frac{1}{K}\sum_{k=1}^{K}\sum_{p=j-1}^{j+1} \alpha^k_{i,j,p}\mathbf{W}^k h_{O_{ip}}\right) \tag{18}$$

$$h^t_{\mathcal{G}} = 1/\mathcal{O}\sum_{O_{ij}\in\mathcal{O}} h^t_{O_{ij}} \tag{19}$$

Job operation decoder

$$sor^o_{t,O_{ij}} = MLP_{\theta_{\pi_o}}([h^t_{O_{ij}}, h^t_{\mathcal{G}}]), O_{ij} \in \{1, 2, \ldots, \text{O}\} \tag{20}$$

Method Design

Machine encoder

$$P = \{ M_k, M_q, \ldots, M_v \}$$

$$Attention(Q, K, V) = Softmax(\frac{(QK^T)}{\sqrt{d_k}})V \tag{21}$$

$$\begin{aligned} &\text{MutiHead}(Q, K, V) = \left[\text{head}_1, \ldots, \text{head}_{\mathcal{M}}\right] W^O \\ &\text{where head}_i = \text{Attention}\left(QW_i^Q, KW_i^K, VW_i^V\right) \end{aligned} \tag{22}$$

Machine decoder

$$sor_{t,M_P}^m = MLP_{\theta_{\pi_m}}([Z_{M_{P_i}}^t, h_{O-M}^t]), P_i \in P \tag{23}$$

$$a_t^m = \begin{cases} \arg\max_{a_{t,k}^m} \left(p_k\left(a_t^m\right)\right), & \text{random} < \varepsilon \\ \text{random.choice}\left(a_{t,k}^m\right), & \text{random} > \varepsilon \end{cases} \tag{24}$$

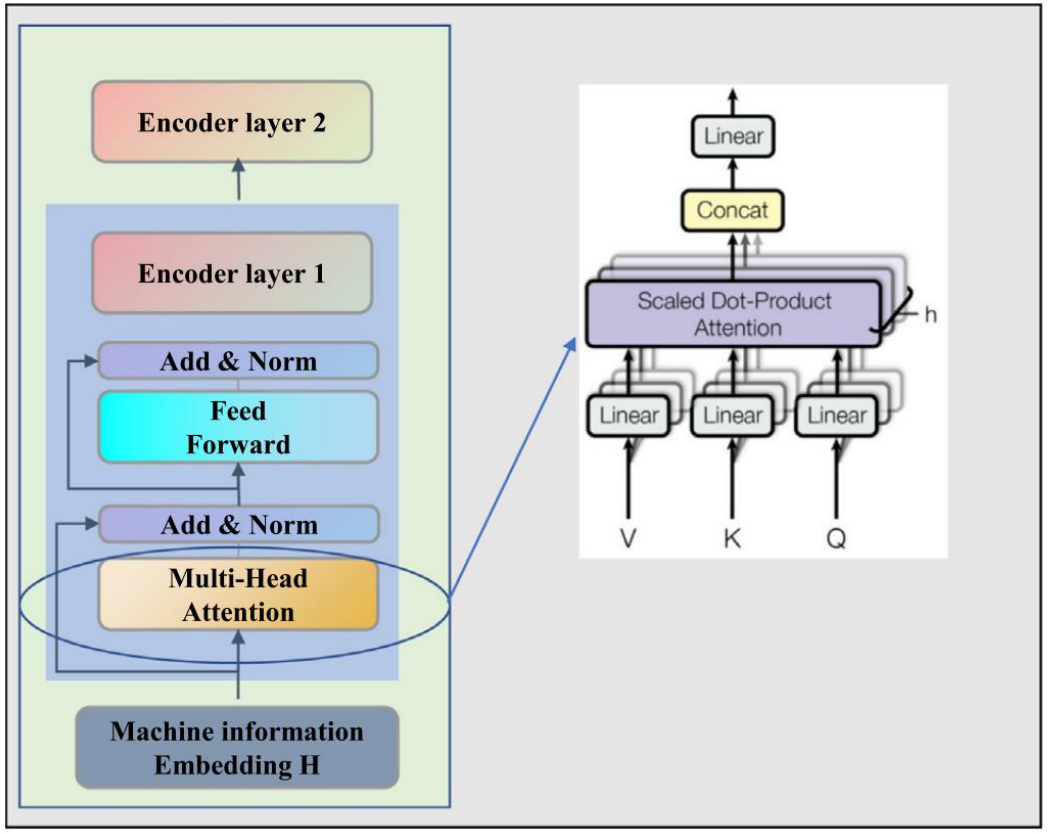

Fig. 5. Model competition machine information via a Transformer Encoder.

Method Design

Algorithm 1 Training CARL-FJSP Algorithm to dispatch

Input: Training episodes E_t, network update episodes E_s, batch size B;empty replay buffer D and fixed validation data ς_{val}; SAC algorithm: Training the actor network π_{θ_o} (parameter θ_o) and the critic network v_ϕ (parameter ϕ_1, ϕ_2). D5QN algorithm: Training the primary network Q_{θ_m} (parameter θ_m), target network $Q^-_{\theta_m^-}$(parameters $\theta_m^- = \theta_m$), execution network $\pi_{\theta_m^{old}}$, action selection probability parameter ε, Update network interval C.

Output: π_{θ_o} (parameter θ_o) , v_ϕ (parameter ϕ_1, ϕ_2), Q_{θ_m} (parameter θ_m)

Init θ_m 、 θ_o 、 ϕ_1 、 ϕ_2、 $\phi_o^{old} = \phi_o$ 、 $\theta_m^{old} = \theta_m$;
for $e = 1, 2, ..., E_t$ **do**
  Draw B FJSP Instances from GenerateInstance
  for $b = 1, 2, ..., B$ **do**
    for $t = 1 \rightarrow T$ **do**
      Based on $\pi_{\theta_o^{old}}$ using a greedy decision to execute $a^o_{b,t}$ under $s^o_{b,t}$ (c.f. Section 3.2) ;
      Based on $\pi_{\theta_m^{old}}$ a probability ε to execute $a^m_{b,t}$ according to $s^m_{b,t}$ (c.f. Section 3.3) ;
      Observe reward $r_{b,t}$ and next state $s_{b,t+1}$;
      $$y_{b,t} = \begin{cases} r_{b,t} + \gamma Q^-_{\theta_m^-}\left(s_{b,t+1}, \arg\max_{a'^m_{b,t}} Q_{\theta_m^{\text{old}}}\left(s_{b,t+1}, a'^m_{b,t}; \theta_m^{\text{old}}\right); \theta_m^-\right) \\ r_{b,t} \end{cases};$$
      Store $(s_{b,t}, a_{b,t}, r_{b,t}, s_{b,t+1})$ in replay buffer D;
    end for
  end for
  for $k = 1, 2, ..., E_s$ **do**
    SAC cumulative lOSS: $J_Q(\phi)$, $J_\pi(\theta_i)$, $J(\alpha)$ (c.f. Section 2.6);
    D5QN-loss:$\text{Loss}_{\text{D5QN}} = \left(y_b - Q_{\theta_m}\left(s^m_{b,t}, a^m_{b,t} \mid \theta_m\right)\right)$;
    Every c steps reset $Q^-_{\theta_m^-} = Q_{\theta_m^{\text{old}}}$, soft update $\phi_o = 0.8 * \phi_o + 0.2 * \phi_o^{old}$;
    Gradient descent updates all parameters;
  end for
  if Every Nr episodes **then**
    Resample B instances to form the training data;
  end if
  if Every N_{val} episodes **then**
    Validate π_θ on ς_{val};
  end if
end for

Contents

Experiment Results

Dataset

Table 1
The top 6 results in hyperparameter tuning.

CARL-FJSP		Hyperparameters	1	2	3	4	5	6
Agent 1	GAT	number of attention heads	4	4	6	2	6	6
		out feature dimension	8	8	16	8	32	16
		dropout rate	0.9	0.9	0.95	0.9	0.9	0.95
	SAC	learning rate	3e-4	3e-4	3e-3	3e-3	1e-3	3e-3
		tau	5e-3	5e-3	5e-3	5e-3	5e-3	5e-3
		decay ratio	0.9	0.95	0.95	0.95	0.95	1
Agent 2	Transformer Encoder	hidden size	32	32	64	64	128	128
		number of attention heads	4	4	8	2	4	8
		number of encoder layers	2	2	2	3	3	3
	D5QN	epsilon	0.8	0.8	0.85	0.8	0.8	0.8
		gamma	1	1	1	1	1	1
		learning rate	3e-4	3e-4	3e-3	3e-3	3e-4	3e-4
$Cmax$			334.6	336.8	338.4	346.7	361.6	367.0

Experiment Results

Baseline methods

Table 2
Heuristic scheduling rules.

Baseline rule	No.	Rule	Content
Operation selection rules	1	FIFO	select the earliest arriving job in the queue of a machine.
	2	MOPNR	select a job that has the greatest number of remaining operations to be done.
	3	LWKR	select a job that has the least total processing time remaining to be done
	4	SPT	select a job with the shortest processing time
	5	MWKR	select a job that has the most total processing time remaining to be done
Machine selection rules	1	SPT	select a machine with the shortest processing time for the operation of a job
	2	FIFO	select the earliest ready compatible machine.
	3	EET	select a machine that is idle at the earliest time

RPD (Relative Percent Deviation) measures the relative percentage deviation from the optimal values for different algorithms.

$$RPD = (C_{\max}/C_{\max}^{BS} - 1) \times 100\%$$

Experiment Results

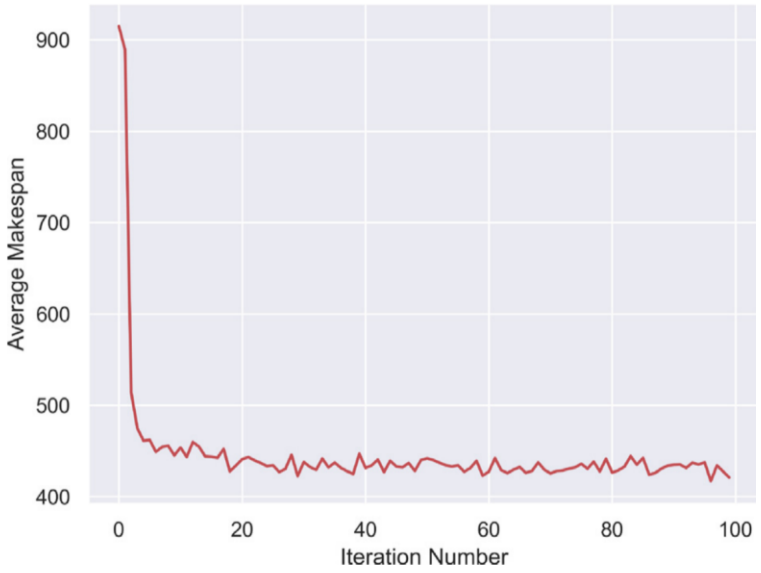

Fig. 6. Training curve on 15×10 instances.

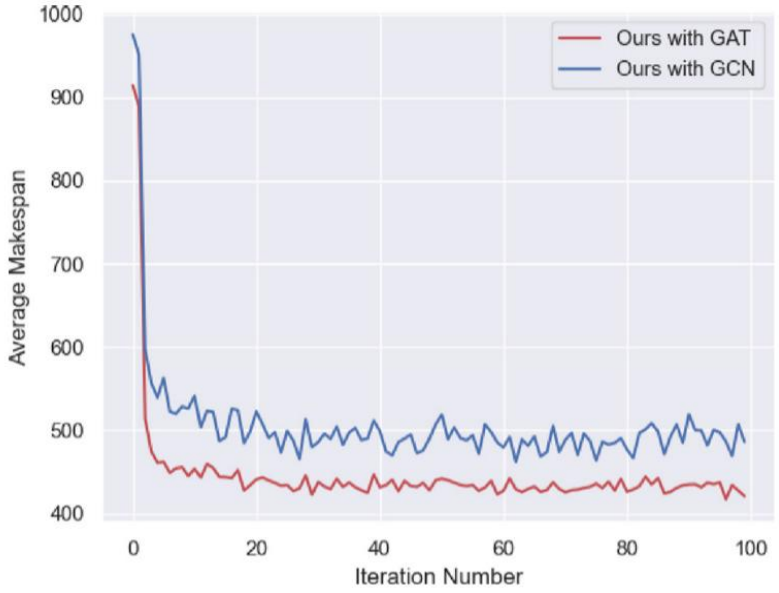

Fig. 7. Verification of the effectiveness of the GAT component.

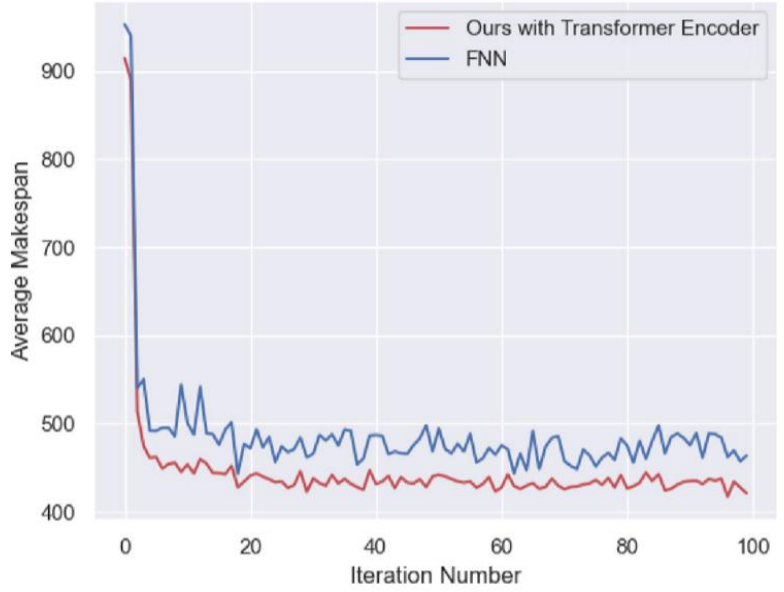

Fig. 8. Verification of the effectiveness of the Transformer Encoder component.

Experiment Results

Table 3
Results of all methods on synthetic instances of training size.

Size		Ours	FIFO +FIFO	SPT +SPT	MOPNR +EET	MWKR +EET	LWKR +SPT	FIFO +SPT	FIFO + EET	MWKR + SPT	MOPNR +SPT	LWKR +EET	[41] 20×5	[41] 20×10	OR-Tools
10×5	Obj	**398.6**	567.85	515.9	558.36	548.54	562.85	479.54	571.01	484.12	484.16	795.5	572.01	552.72	326.24(100%)
	Gap	**22.2%**	76.10%	58.42%	72.83%	69.61%	72.53%	46.99%	75.03%	48.39%	48.41%	143.84%	75.33%	69.42%	-
	Time(s)	2.03	0.052	0.057	0.058	0.059	0.016	0.019	**0.014**	0.016	0.016	0.015	0.324	0.318	8.945
10×10	Obj	**403.53**	718.34	542.6	696.98	690.7	618.25	486.03	698.5	476.36	485.54	1205.99	675.5	692.44	329.31(100%)
	Gap	**22.5%**	120.63%	66.19%	113.99%	112.19%	87.74%	47.59%	112.11%	44.65%	47.44%	266.22%	105.13%	110.27%	-
	Time(s)	4.87	0.073	0.086	0.085	0.086	0.034	0.041	**0.031**	0.035	0.036	0.034	0.63	0.623	2.40
15×5	Obj	**540.02**	802.46	676.61	801.62	793.81	731.35	656.06	806.81	665.57	664.71	1056.3	798.24	789.93	462.27(27%)
	Gap	**16.82%**	74.41	46.62%	74.40%	72.61%	58.21%	41.92%	74.53%	43.98%	43.79%	128.50%	72.68%	70.88%	-
	Time(s)	3.36	0.053	0.056	0.056	0.057	0.028	0.033	**0.023**	0.028	0.029	0.026	0.498	0.514	1438.4
15×10	Obj	**491.32**	868.76	701.98	840.73	868.76	784.61	610.08	874.68	593.15	612.14	1513.02	841.55	832	377.13(15%)
	Gap	**30.28%**	131.69	86.47	124.29	121.20%	108.05%	61.77%	131.93%	57.28%	62.32%	301.19%	123.15%	120.61%	-
	Time(s)	6.62	0.112	0.116	0.121	0.123	0.061	0.073	**0.051**	0.059	0.063	0.057	1.008	1.008	1582.4
20×5	Obj	**679.25**	1044.95	836.1	1054	1023.98	895.44	810.23	1050.38	818.08	813.92	1299.5	1030.44	1025.5	598.15(0%)
	Gap	**13.56%**	75.74%	40.05%	77.26%	72.36%	49.70%	35.46%	75.60%	36.77%	36.07%	117.25%	72.27%	71.45%	-
	Time(s)	4.54	0.072	0.09	0.089	0.09	0.043	0.049	**0.034**	0.041	0.045	0.04	0.644	0.644	1800

(.%): The number of scheduling results that can be obtained within 1800s;

For OR-Tools, the solution and the ratio of optimally solved instances are reported.

Experiment Results

Table 4
Results on the large-sized synthetic instances.

Size		Ours	FIFO +FIFO	SPT +SPT	MOPNR +EET	MWKR +EET	LWKR +SPT	FIFO +SPT	FIFO + EET	MWKR + SPT	MOPNR +SPT	LWKR +EET	[41] 20×5	[41] 20×10	OR-Tools
20×10	Obj	**579.63**	1089.61	825.4	1055.46	1041.89	925.18	725.69	1082.34	712.86	724.71	791.18	1044.53	1045.1	456.58(1%)
	Gap	**26.95%**	139.55%	80.83%	132.05%	129.09%	102.63%	58.94%	137.05%	56.13%	58.73%	73.28%	128.77%	128.90%	-
	Time(s)	9.42	0.161	0.176	0.181	0.178	0.087	0.107	0.075	0.09	0.097	**0.016**	1.412	1.369	1783.6
30×20	Obj	**674.53**	1671.18	1158.75	1586.53	1573.13	1202.55	856.6	1672.89	832.09	852.87	3525.68	1574.22	1620.11	598.15(0%)
	Gap	**12.77%**	180.31%	94.06%	166.05%	163.86%	101.04%	43.21%	179.68%	39.11%	42.58%	489.43%	163.18%	170.85%	-
	Time(s)	31.85	0.812	0.833	0.84	0.842	0.4	0.507	**0.348**	0.415	0.457	0.398	4.076	4.206	1802

(.%): The number of scheduling results that can be obtained within 1800s;

For OR-Tools, the solution and the ratio of optimally solved instances are reported.

Experiment Results

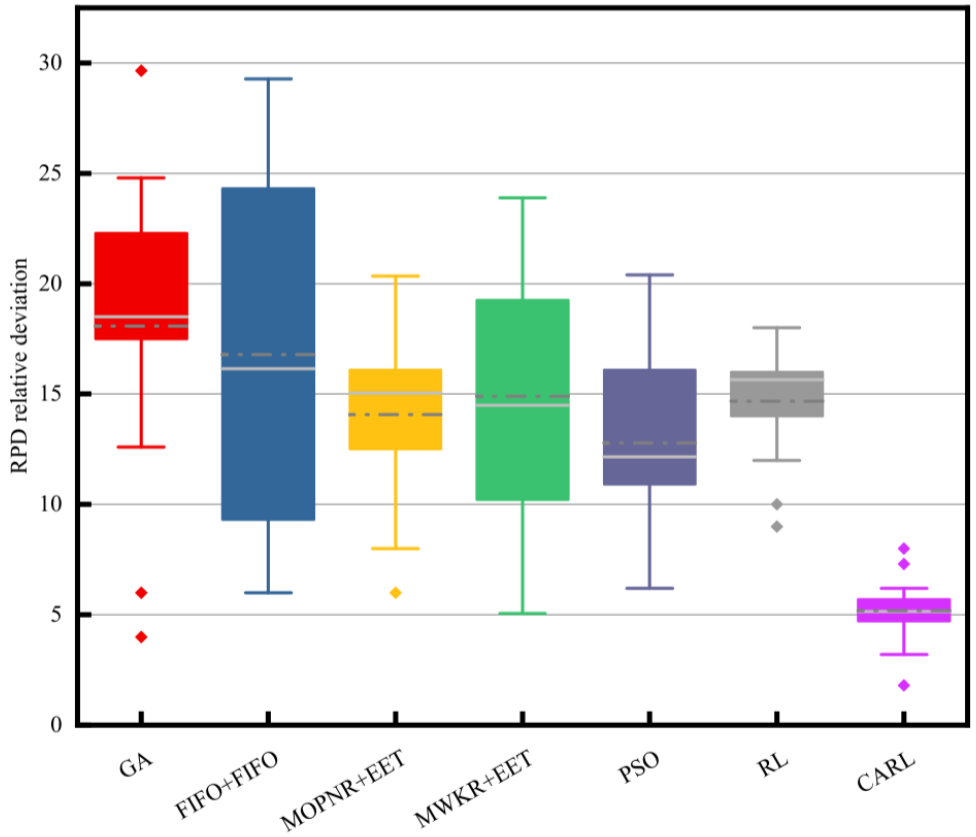

Fig. 9. RPD comparison box chart of different algorithms on the mk dataset. (the statistics are computed from 100 simulations).

Experiment Results

Table 5
Result comparison on Brandimarte's instances between CARL algorithm and Other algorithms.

Instance(size)		Ours	FIFO +FIFO	SPT +SPT	MOPNR +EET	MWKR +EET	LWKR +SPT	FIFO +SPT	FIFO + EET	MWKR + SPT	MOPNR +SPT	LWKR +EET	[41] 20×5	[41] 20×10	GA	PSO	UB
MK01(10×6)	Obj	44	48	59	49	46	76	64	47	53	61	78	55	48	**42**	46	39
	RPD	12.8%	23.1%	51.3%	25.6%	17.9%	94.9%	64.1%	20.5%	35.9%	56.4%	100.0%	41%	23.1%	**7.7%**	17.9%	
MK02(10×6)	Obj	**31**	46	46	40	41	43	42	40	37	41	59	42	43	41	35	26
	RPD	**19.2%**	76.9%	76.9%	53.8%	57.7%	65.4%	61.5%	53.8%	42.3%	57.7%	126.9%	61.5%	65.4%	57.5%	34.6%	
MK03(15×8)	Obj	**207**	220	303	216	213	362	338	207	342	330	325	232	213	238	212	204*
	RPD	**1.5%**	7.8%	48.5%	5.9%	4.4%	77.5%	65.7%	1.5%	67.6%	61.8%	59.3%	13.7%	4.4%	16.7%	3.9%	
MK04(15×8)	Obj	**69**	78	76	80	71	181	169	76	167	174	108	82	75	74	71	60
	RPD	**15.0%**	30.0%	26.7%	33.3%	18.3%	201.7%	181.7%	26.7%	178.3%	190.0%	80.0%	36.7%	25.0%	23.3%	18.3%	
MK05(15×4)	Obj	**177**	186	226	191	186	279	251	194	280	269	250	205	185	188	185	172
	RPD	**2.9%**	8.1%	31.4%	11.0%	8.1%	62.2%	45.9%	12.8%	62.8%	56.4%	45.3%	19.2%	7.6%	9.3%	7.6%	
MK06(10×10)	Obj	**77**	99	89	102	108	123	108	99	104	104	185	110	103	115	98	58
	RPD	**32.8%**	70.7%	53.4%	75.9%	86.2%	112.1%	86.2%	70.7%	79.3%	79.3%	219.0%	89.7%	77.6%	98.3%	69.0%	
MK07(20×5)	Obj	**151**	214	214	219	212	230	232	212	217	217	273	215	214	183	176	139
	RPD	**8.6%**	54.0%	54.0%	57.6%	52.5%	65.5%	66.9%	52.5%	56.1%	56.1%	96.4%	54.7%	54.0%	31.7%	26.6%	
MK08(20×10)	Obj	531	531	664	**523**	535	651	587	531	587	592	736	525	523	523	557	523*
	RPD	1.5%	1.5%	27.0%	**0.0%**	2.3%	24.5%	12.2%	1.5%	12.2%	13.2%	40.7%	0.4%	0.0%	0.0%	6.5%	
MK09(20×10)	Obj	334	372	448	342	355	511	466	349	456	462	616	424	**333**	361	345	307
	RPD	8.8%	21.2%	45.9%	11.4%	15.6%	66.4%	51.8%	13.7%	48.5%	50.5%	100.7%	38.1%	**8.5%**	17.6%	12.4%	
MK10(20×15)	Obj	**245**	278	358	268	264	427	365	279	369	358	492	266	266	319	247	197
	RPD	**24.4%**	41.4%	81.7%	36.0%	34.0%	116.8%	85.3%	41.6%	87.3%	81.7%	149.7%	35.0%	35.0%	61.9%	25.4%	
Average	Obj	**186**	207	248	203	203	288	262	203	261	261	312	216	200	208	197	173
	RPD	**5.7%**	19.7%	43.4%	17.3%	17.3%	66.5%	51.4%	17.3%	50.9%	50.9%	80.3%	24.9%	15.6%	20.2%	13.9%	

UB column that is the best result from literature, and '*' denotes the result is optimal

Experiment Results

Table 6
Result comparison on Hurink's vdata instances between CARL algorithm and Other algorithms.

Instances(size)		Ours	FIFO +FIFO	SPT +SPT	MOPNR +EET	MWKR +EET	LWKR +SPT	FIFO +SPT	FIFO + EET	MWKR + SPT	MOPNR +SPT	LWKR +EET	[41] 20×5	[41] 20×10	UB
la1-5(10×5)	Obj	**544.4**	576.1	631.9	559.6	555.4	803.0	790.0	613.4	788.0	602.0	749.6	580.4	550.4	507*
	RPD	**7.4%**	13.6%	24.6%	10.4%	9.5%	58.4%	55.8%	21.0%	55.4%	18.7%	47.9%	14.5%	8.6%	
la6-10(15×5)	Obj	822.2	850.8	973.0	838.4	823.3	1263.	1146.0	842.8	1196.0	861.8	1061.4	845.6	**821.8**	794*
	RPD	3.6%	7.2%	22.5%	5.6%	3.7%	659.1%	44.3%	6.1%	50.6%	8.5%	33.7%	6.5%	**3.5%**	
la11-15(20×5)	Obj	**1062.8**	1089.6	1181.1	1080.6	1063.5	1464.6	1283.4	1090	1398.6	1094.8	1355.6	1072.8	1064	1040.8*
	RPD	**2.1%**	4.7%	13.5%	3.8%	2.2%	40.7%	23.3%	4.7%	34.4%	5.2%	30.2%	3.1%	2.2%	
la16-20(10×10)	Obj	**695**	716.6	728.7	719.1	714.0	1339.2	1002.6	716.4	1360	737.6	1138.0	715.6	703.2	679.8*
	RPD	**2.2%**	5.4%	7.2%	5.8%	5.0%	97.0%	47.5%	5.4%	100.1%	8.5%	67.4%	5.3%	3.4%	
la21-25(15×10)	Obj	858.4	874.1	981.3	847.9	866.9	1607.8	1232.6	894.4	1702.8	936.8	1277.2	848.2	**825.2**	777.2
	RPD	10.4%	12.5%	26.3%	9.1%	11.5%	106.9%	58.6%	15.1%	119.1%	20.5%	64.3%	9.1%	**6.2%**	
la26-30(20×10)	Obj	1100	1141.4	1376.7	1101.2	1119.8	2169.4	1603.6	1119.8	2136.6	1175.	1538.8	1107.8	**1085.4**	1054.2
	RPD	4.3%	8.3%	30.6%	4.5%	6.2%	105.8%	52.1%	6.2%	102.7%	411.5%	46.0%	5.1%	**3.0%**	
la31-35(30×10)	Obj	**1580.6**	1619.4	1786.7	1595.0	1589.5	2598.0	2136.0	1611.2	2639.6	1657.2	2322.4	1588.2	1614.0	1552.2*
	RPD	**1.8%**	4.3%	15.1%	2.8%	2.4%	67.4%	37.6%	3.8%	70.1%	6.8%	49.6%	2.3%	4.0%	
la36-40(15×15)	Obj	**970.8**	995.0	1003.7	986.4	986.8	1991.4	1589.6	1002.4	2039.2	1087.8	1601.2	983.6	983.4	950.8*
	RPD	**2.1%**	4.6%	5.6%	3.7%	3.8%	109.4%	67.2%	5.4%	114.5%	14.4%	68.4%	3.4%	3.4%	
Average	Obj	**954**	980.0	1083.0	966.0	961.8	1655	1348	986.0	1658.0	1019.0	1381.0	968	959	920
	RPD	**3.7%**	7.6%	17.8%	5.1%	4.6%	79.9%	46.5%	7.3%	80.3%	10.8%	50.1%	5.2%	3.8%	

UB column that is the best result from literature, and '*' denotes the result is optimal

Experiment Results

Table 7
Result comparison on Hurink's rdata instances between CARL algorithm and Other algorithms.

Instances(size)		Ours	FIFO +FIFO	SPT +SPT	MOPNR +EET	MWKR +EET	LWKR +SPT	FIFO +SPT	FIFO + EET	MWKR + SPT	MOPNR +SPT	LWKR +EET	[41] 20×5	[41] 20×10	UB
la1-5(10×5)	Obj	**549.8**	585.6	676.8	576	594.8	893.6	677	598.4	784.6	804.4	781.4	617.2	574.8	507.6
	RPD	**8.30%**	15.40%	33.30%	13.50%	17.20%	76.00%	33.40%	17.90%	54.60%	58.50%	53.90%	21.60%	13.20%	
la6-10(15×5)	Obj	**838.2**	865.6	1012	855.7	841.2	1256.4	1002.8	856.8	1090.4	1036.4	1129.8	878.8	839.6	794.2
	RPD	**5.50%**	9.00%	27.40%	7.70%	5.90%	58.20%	26.30%	7.90%	37.30%	30.50%	42.30%	10.70%	5.70%	
la11-15(20×5)	Obj	**1093**	1137.6	1223.7	1126.2	1095	1500.6	1327.4	1147	1354.4	1343.4	1416.4	1121.2	1105.4	1041
	RPD	**5.00%**	9.30%	17.60%	8.20%	5.20%	44.10%	27.50%	10.20%	30.10%	29.00%	36.10%	7.70%	6.20%	
la16-20(10×10)	Obj	**823**	864.1	887.8	860	842.4	1294.6	1063.6	830.2	1030.4	1042.8	1303.2	875.8	884.4	697
	RPD	**18.10%**	24.00%	27.40%	23.40%	20.90%	85.70%	52.60%	19.10%	47.80%	49.60%	87.00%	25.70%	26.90%	
la21-25(15×10)	Obj	958.2	1037.6	1140.9	1003.8	987.3	1816.4	1334.4	1043	1261.4	1398.2	1654.4	1004.6	**947.6**	807.2
	RPD	18.70%	28.50%	41.30%	24.40%	22.30%	125.00%	65.30%	29.30%	56.30%	73.20%	105%	24.50%	**17.40%**	
la26-30(20×10)	Obj	1182.4	1252	1441	1224.6	1191	2095.8	1772	1236	1585.4	1646.4	2068	1247.6	**1175.6**	1062
	RPD	11.30%	17.90%	35.70%	15.30%	12.10%	97.30%	66.90%	16.40%	49.30%	55.00%	94.70%	17.50%	**10.70%**	
la31-35(30×10)	Obj	1651	1692.2	1910	1656.3	1642	2650.6	2050.2	1683.4	2217	2111.8	2578	1637.4	**1612.8**	1553
	RPD	6.30%	9.00%	23.00%	6.70%	5.70%	70.70%	32.00%	8.40%	42.80%	36.00%	66.00%	5.40%	**3.90%**	
la36-40(15×15)	Obj	**1198.8**	1262	1311	1231	1231	2095.6	1612.8	1273	1579	1603.4	2132.4	1259.8	1212	1013
	RPD	**18.30%**	24.60%	29.40%	21.50%	21.50%	106.90%	59.20%	21.50%	55.90%	58.30%	111%	24.40%	19.60%	
Average	Obj	**1037**	1087	1200	1043	1053	1700	1355	1083	1363	1373	1633	1080	1044	934
	RPD	**11.00%**	16.30%	28.40%	11.70%	12.70%	82.00%	45.10%	15.90%	45.90%	47.00%	74.80%	15.60%	11.80%	

UB column that is the best result from literature

Experiment Results

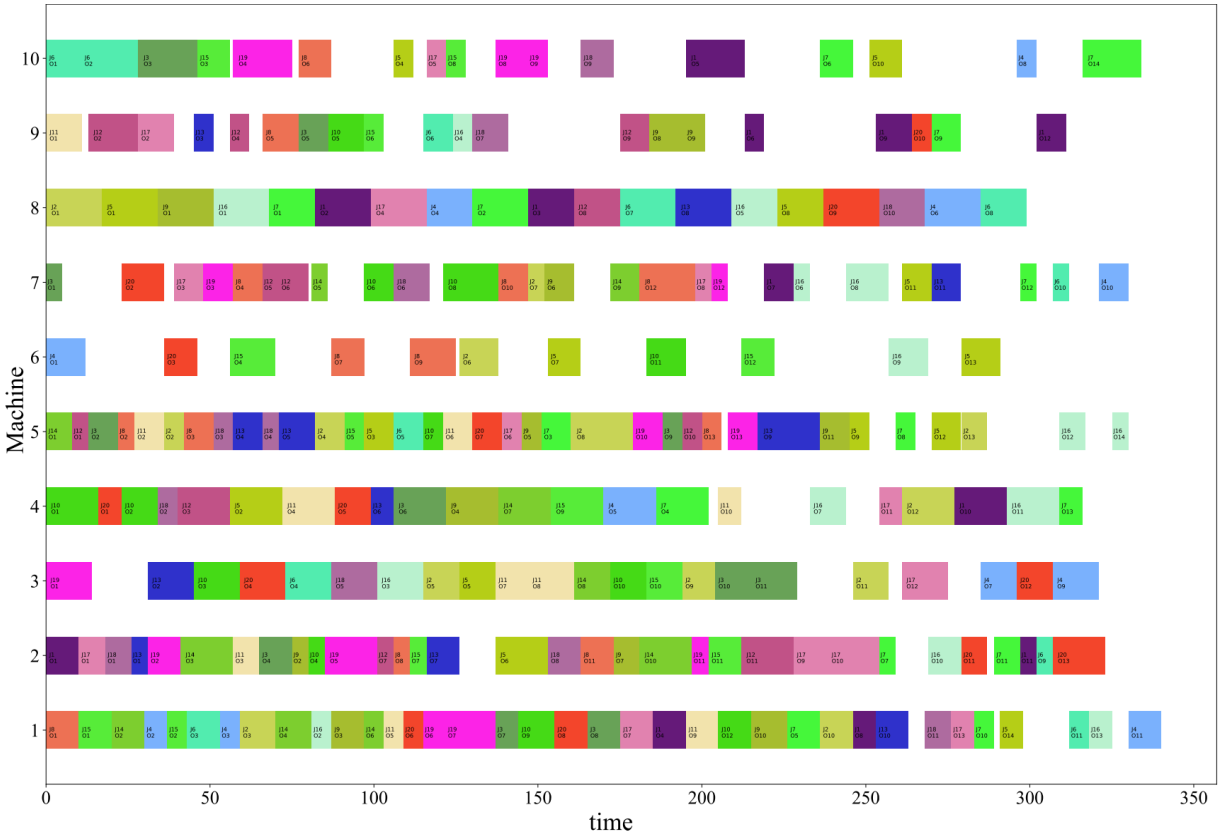

Fig. 10. The Gantt charts of our method on the mk09 dataset.

Fig. 11. The Gantt charts of our method on the vdata40 dataset.

Experiment Results

Table 8

Result comparison on DPpaulli's instances between CARL algorithm and dispatching rules.

Instances Size		Ours	FIFO +FIFO	SPT +SPT	MOPNR +EET	MWKR +EET	LWKR +SPT	FIFO +SPT	FIFO + EET	MWKR + SPT	MOPNR +SPT	LWKR +EET
10×5	DPpaullii1a	2980	3113	**2852**	3078	3179	3983	3123	3189	3313	3263	3718
	DPpaullii2a	**2483**	2526	2772	2973	2651	4388	3254	2839	3039	3236	4244
	DPpaullii3a	**2366**	2398	3128	2580	2432	4396	3016	3344	3105	3164	3760
	DPpaullii4a	3055	3000	**2889**	3018	3106	3917	3126	3102	3136	3206	3878
	DPpaullii5a	2422	**2419**	2485	2769	2602	3895	3020	3146	2977	2959	4141
	DPpaullii6a	**2330**	2502	3054	2527	2446	4233	3139	2993	3109	3157	3792
15×8	DPpaullii7a	2854	**2768**	2974	3052	3047	4073	3200	3087	3121	3149	3812
	DPpaullii8a	2327	**2319**	2632	2454	2452	3771	2943	3312	2933	3207	3999
	DPpaullii9a	**2171**	2240	2521	2368	2257	4321	3183	3087	3011	3263	3720
	DPpaullii10a	2819	2840	**2808**	3000	3018	4015	3110	3312	3202	3098	4145
	DPpaullii11a	2352	**2260**	2596	2544	2455	3734	3032	3104	3291	3038	3682
	DPpaullii12a	**2147**	2236	2255	2361	2233	3872	2720	2957	2855	2796	4016
20×10	DPpaullii13a	**2836**	2924	3487	2967	2838	4368	3095	3168	3054	3193	4482
	DPpaullii14a	**2351**	2374	2716	2578	2441	3930	3550	3315	3220	3165	4065
	DPpaullii15a	**2301**	2400	2505	2435	2306	4259	3339	3298	3181	3249	4482
	DPpaullii16a	**2815**	3050	2989	2843	2852	3899	3202	3178	3012	3078	3731
	DPpaullii17a	**2392**	2467	2441	2479	2416	4167	3200	3252	3301	3092	4209
	DPpaullii18a	**2242**	2328	2677	2422	2290	4025	2897	2976	2891	2978	4826

Experiment Results

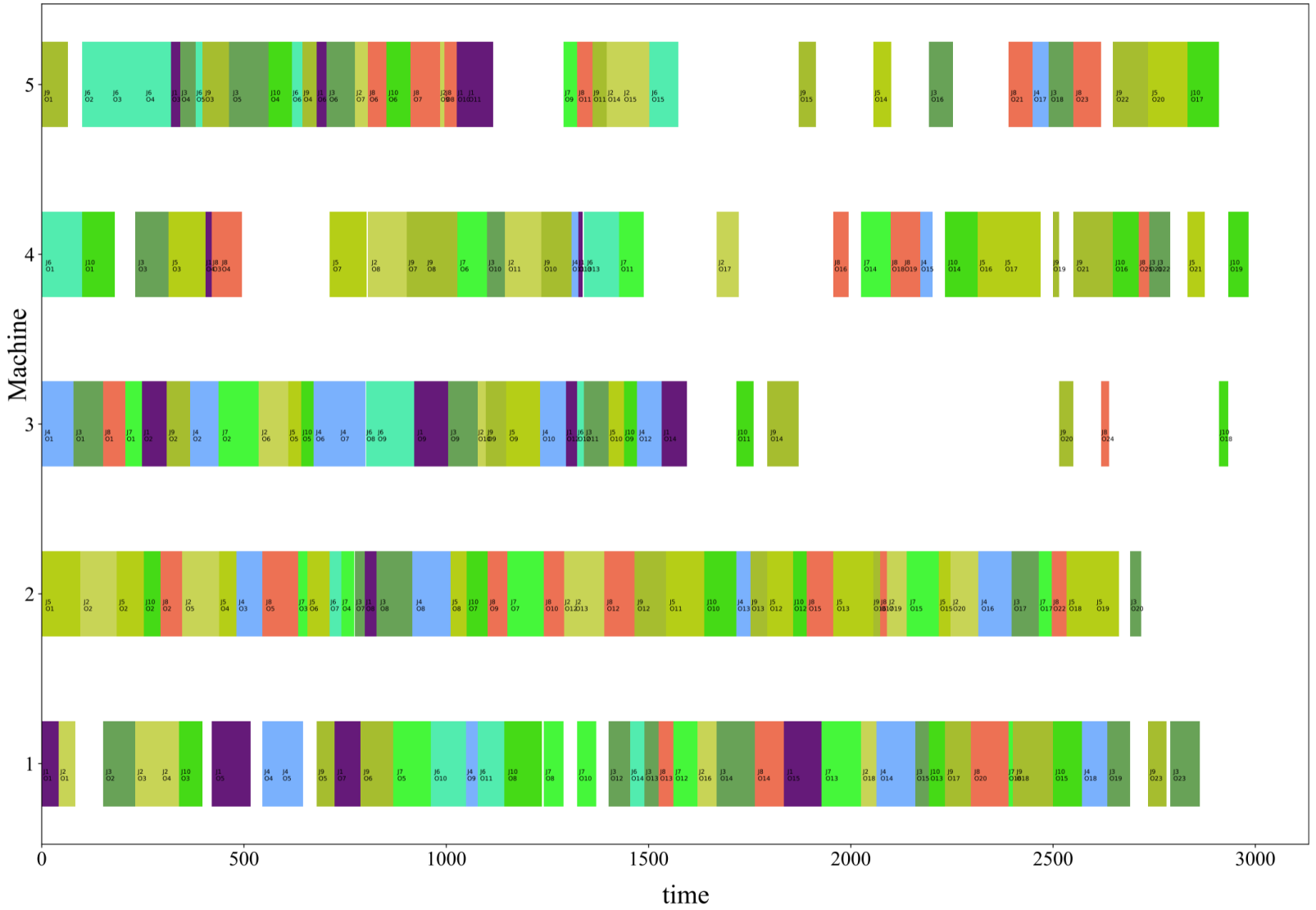

Fig. 12. The Gantt charts of our method on the DPpaullii1a dataset.

Contents

Conclusion

① This study proposes the CARL model to tackle FJSP, integrating cooperative DRL for operation selection and machine allocation, achieving a 55.52% performance improvement on large-scale instances without specific training while demonstrating strong generalization and robustness.

② Future research may explore innovative disjunctive graph embeddings and advanced machine modeling, alongside diverse RL agents such as SARSA, DQN, PPO, and A2C for job and machine selection.

Paper 2

北京工業大學
BEIJING UNIVERSITY OF TECHNOLOGY

Dynamic job shop scheduling based on deep reinforcement learning for multi-agent manufacturing systems

Yi Zhang, Haihua Zhu *, Dunbing Tang, Tong Zhou, Yong Gui

Publish Journal: Robotics and Computer-Integrated Manufacturing（2022）

Contents

Contents

Problem Description

- This study proposes a multi-agent manufacturing system based on deep reinforcement learning to enhance the dynamic response and self adjustment capabilities of workshops to personalized orders.
- **Challenge:** Traditional scheduling methods struggle to maintain efficient operation in dynamic workshop environments with uncertainties such as random job insertions and equipment failures.
- **Method:** The system utilizes an improved Contract Network Protocol (CNP) to coordinate agent competition and cooperation, and optimizes the decision-making ability of the AI scheduler through PPO algorithm to achieve autonomous scheduling and real-time adjustment.

Contents

Method Design

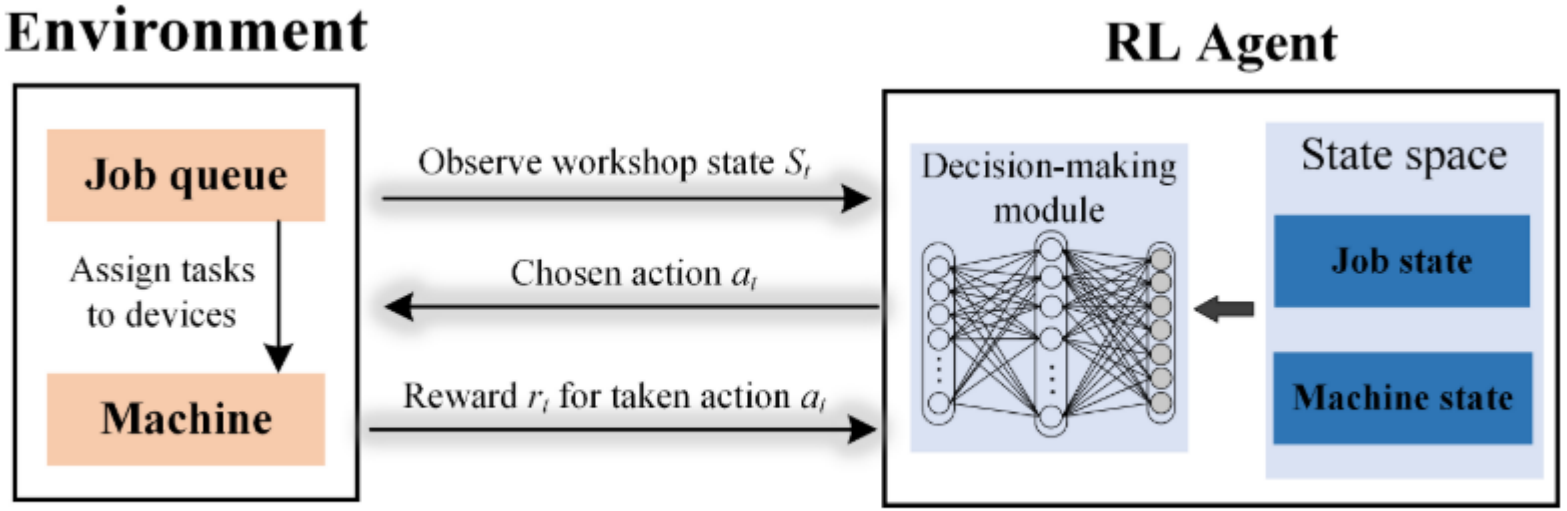

Fig. 1. The design of RL-based scheduling method in a smart workshop.

Method Design

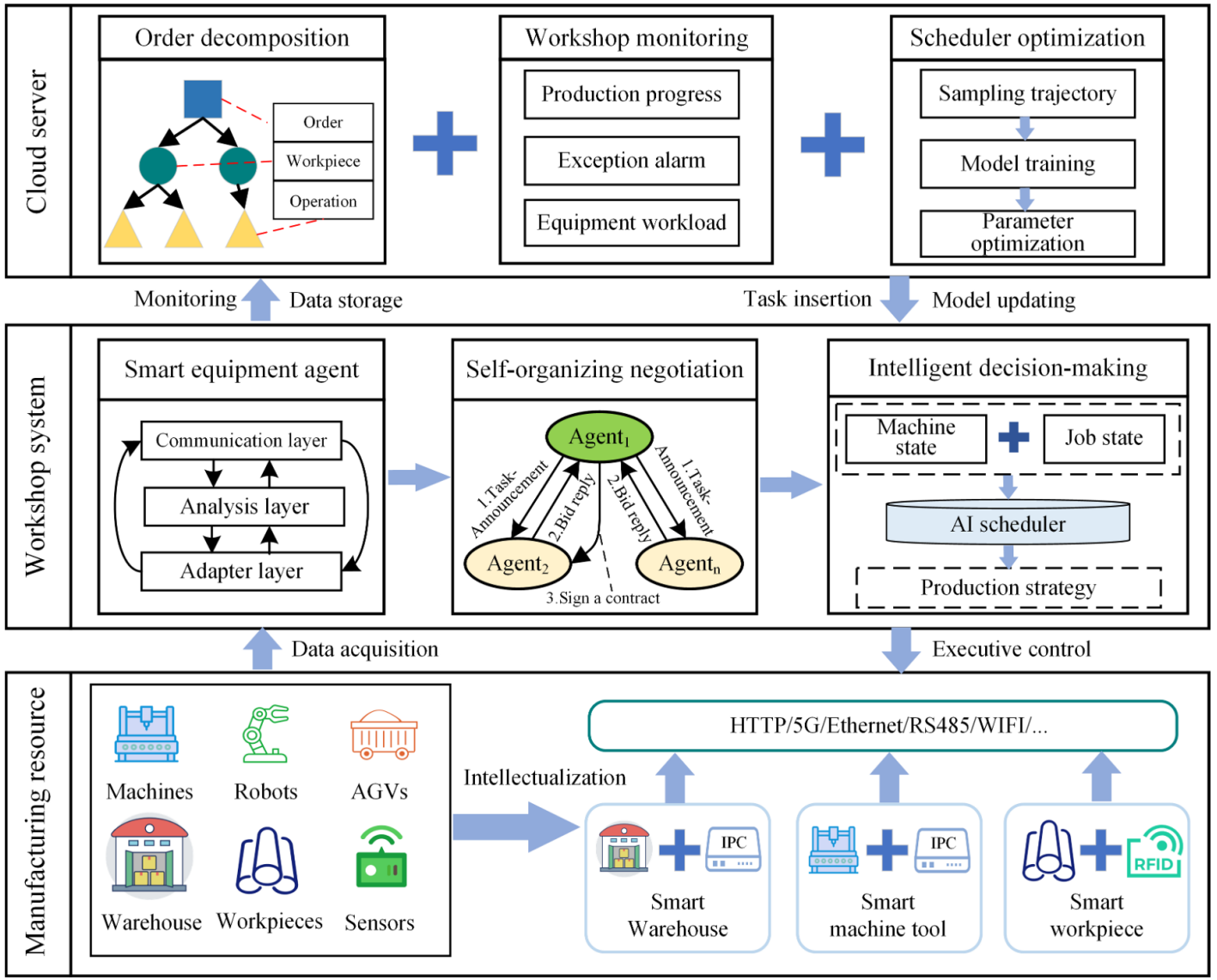

Fig. 2. The architecture of multi-agent manufacturing system.

Method Design

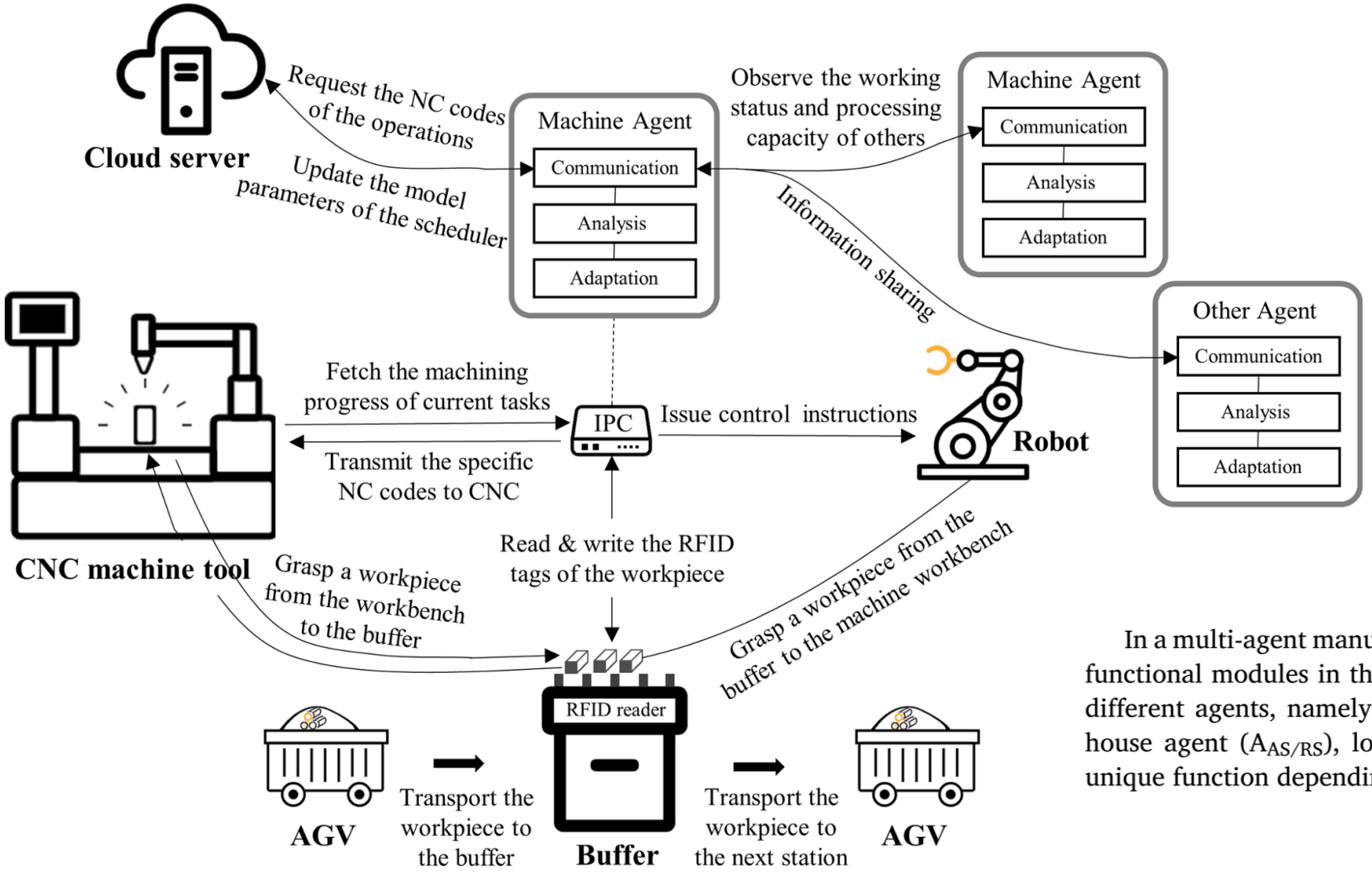

Fig. 3. The operation logic of a machine agent.

In a multi-agent manufacturing system, the machine, workpiece, and functional modules in the workshop are abstracted and constructed as different agents, namely, machine agent (A_M), part agent (A_P), warehouse agent ($A_{AS/RS}$), logistics agent (A_{AGV}). Each agent has its own unique function depending on its characteristics.

Method Design

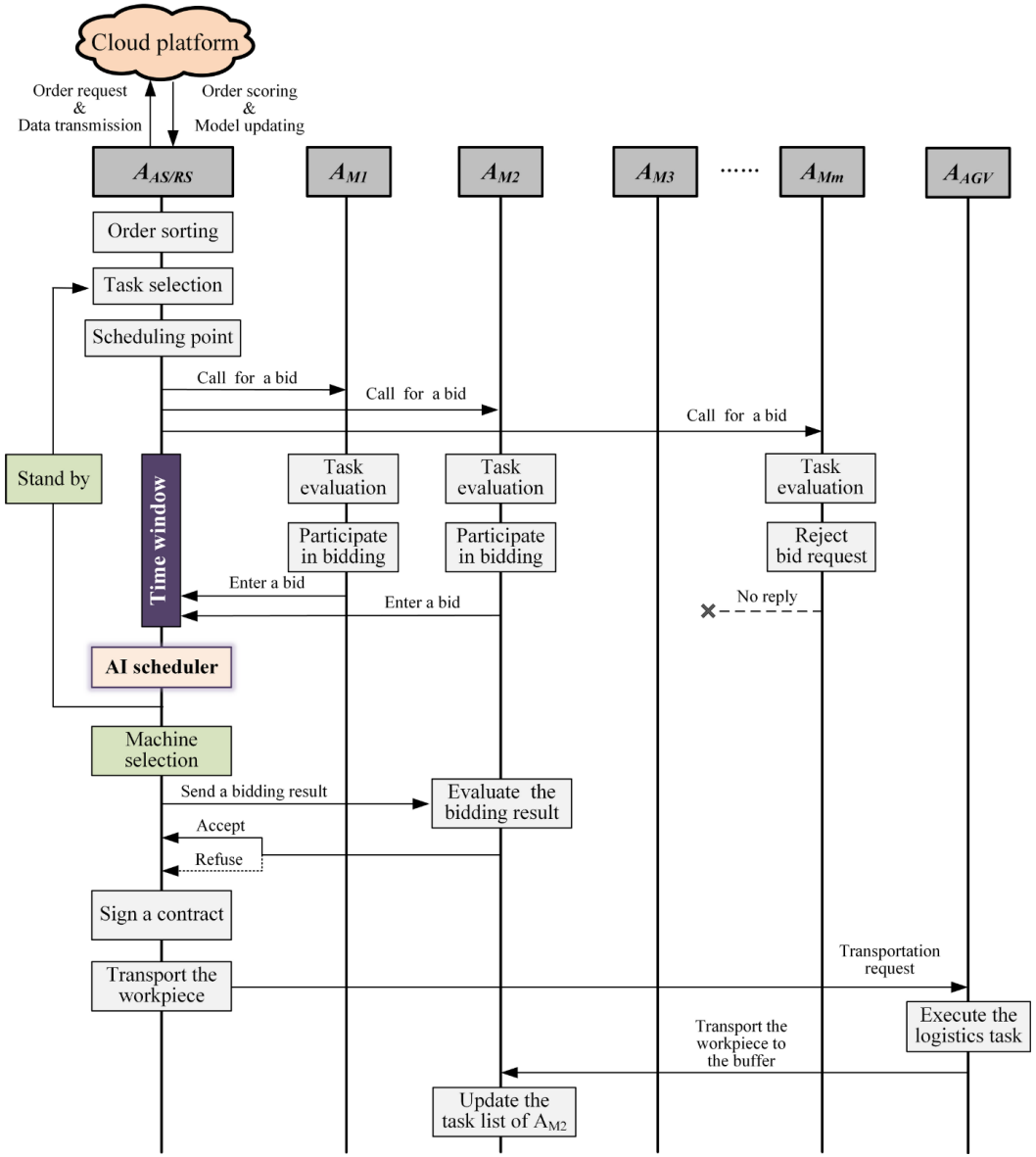

Fig. 4. Self-organizing negotiation process among multiple agents.

Method Design

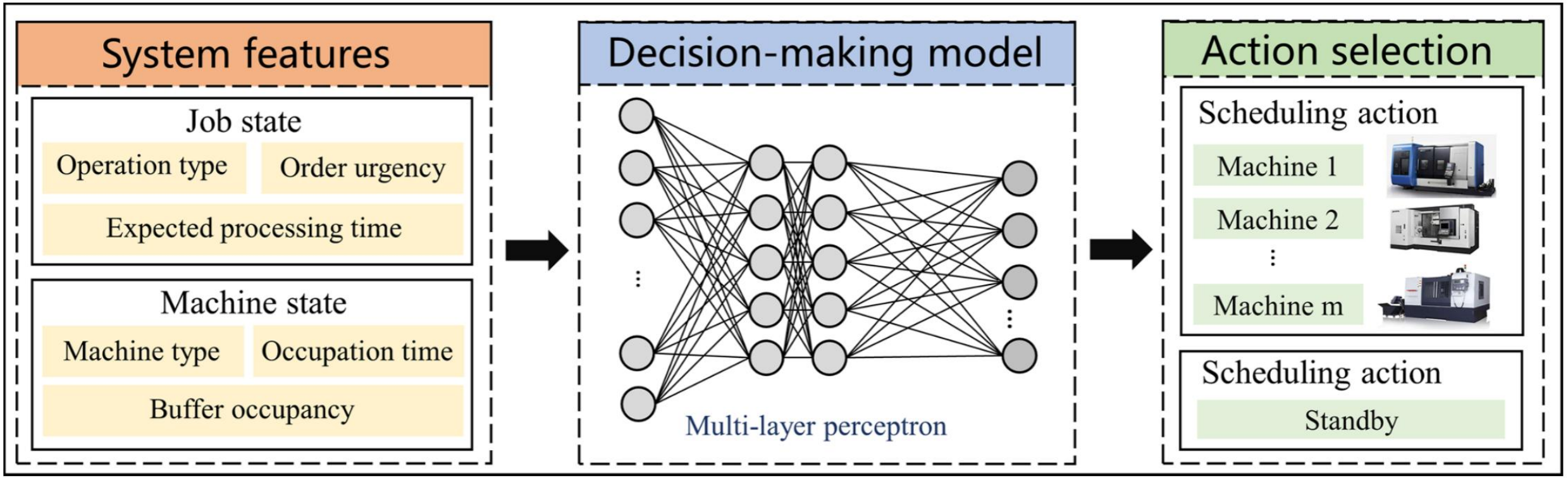

Fig. 5. Adaptive decision-making process of AI scheduler.

Method Design

State Space

State space is an accurate representation of workshop environment characteristics and the key basis for AI scheduler to make decisions. At the scheduling moment t, the state space S_t of workshop environment consists of operation attributes O_t of the workpiece J_i to be scheduled and working status M_t of all available machining tools, and can be described as $S_t = \{O_t, M_t\}$. The operation attributes of the workpiece to be scheduled $O_t = \{O_{1t}, O_{2t}, O_{3t}\}$ are composed of processing technology type O_{1t}, ideal operating time O_{2t} and order urgency O_{3t}, and the dimension of job state is 3. O_{1t} denotes the numerical expression of operation types (i.e., 1: turning, 2: milling). O_{2t} indicates the workload time required to complete the operation. Order urgency O_{3t} indicates the difference between due time and current timepoint t, as shown in Eq. (6).

$$O_{3t} = \frac{\widehat{T}_{i,j}^{(C)} - t}{\sum_{j<N_i} T_{i,j}} \tag{6}$$

Action Space

A_t. The action space is a collection of all optional production actions $A_t = \{a_0, a_1, \ldots, a_m\}$ for AI scheduler in a workshop environment, as shown in Fig. 5. In this paper, there are two kinds of actions within A_t: standby "a_0", and machine allocation "$a_1, \ldots, a_m$". The standby action indicates

Reward function design

$$r_t = \begin{cases} -50 & invalid\ action \\ w_1 \times r_{tard} - w_2 \times r_{load} + w_3 \times r_{profit} & order\ to\ machine\ or\ standby \end{cases} \tag{7}$$

$$r_{tard} = \frac{\widehat{T}_{i,j}^{(c)} - T_{i,j}^{(c)}}{\widetilde{T}_{i,j}} \tag{8}$$

Where $\widehat{T}_{i,j}^{(c)}$ and $T_{i,j}^{(c)}$ are the expected completion time and actual completion time of operation $O_{i,j}$, and $\widetilde{T}_{i,j}$ is the nominal operating time of operation $O_{i,j}$. If the actual completion time of operation is earlier than expected, r_{tard} will be positive. The goal of AI scheduler is to maximize the value of r_{tard}.

$$LD_m = \int_{t_0}^{t} \sum_{i,j} K_m^{(S)} \times T_{i,j} \tag{9}$$

Where LD_m represents the cumulative workload time of machine M_m from timestep t_0 to t.

$$r_{load} = \sqrt{\frac{\sum_{m \in c} (LD_m - \overline{LD})^2}{M_c}} \tag{10}$$

Where r_{load} indicates the workload deviation between isomorphic machine tools, $\overline{LD}$ represents the average workload time of isomorphic machine tool., and M_c denotes the number of types of machine tools.

$$r_{profit} = e - K_m^{(E)} \tag{11}$$

Where r_{profit} indicates the production profit of the work order.

Method Design

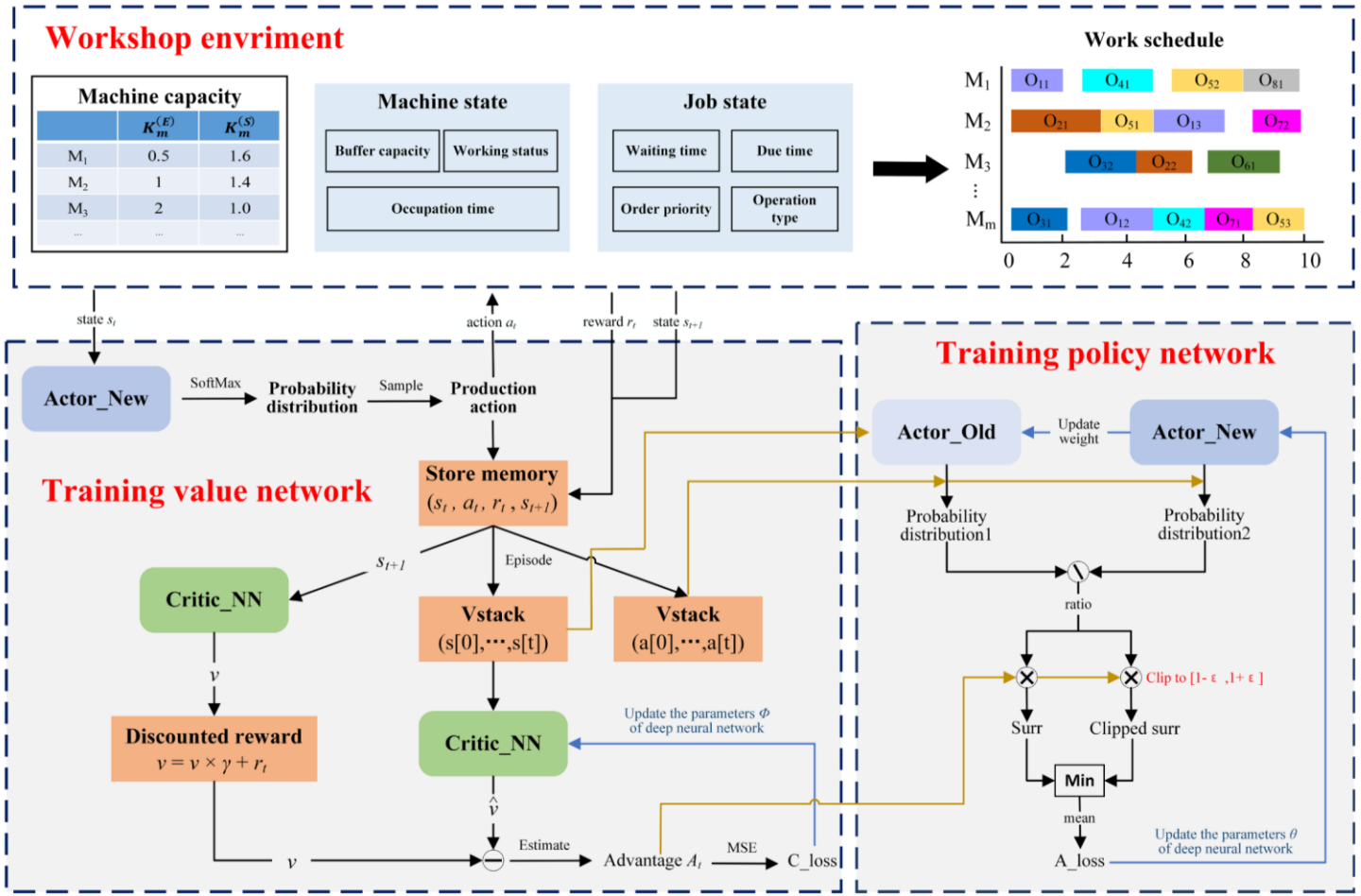

Fig. 6. Self-learning mechanism of decision-making model.

Table. 2
Adaptive optimization method of AI scheduler based on DRL.

Algorithm 1: the pseudo-code of adaptive optimization method of AI scheduler based on DRL

1: Initialization: hyper parameter α_p, α_v, γ, ε and the network parameter of PPO algorithm
2: Generate a simulated job shop environment for training according to predefined criteria
3: For episode number $e = 1, 2, \ldots, N$ do
4: Reset the simulated workshop environment
5: For epoch number $t = 1, 2, \ldots, T$ do
6: AI scheduler observes the state S_t of workshop environment: operation characteristics of the workpiece
to be scheduled, running status of machine sets
7: AI scheduler run policy $\pi(\theta)$ to choose a production action a_t based on the workshop state S_t
8: The workshop environment feeds back a composite reward value r_t to AI scheduler after the action a_t
executed, and makes a translation to a new state S_{t+1}
9: Store the (s_t, a_t, r_t) in the trajectory buffer $(s_1, a_1, r_1, \ldots, s_\tau, a_\tau, r_\tau)$
10: End for
11: AI scheduler runs critic network and estimates the value of advantage function $\widehat{A}_t$
12: For epoch number $i = 1, 2, \ldots, M$ do
13: Sample mini-batches from the trajectory buffer
14: Update θ by a gradient method to optimize the loss function $J_{ppo}(\theta)$
15: End for
16: For epoch number $j = 1, 2, \ldots, B$ do
17: Sample mini-batches from the trajectory buffer
18: Update ∅ by a gradient method to optimize the loss function $L_{BL}(\varnothing)$
19: End for
20: Replace the parameters of actor network $\pi(\text{old}) \leftarrow \pi(\theta)$
21: End for

Contents

Experiment Results

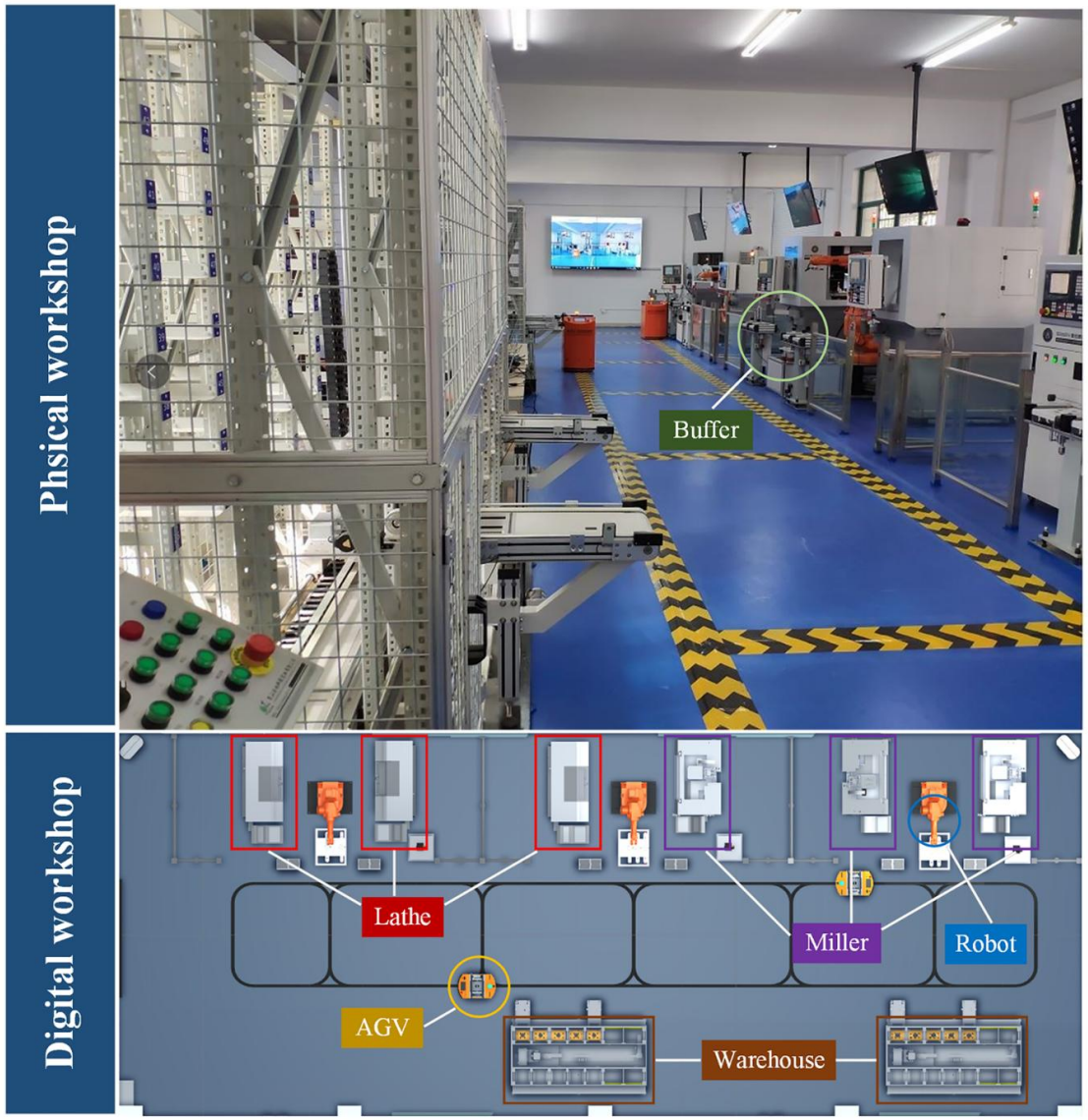

Fig. 7. The overall layout of a smart workshop.

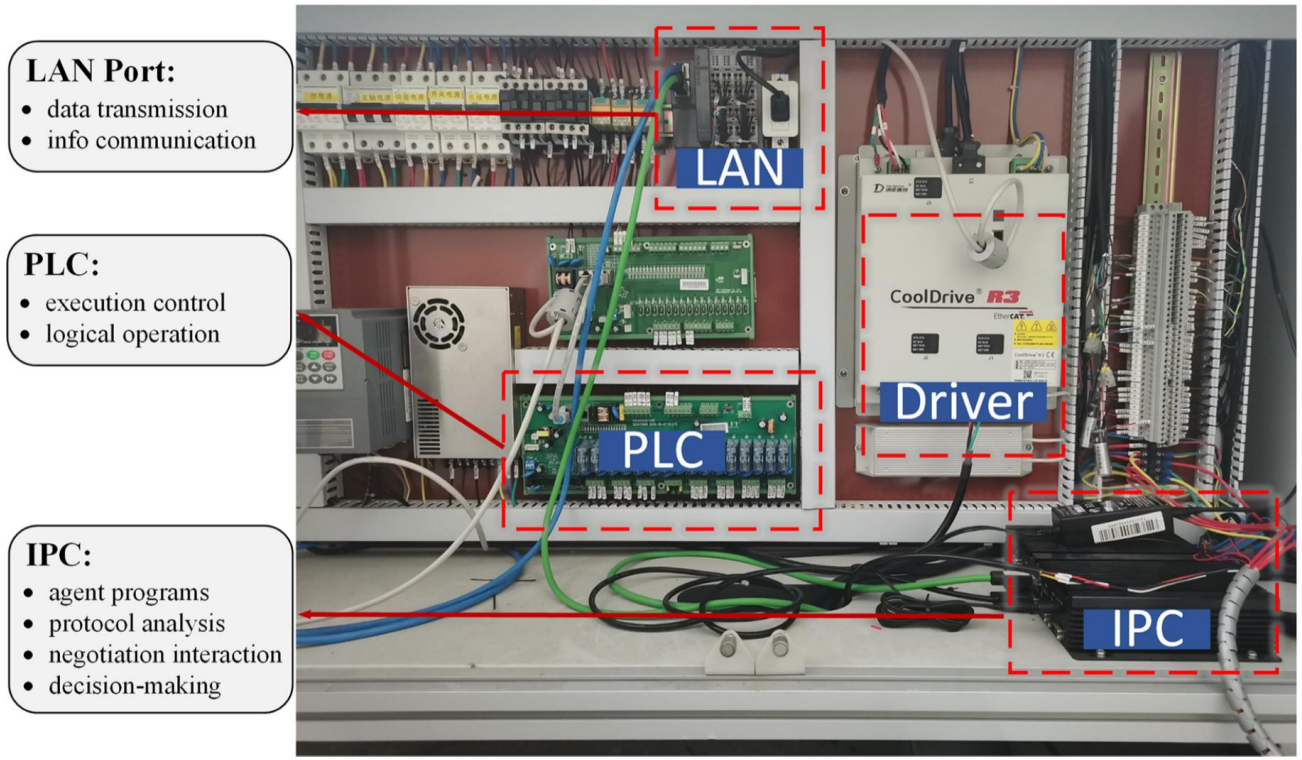

Fig. 8. The internal view of a smart machine.

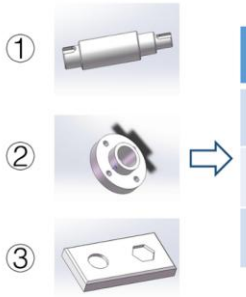

Job type	Process route	Available machines
Shaft	Turning→ Milling	(M_1,M_2,M_3), (M_4,M_5,M_6)
Flange	Turning→ Milling	(M_1,M_2,M_3), (M_4,M_5,M_6)
Plate	Milling	(M_4,M_5,M_6)

Fig. 9. The process route of jobs and available machines of operations.

Experiment Results

Table. 4
Test case.

Index	Job type	Arrival time	Due time	Ideal workload time
1	Shaft	10	151	35,12
2	Flange	45	171	32,10
3	Plate	70	199	43
4	Plate	95	209	38
5	Plate	125	266	47
6	Flange	150	282	30,14
7	Shaft	175	307	33,11
8	Plate	190	340	50
9	Flange	200	368	39,17
10	Plate	210	297	29
11	Flange	235	373	33,13
12	Plate	260	392	44
13	Plate	270	384	38
14	Shaft	295	412	29,10
15	Flange	320	425	26,9
16	Shaft	350	464	28,10
17	Plate	370	475	35
18	Plate	385	496	37
19	Shaft	430	571	31,16
20	Flange	495	651	34,18

Experiment Results

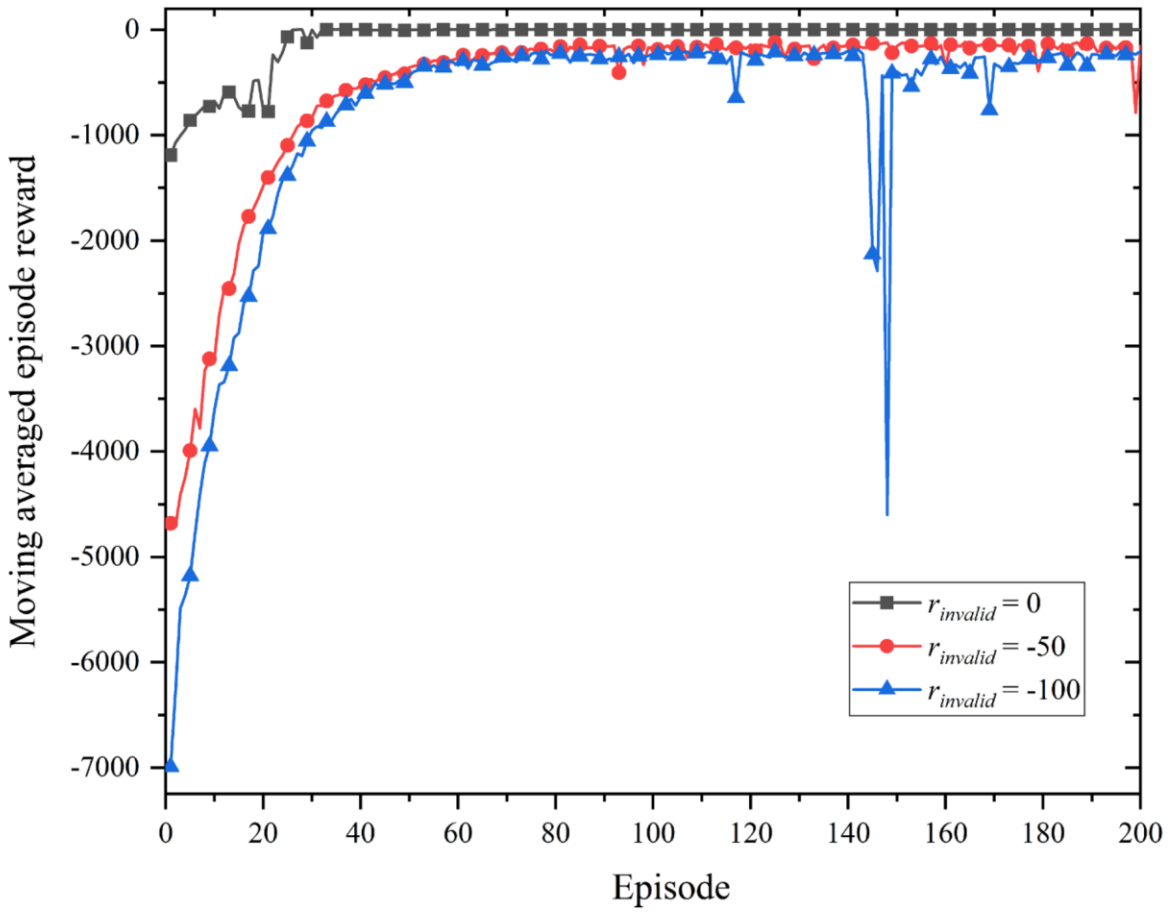

Fig. 10. The learning curves of accumulated reward under three kinds of reward settings.

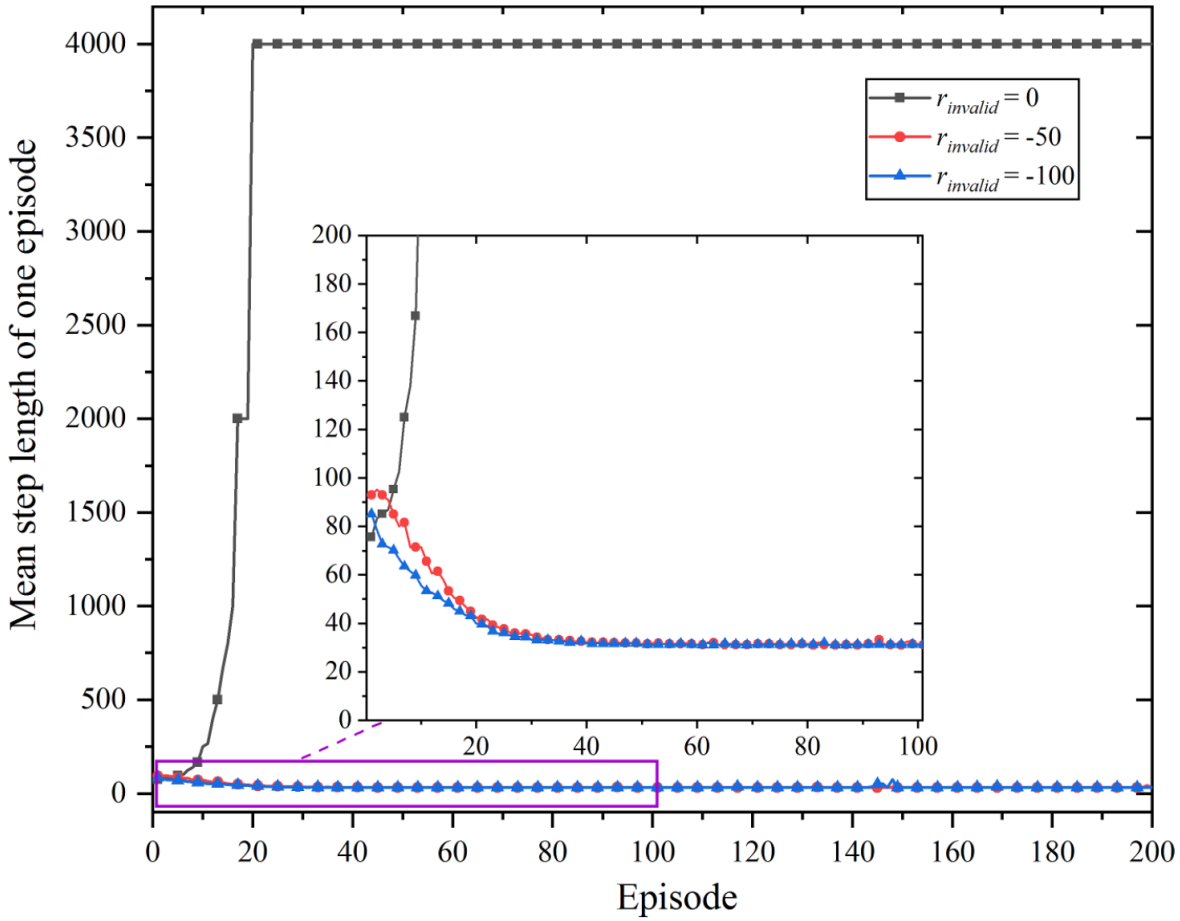

Fig. 11. The learning curves of step length under three kinds of reward settings.

Experiment Results

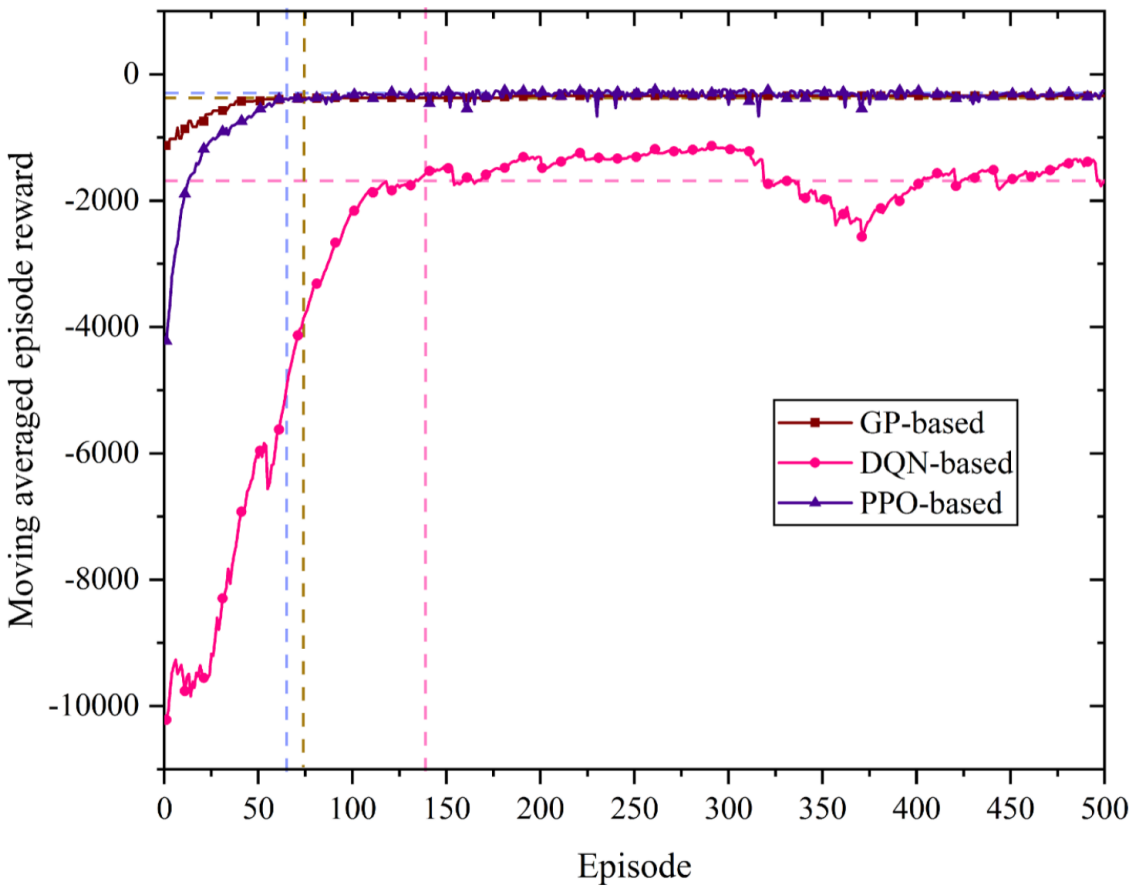

Fig. 12. The learning curve of three different methods in training process.

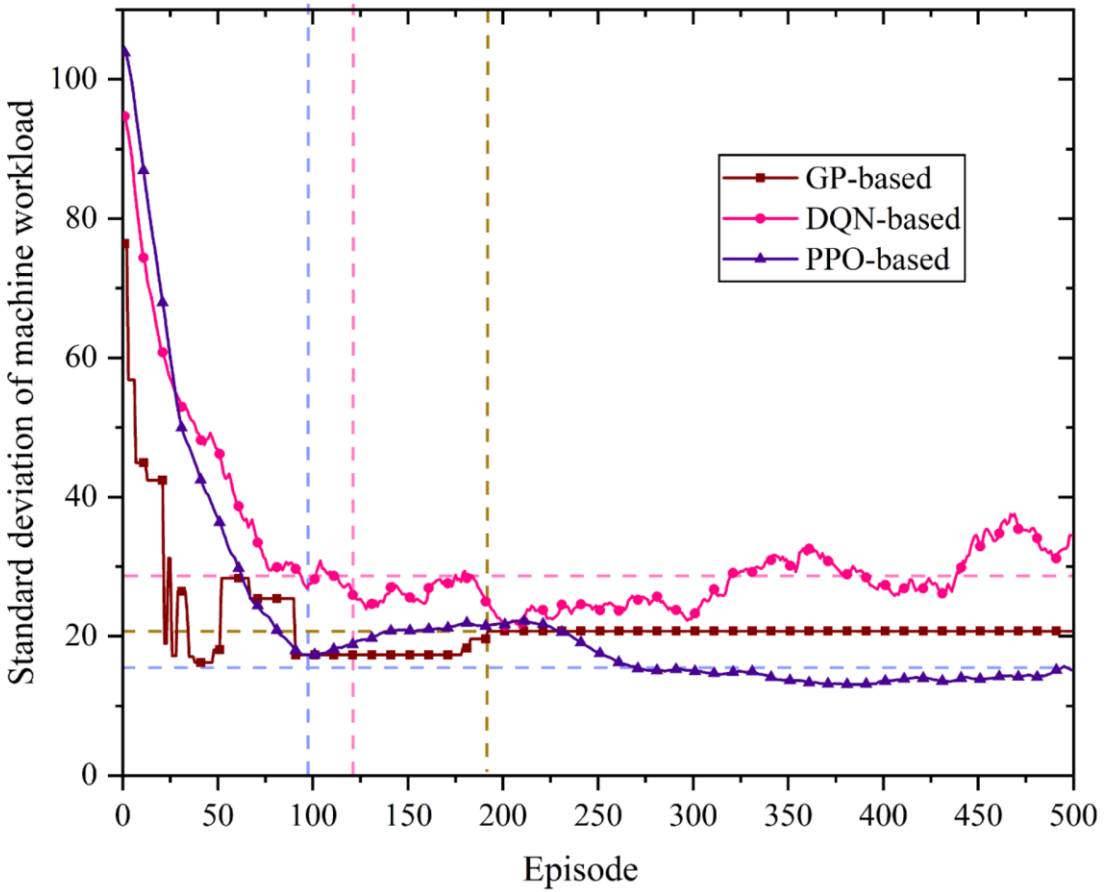

Fig. 13. The learning curve of workload balance between isomorphic machine tools.

Experiment Results

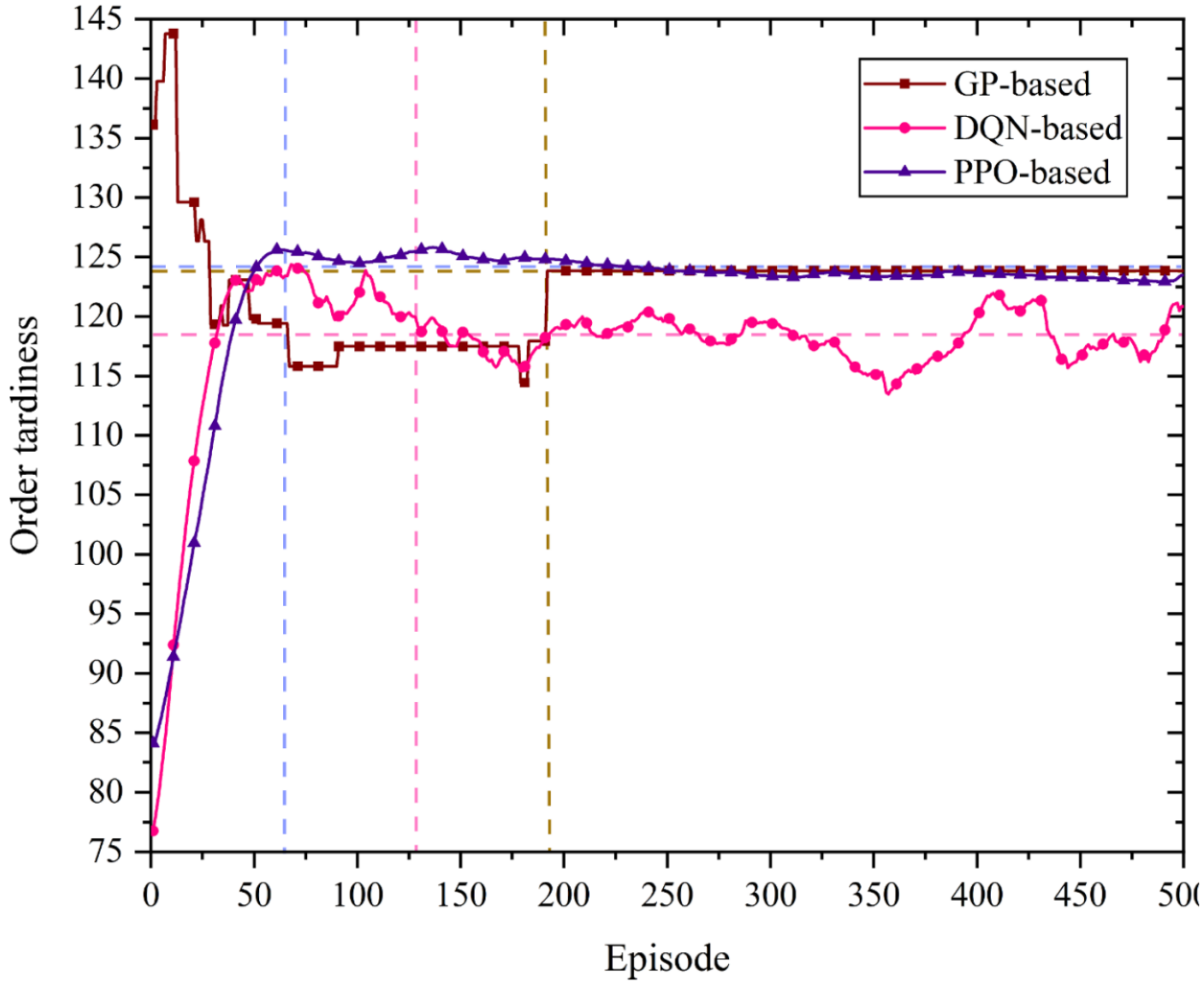

Fig. 14. The learning curve of order tardiness by three different methods.

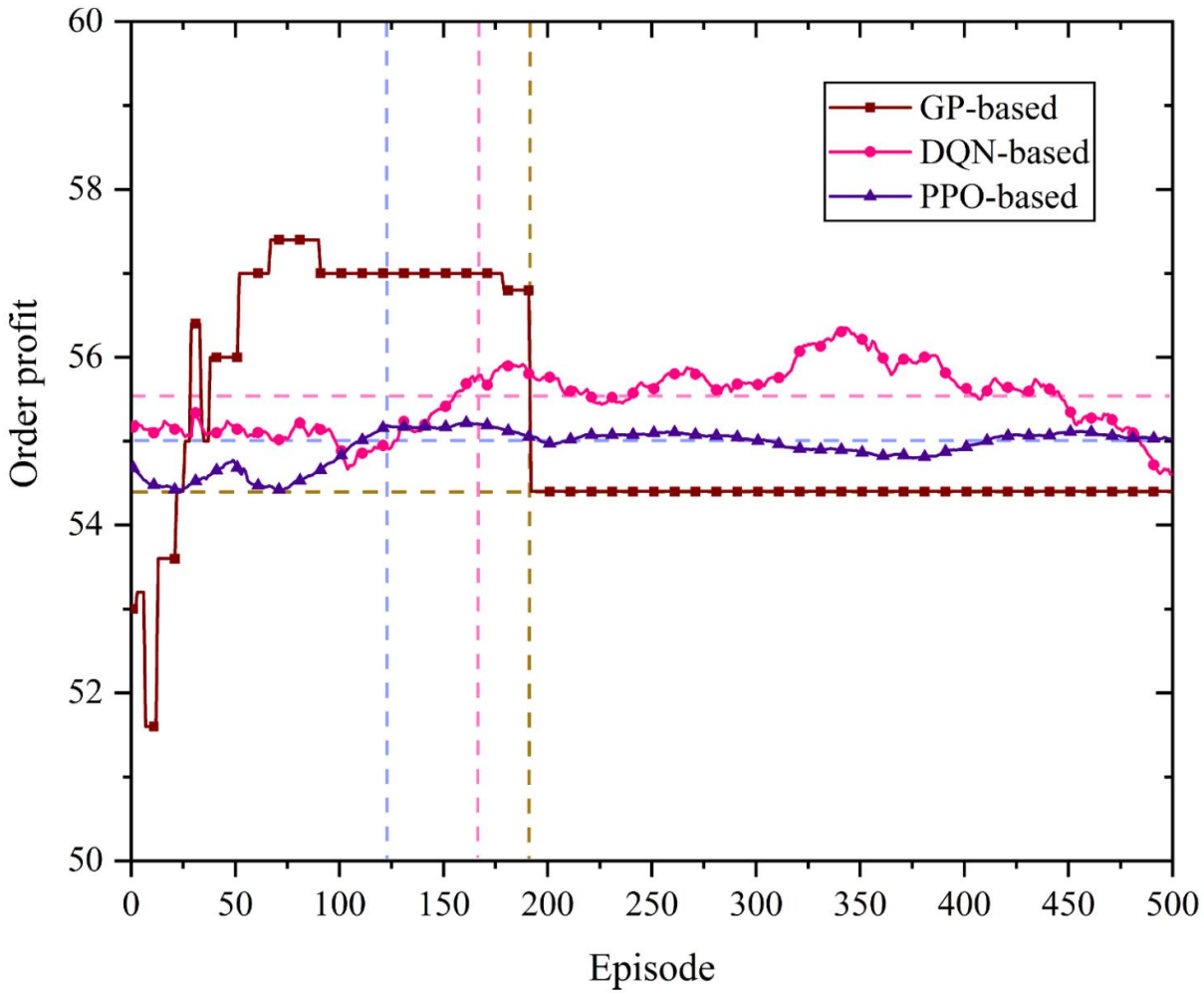

Fig. 15. The learning curve of order profit by three different methods.

Experiment Results

Table. 6
Comparison of results on test case by five scheduling methods.

	GA-based	SPT+FIFO		GP-based		DQN-based		PPO-based	
Tardiness	125.3	146.8		124.9		121.9		123.0	
Workload balance	15.6	79.6		20.8		43.9		15.3	
Profit	55.6	50.4		54.4		54.4		55.8	
Evaluation value	165.3	117.6		158.5		132.4		163.5	
Architecture	☆	☆	★	☆	★	☆	★	☆	★
Execution time (s)	28.23	6.33	1.32	6.52	1.52	6.05	1.06	5.99	0.98

Table. 7
Comparison of results on test case under new order insertion.

	GA-based	SPT+FIFO		GP-based		DQN-based		PPO-based	
Tardiness	123.0	145.8		122.9		124.2		117.6	
Workload balance	20.1	71.8		23.1		29.2		17.7	
Profit	54.9	50.8		54.8		55.2		56.6	
Evaluation value	157.8	124.8		154.6		150.2		156.5	
Architecture	☆	☆	★	☆	★	☆	★	☆	★
Execution time (s)	54.22	6.35	1.34	6.56	1.55	6.07	1.07	6.01	0.99

Table. 8
Comparison of results on test case under machine failure.

	GA-based	SPT+FIFO		GP-based		DQN-based		PPO-based	
Tardiness	122.5	143.8		122.4		122.2		121.6	
Workload balance	28.6	60.0		31.7		35.6		31.1	
Profit	55.1	51.6		55.0		55.4		56.0	
Evaluation value	149.0	135.4		145.7		142.0		146.5	
Architecture	☆	☆	★	☆	★	☆	★	☆	★
Execution time (s)	42.53	6.52	1.42	6.67	1.58	6.19	1.08	6.12	1.01

Contents

Future Work

Contributions

This paper constructs a multi-agent manufacturing system with an AI scheduler based on deep reinforcement learning to improve dynamic responsiveness and production efficiency for personalized orders.

Future Work

Future research will focus on expanding the system's scale, enhancing the state space design, and incorporating various dispatching rules.

Paper 3

北京工業大學
BEIJING UNIVERSITY OF TECHNOLOGY

A Hierarchical Multi-Action Deep Reinforcement Learning Method for Dynamic Distributed Job-Shop Scheduling Problem With Job Arrivals

Jiang-Ping Huang , Liang Gao , Senior Member, IEEE, and Xin-Yu Li , Member, IEEE

Publish Journal: IEEE TRANSACTIONS ON AUTOMATION SCIENCE AND ENGINEERING (2025)

Contents

Contents

Problem Description

- This paper addresses the Distributed Job-shop Scheduling Problem (DJSP) with job arrivals using a Multi-action Deep Reinforcement Learning (MDRL) method, incorporating a hierarchical action space and Graph Neural Network (GNN) for scheduling optimization.

- **Challenges:** The main challenge is managing job arrival uncertainties and designing a reward function and state transition that can effectively handle dynamic disturbances in the scheduling process.

- **Method:** The MDRL approach utilizes Proximal Policy Optimization (PPO) with two actor-critic frameworks to enable intelligent decision-making, outperforming other methods in both experimental and industrial settings.

Contents

Method Design

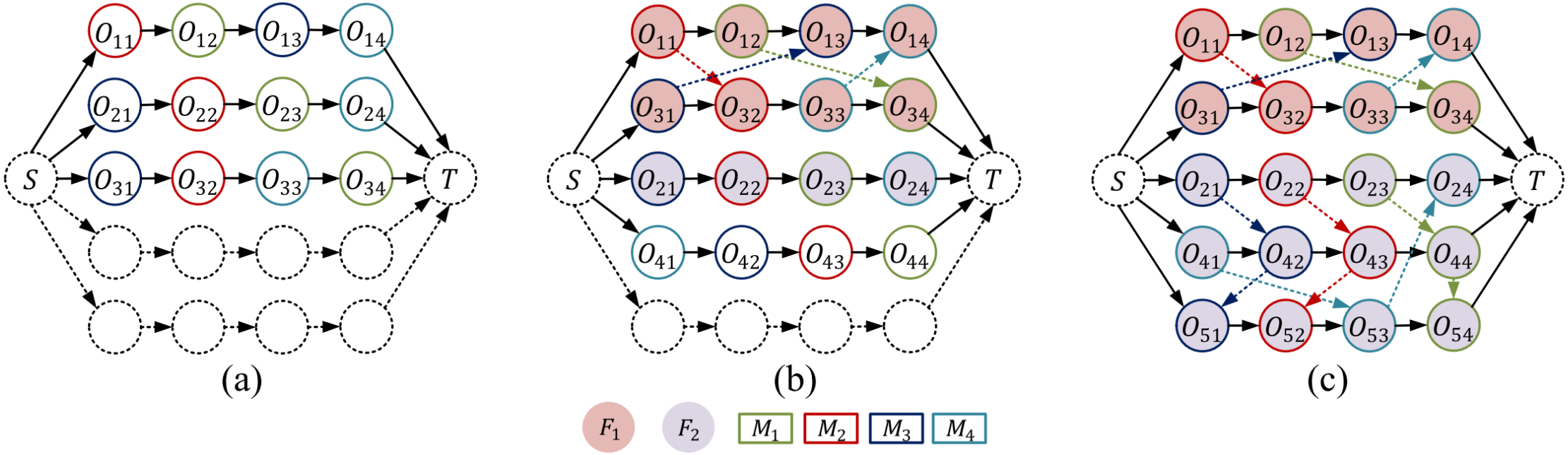

Fig. 1. Stitched disjunctive graph model.

Method Design

$$A = A_{op} \times A_{fac}$$

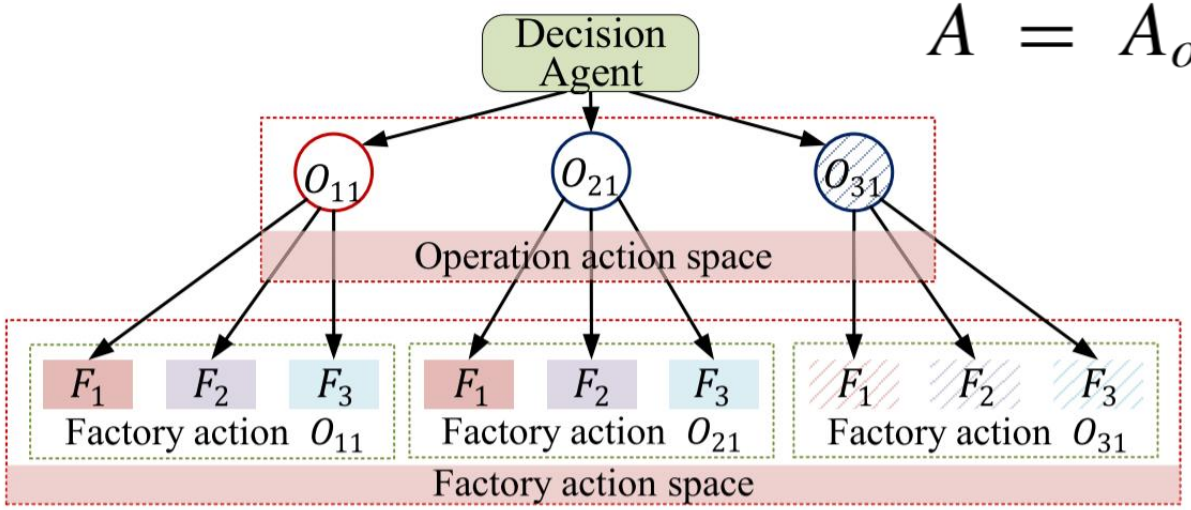

(a)

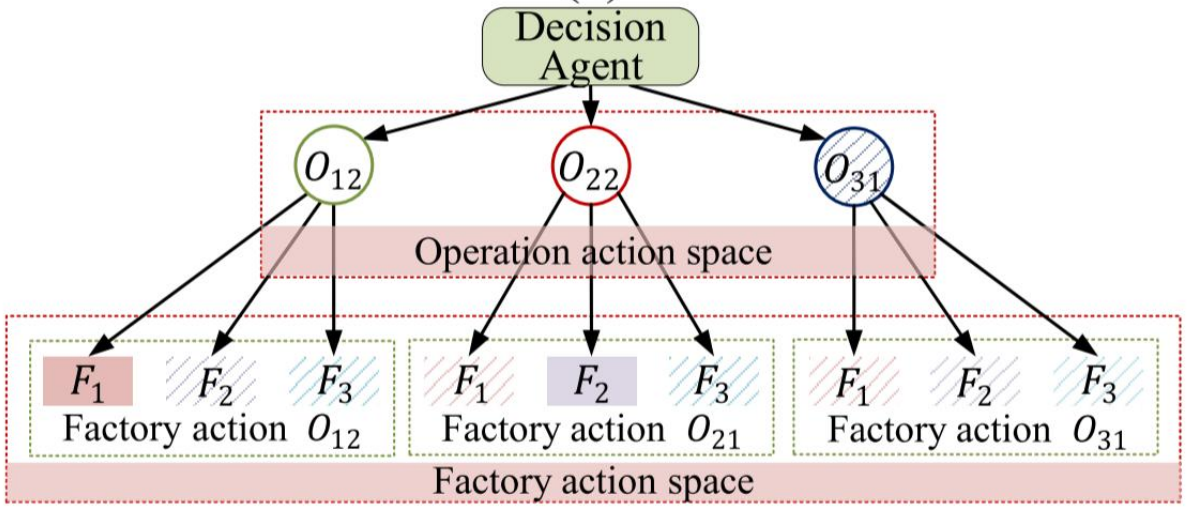

(b)

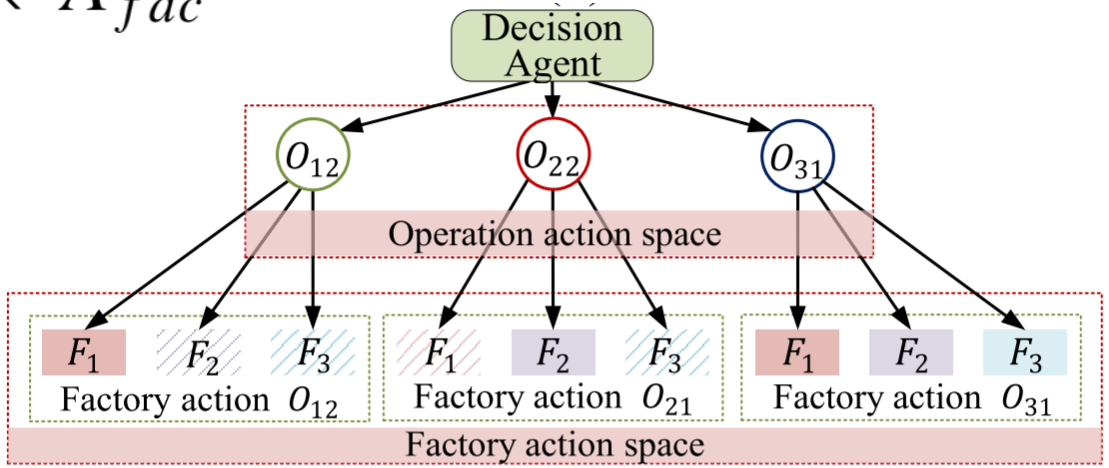

(c)

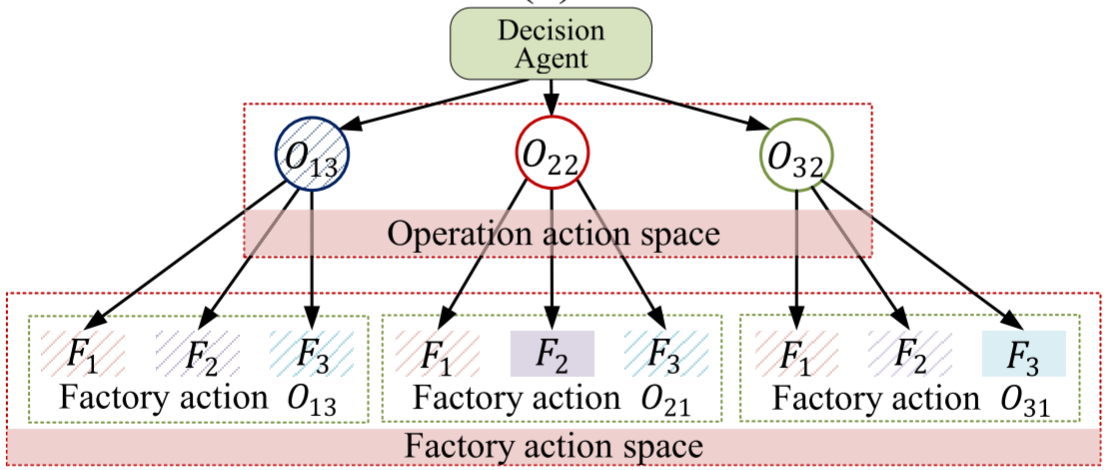

(d)

Method Design

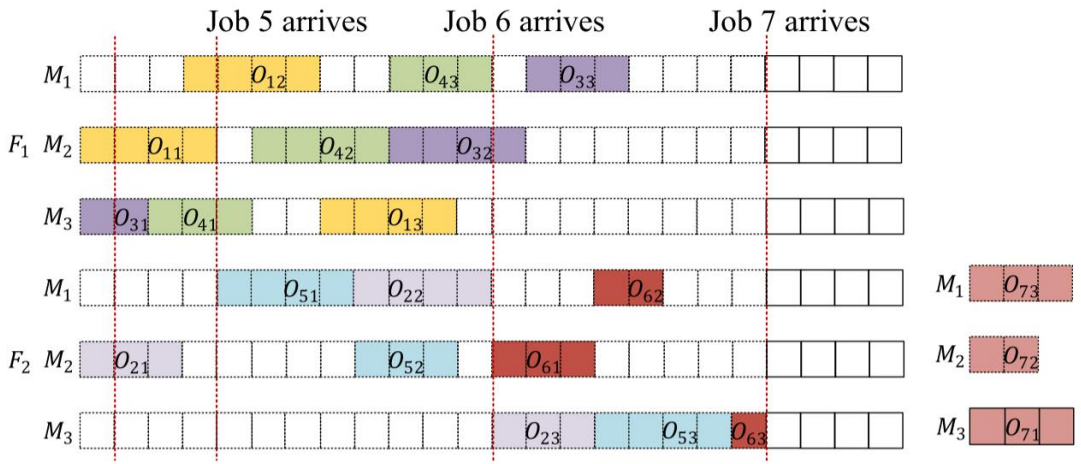

(a) Current state s_t and the information of the arrived job

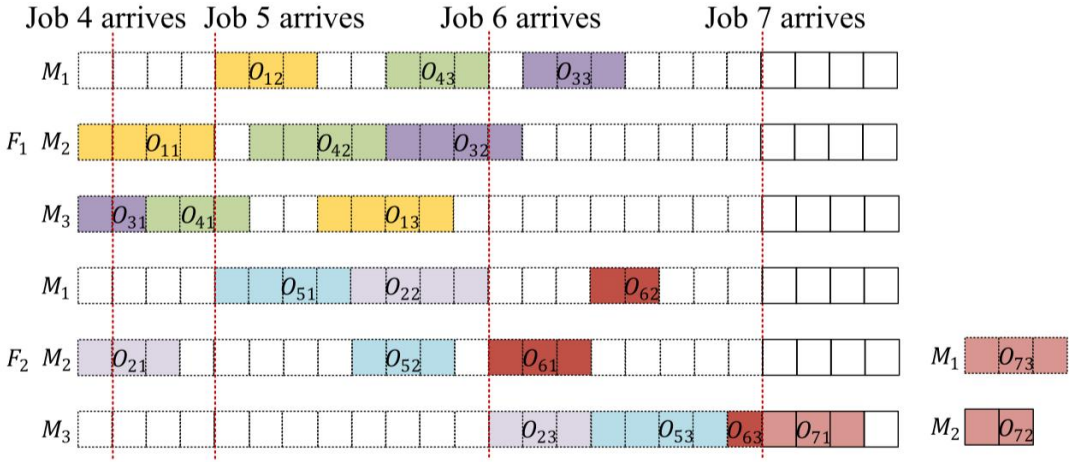

(b) Next state s_{t+1} based on the selected action

Fig. 3. Illustration of the state transition in Case 2.

TABLE I

SYMBOLS FOR CLASSIFYING THE STATE TRANSACTION

Symbol	Definition
$\mathcal{J}_{a\&u}$	Set of jobs that have arrived, but have not yet been scheduled
$\mathcal{A}_{a\&u}$	Set of the arrival times of the jobs in set $\mathcal{J}_{a\&u}$
$\mathcal{C}_s$	Set of the completion times of the operations that have been scheduled
$\mathcal{CF}_s$	Set of the completion times refers to the completion times of the first operations of each job in the scheduling scheme

Case 1: $\boldsymbol{\mathcal{J}_{a\&u} = \emptyset}$, *i.e.*, no job that has arrived has not been scheduled. In this case, if there is at least an eligible operation available in the operation action space, the agent will select a suitable operation and determine the earliest start processing time. However, if there are no eligible operations available, the agent will wait until a new job arrives.

Case 2: $\boldsymbol{\mathcal{J}_{a\&u} \neq \emptyset}$ **and** $\boldsymbol{min(\mathcal{A}_{a\&u}) \geq max(\mathcal{C}_s)}$, *i.e.*, at least one job has arrived but not been scheduled. Additionally, the earliest arrival time in set $\mathcal{A}_{a\&u}$ is not less than the maximum completion time of all the operations that have already been scheduled. An example is shown in Fig. 3(a), where $\mathcal{J}_{a\&u} = \{7\}$. The arrival time of job 7 equals the completion time of operation o_{63}.

Method Design

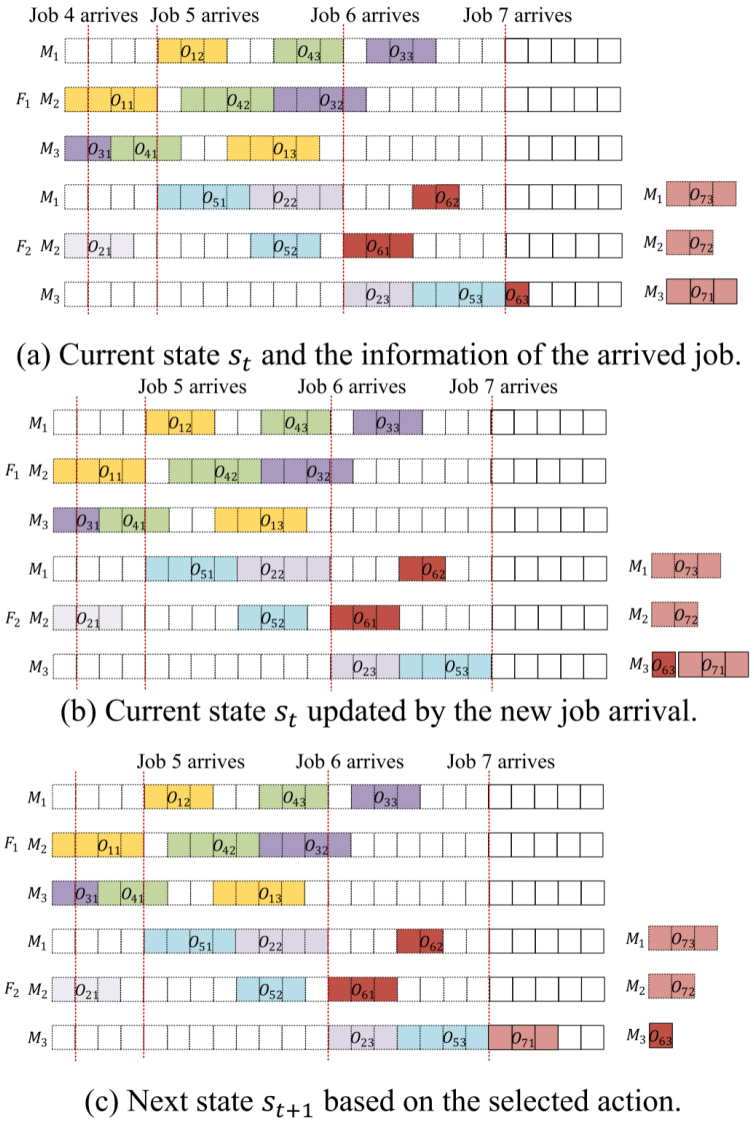

(a) Current state s_t and the information of the arrived job.

(b) Current state s_t updated by the new job arrival.

(c) Next state s_{t+1} based on the selected action.

Fig. 4. Illustration of the state transition in Case 3.

Case 3: $\mathcal{J}_{a\&u} \neq \emptyset$ **and** $\boldsymbol{min}(\mathcal{A}_{a\&u}) \geq \boldsymbol{max}(\mathcal{CF}_s)$ **and** $\boldsymbol{min}(\mathcal{A}_{a\&u}) \leq \boldsymbol{max}(\mathcal{C}_s)$, *i.e.*, at least one job has arrived but not been scheduled, the earliest arrival time in set $\mathcal{A}_{a\&u}$ is not less than the maximum completion times in set $\mathcal{CF}_s$, and it is also not greater than the maximum completion time among all operations that have already been scheduled. For instance, in Fig. 4(a), $\mathcal{J}_{a\&u} = \{7\}$, and the arrival time of job 7 is between the completion times of operation o_{53} and operation o_{63}.

Method Design

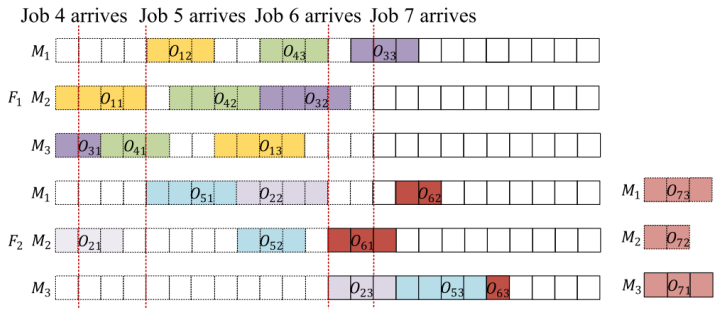

(a) Current state s_t and the information of the arrived job.

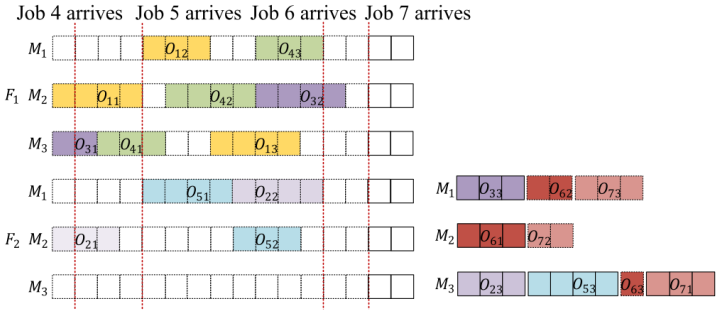

(b) Current state s_t updated by the new job arrival.

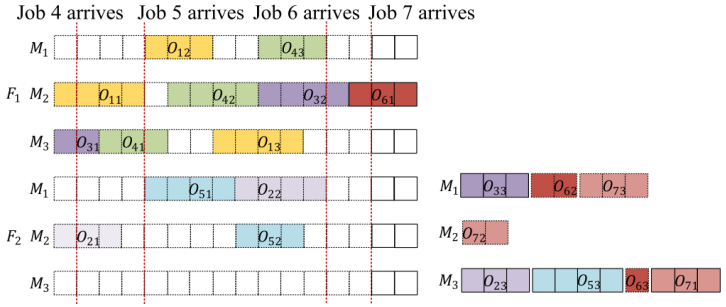

(c) Next state s_{t+1} based on the selected action

Fig. 5. Illustration of the state transition in Case 4.

Case 4: $\mathcal{J}_{a\&u} \neq \emptyset$ **and** $\boldsymbol{min}(\mathcal{A}_{a\&u}) < \boldsymbol{max}(\mathcal{CF}_s)$, *i.e.*, at least one job has arrived but not been scheduled. Additionally, the smallest arrival time in set $\mathcal{A}_{a\&u}$ is less than the maximum completion time in set $\mathcal{CF}_s$. As in Fig. 5(a), the arrival time of job 7 is less than the completion time of operation o_{61}.

Method Design

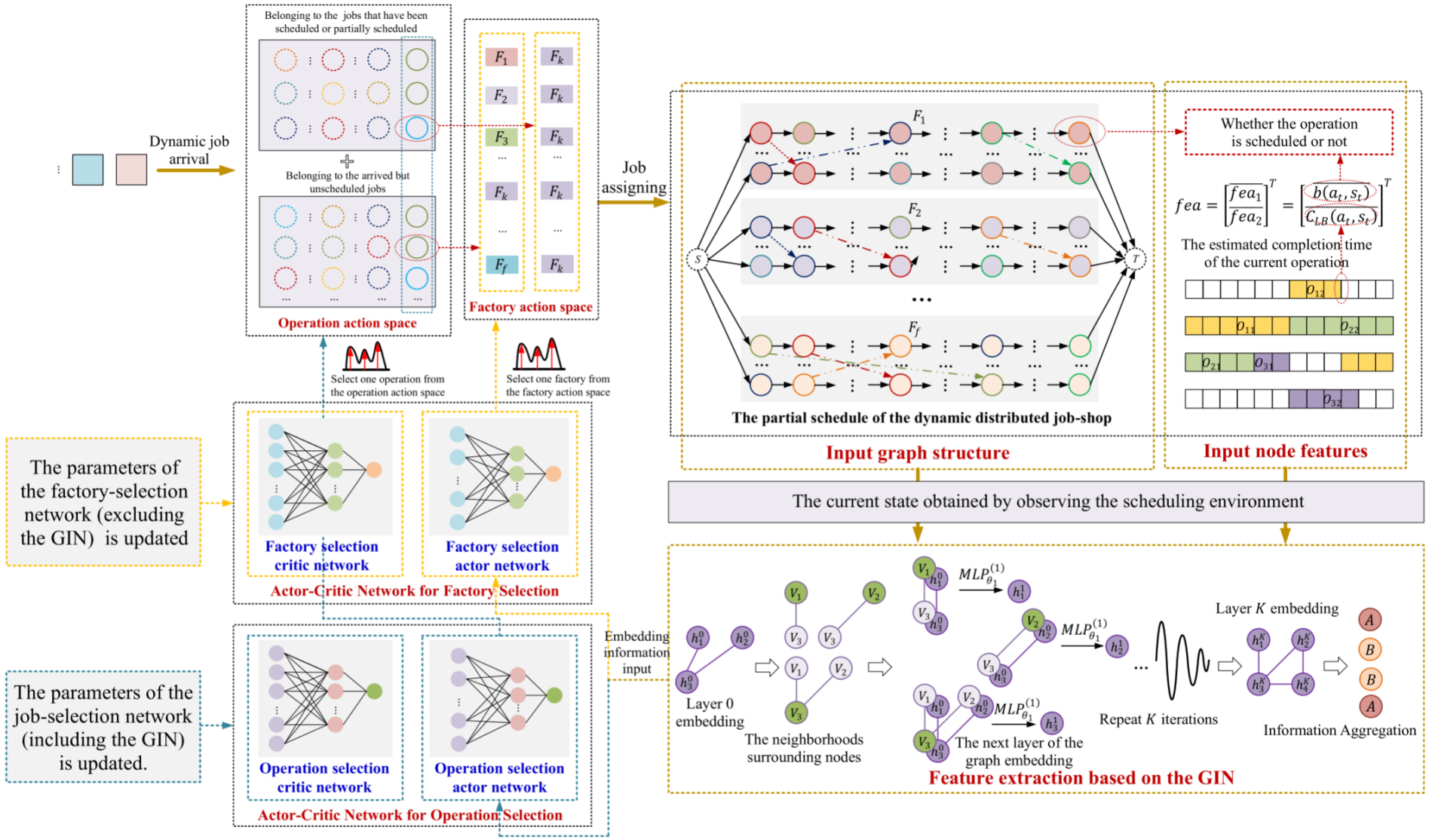

Fig. 6. The framework of GIN-based multi-action scheduling policy.

Contents

Method Design

$$RPI = \frac{Method_{sol} - Best_{sol}}{Best_{sol}} \times 100\% \qquad (10)$$

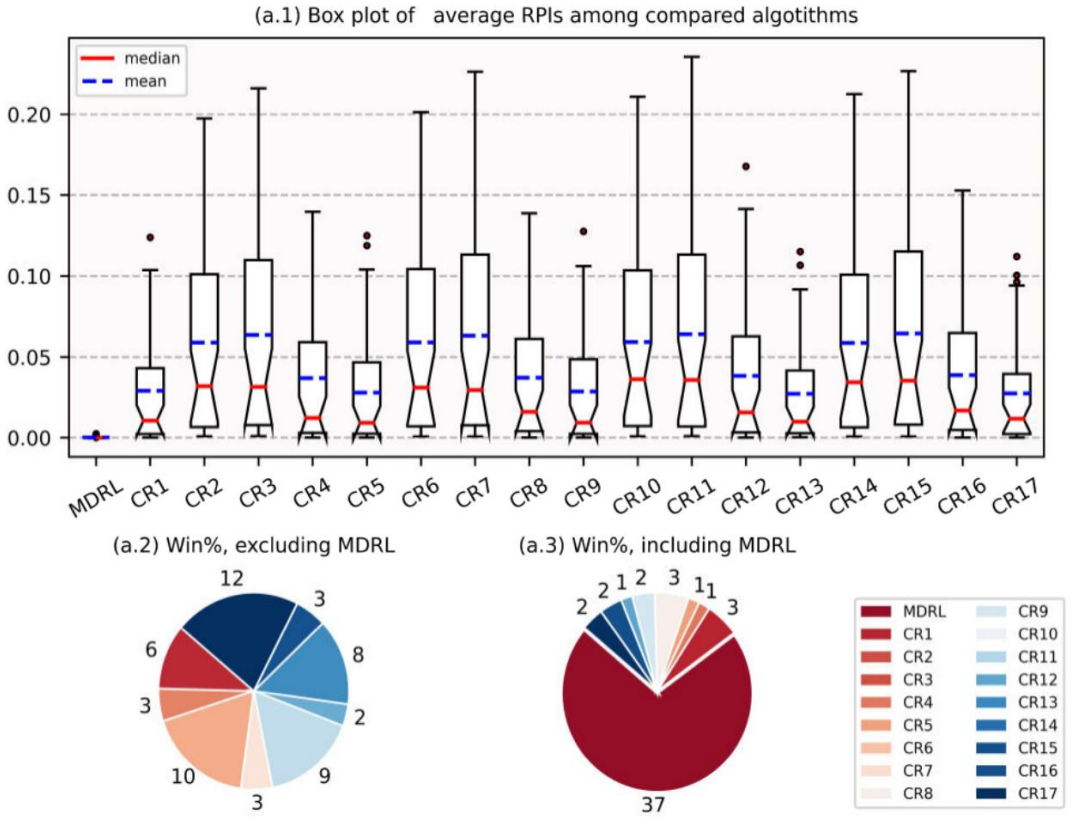

(a) $f = 2$

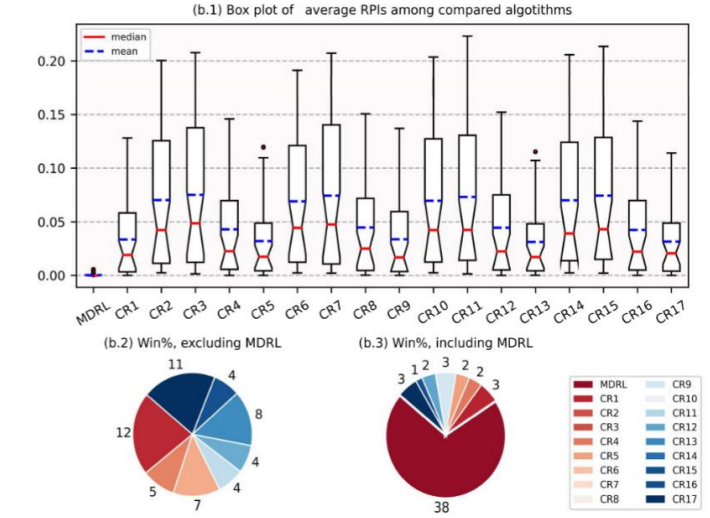

(b) $f = 3$

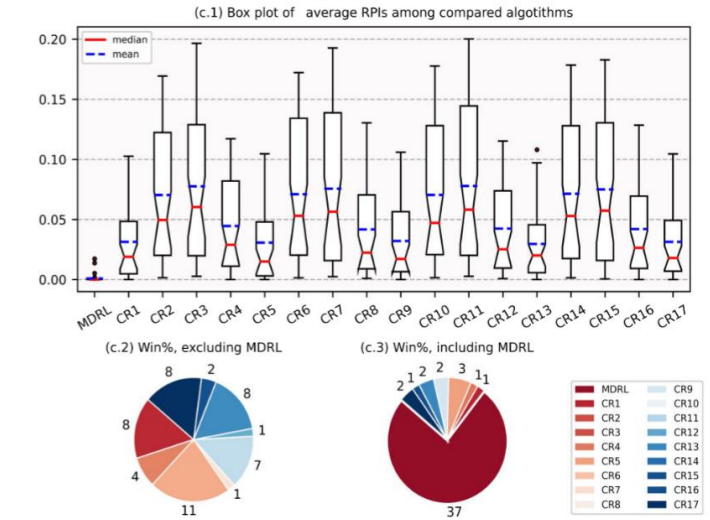

(c) $f = 4$

Fig. 7. Comparison among MDRL and PDRs.

Method Design

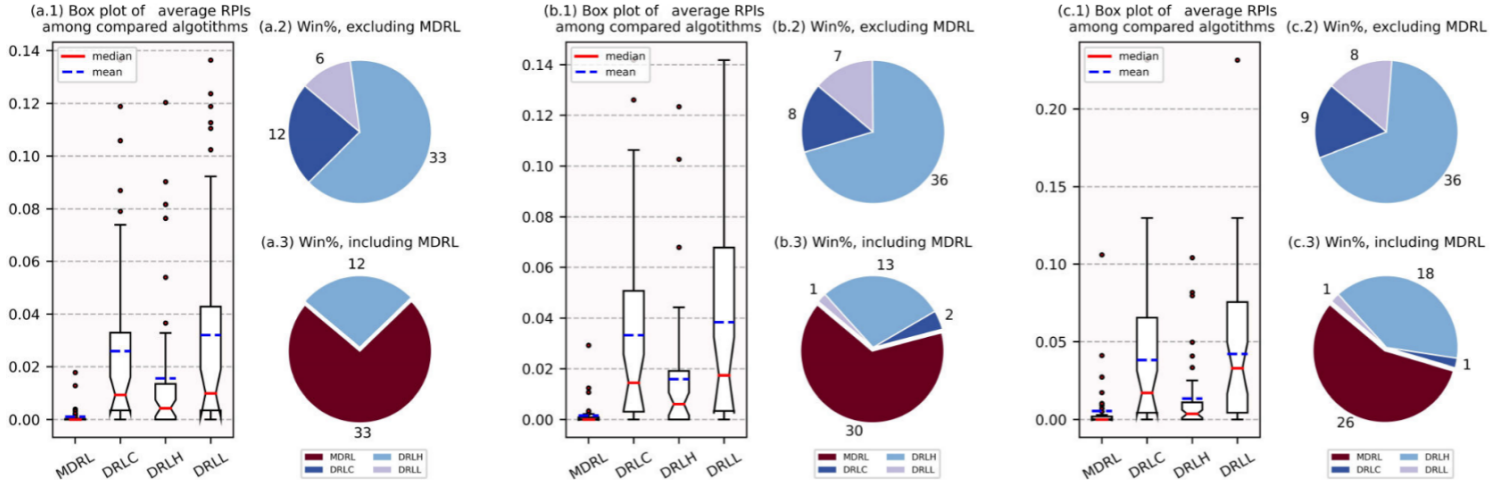

(a) $f = 2$ (b) $f = 3$ (c) $f = 4$

Fig. 8. Comparison among MDRL and DRLs.

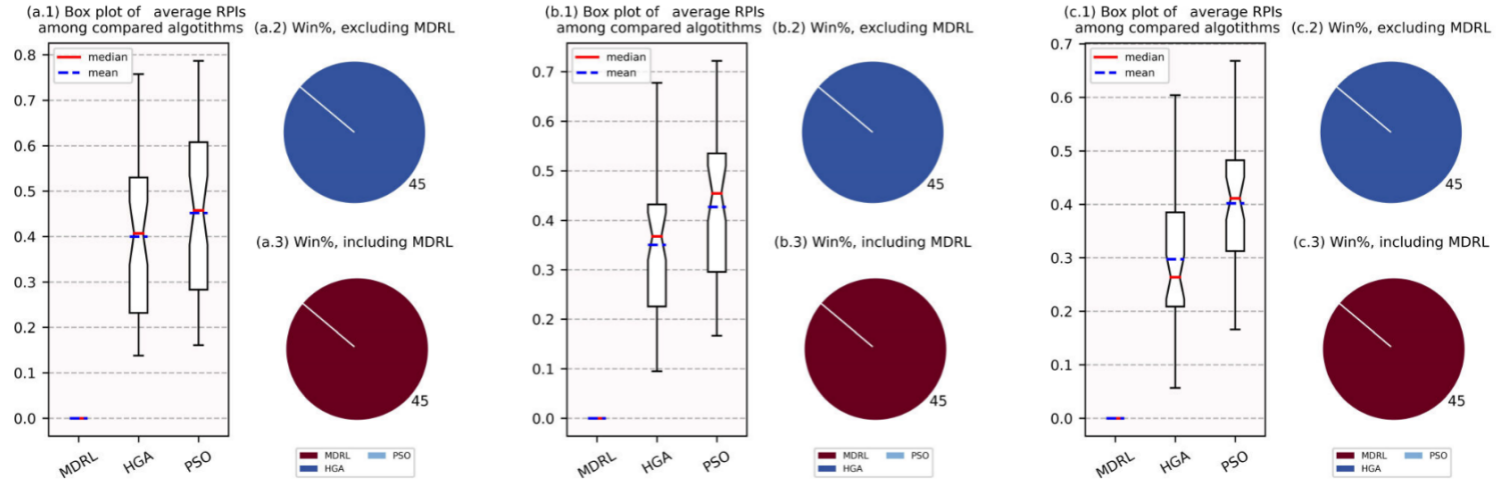

(a) $f = 2$ (b) $f = 3$ (c) $f = 4$

Fig. 9. Comparison among MDRL and metaheuristics.

Contents

Future Work

Contributions

A hierarchical multi-action DRL method has been proposed for the DJSP with job arrivals, utilizing a multi-action MDP framework, GIN-based feature extraction, and dual decision policies to effectively handle dynamic job arrivals, demonstrating superior performance over PDRs, DRL methods, and metaheuristics in extensive experiments and a real-world case study.

Future Work

Future research should incorporate transportation costs and machine breakdowns to further optimize scheduling in distributed manufacturing environments.

Paper 4

北京工業大學
BEIJING UNIVERSITY OF TECHNOLOGY

Real-Time Scheduling for Flexible Job Shop With AGVs Using Multiagent Reinforcement Learning and Efficient Action Decoding

Yuxin Li , Qingzheng Wang, Xinyu Li , Member, IEEE,Liang Gao , Senior Member, IEEE, Ling Fu, Yanbin Yu, and Wei Zhou

Publish Journal: IEEE TRANSACTIONS ON SYSTEMS, MAN, AND CYBERNETICS: SYSTEMS (2025)

Contents

Contents

Problem Description

- **Problem:** The dynamic flexible job shop scheduling problem (DFJSP) involves machine flexibility and limited logistics equipment, increasing the complexity of collaborative scheduling.
- **Challenge:** Frequent dynamic events introduce uncertainty, making it difficult to achieve efficient and reliable real-time scheduling.
- **Method:** A real-time scheduling approach based on multiagent reinforcement learning (MARL) is proposed to optimize task selection, machine allocation, and AGV assignment while enhancing robustness against disturbances.

Contents

Method Design

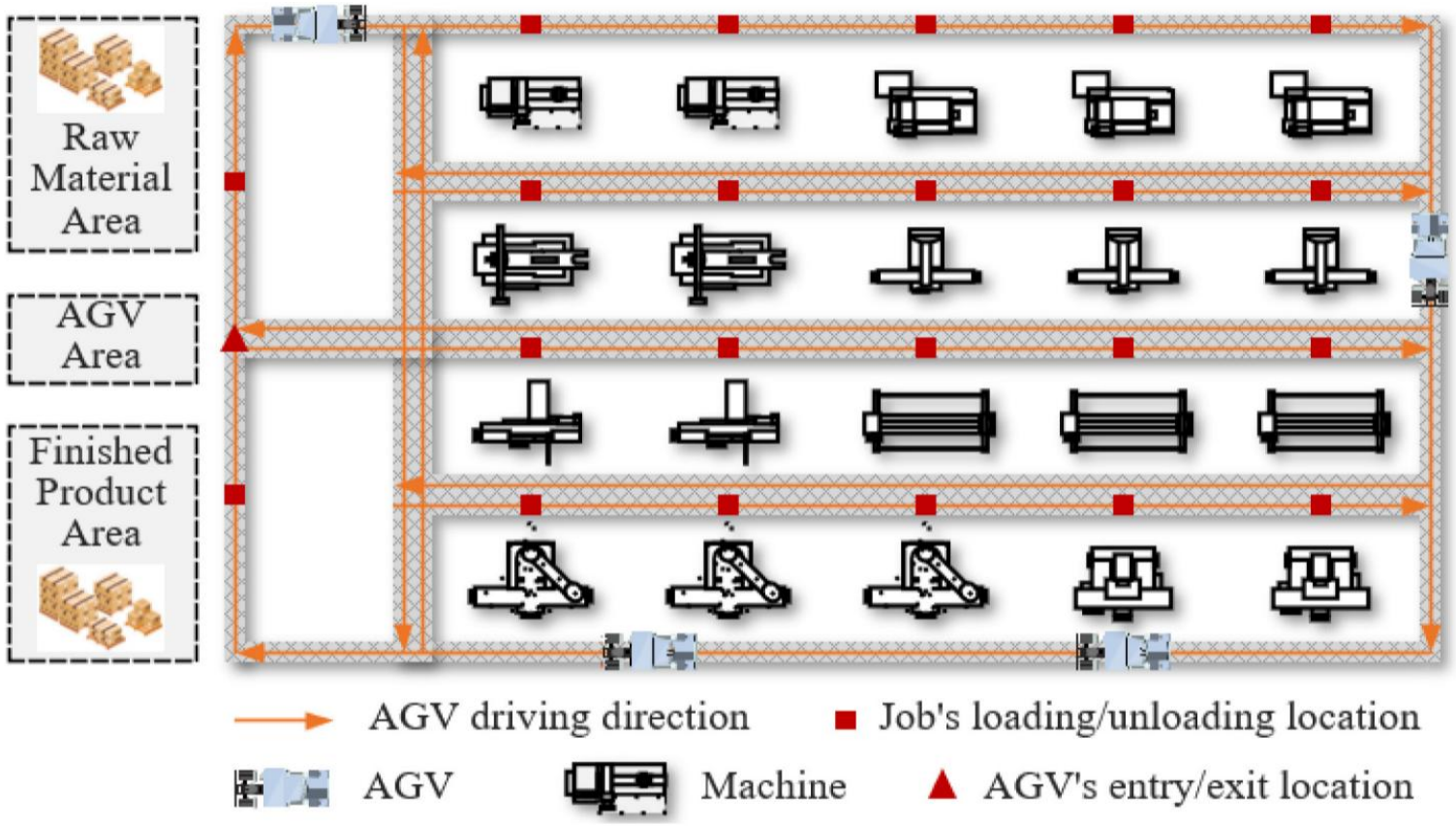

Fig. 1. Layout of flexible job shop with AGVs.

1) New Job Arrivals:

$$\min \mathrm{TTC} = \min \sum_{i=1}^{n} (w_i \cdot \max(0,\ C_i - D_i)) \tag{1}$$

$$\mathrm{MTBA} = \frac{\overline{N_{\mathrm{ope}}} \cdot \overline{T^{\mathrm{PT}}}}{U \cdot \sum_{x=1}^{m} N_x} + \frac{\left(\overline{N_{\mathrm{ope}}} + 1\right) \cdot \overline{T^{\mathrm{LT}}}}{U \cdot l} \tag{2}$$

$$D_i = A_i + \mathrm{DDT}_i \cdot \sum_{j=1}^{N_i} \left(\sum_{k=1}^{N_x} T_{ijxk}^{\mathrm{PT}} / N_x \right) + \mathrm{DDT}_i \cdot (N_i + 1) \cdot \overline{T^{\mathrm{LT}}} \tag{3}$$

2) Machine Breakdowns and Repairs:

$$A_g = \mathrm{MTTR}/(\mathrm{MTBF} + \mathrm{MTTR}). \tag{4}$$

3) Job Reworks: In actual production, the material quality, improper worker operation and other reasons will cause the job quality to be unqualified, which leads to the requirement of job rework.

4) Fuzzy Transportation Time: Due to path congestion, AGV acceleration, AGV deceleration and other reasons, the actual transportation time of AGV will fluctuate based on the predetermined time.

Method Design

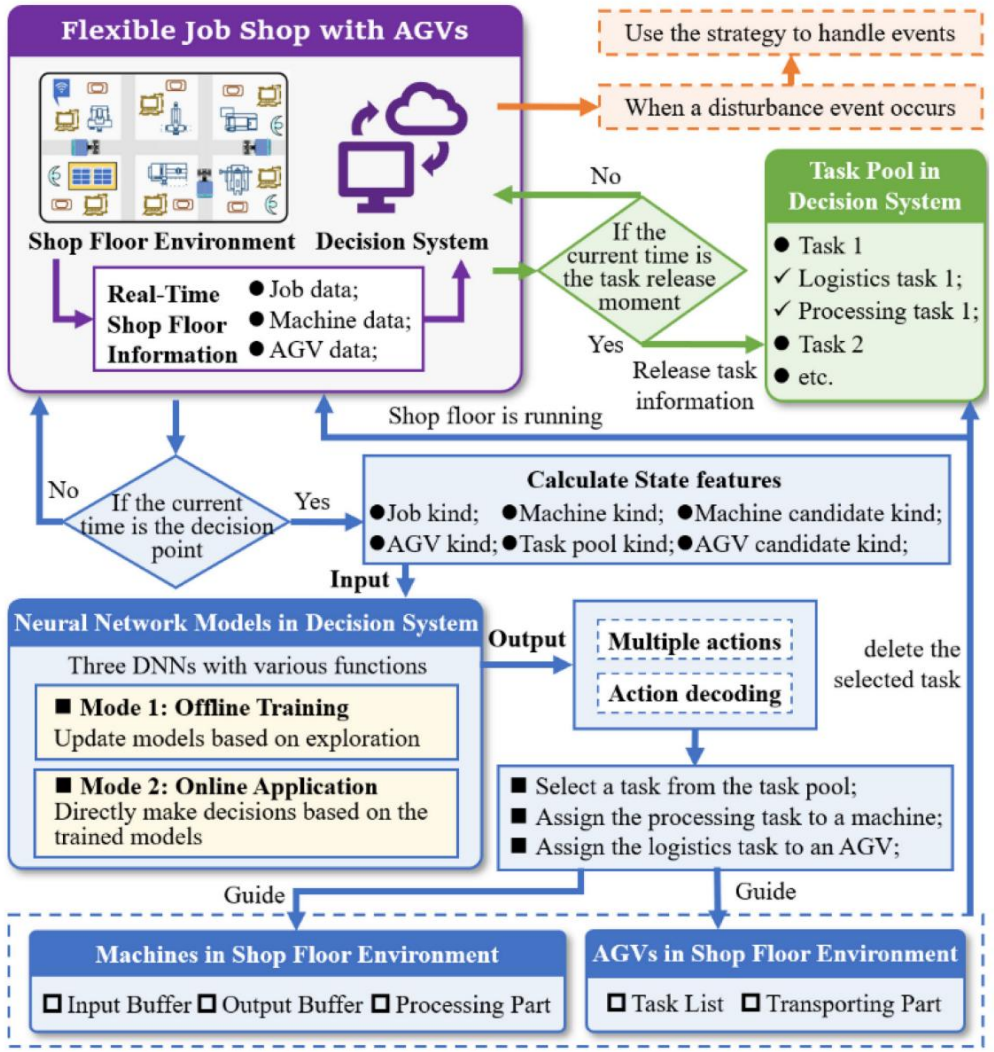

Fig. 2. Proposed real-time scheduling framework.

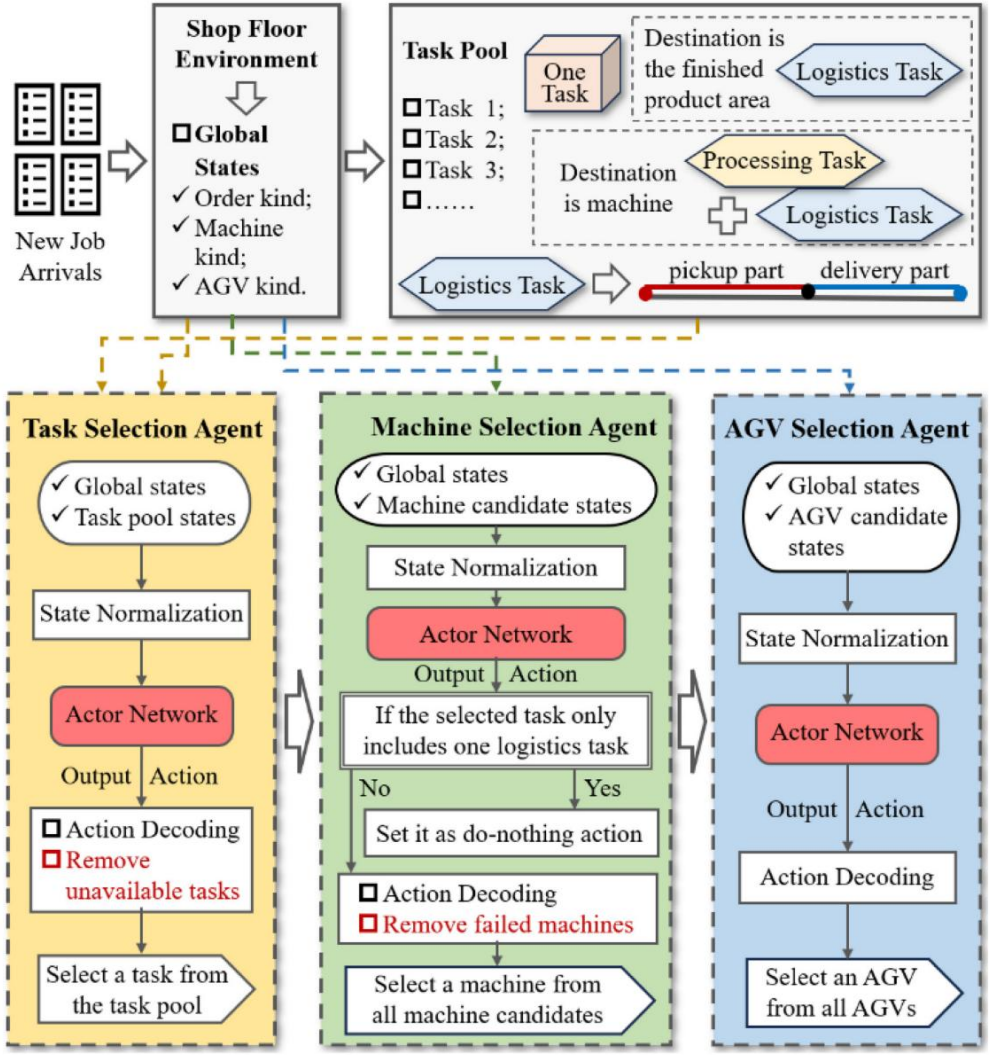

Fig. 3. Resource allocation process of agents.

Method Design

TABLE I
REAL-TIME ATTRIBUTES OF WORKSHOP

Notations	Descriptions
Variables for manufacturing system	
t	Current time
Variables for task pool	
T_g^P	The g-th task in the task pool, $g = 1, \dots, NTP$, where NTP is the number of tasks in the task pool
J_g^P	The job corresponding to task T_g^P
Jth	The sequence number of operation for task T_g^P in job J_g^P
T_{gj}^{PT}	Time of the j-th processing task for job J_g^P
FT_{gj}^{PT}	Time that the j-th processing task for job J_g^P has been finished
T_{ga}^{DLT}	Time of the delivery part of the a-th logistics task for job J_g^P
FT_{ga}^{DLT}	Time that the delivery part of the a-th logistics task for job J_g^P has been finished
RT_g^P	Remaining time of job J_g^P (consider processing and logistics)
EAT_g^P	Earliest available time of job J_g^P
EWT_g^P	Estimated weighted tardiness of job J_g^P
Variables for all machines	
$RTING_{xk}^M$	Remaining time of the in-process task for machine M_{xk}
T_{xkw}^{PT}	Time of the w-th processing task in the buffer for machine M_{xk}, $w = 1, \dots, N_{xk}$, where N_{xk} is the number of processing tasks in the machine's buffer
CT_{xk}^M	Shortest time for completing the in-process task and all tasks in the buffer for machine M_{xk}
DPT_{gxk}	The sum of delivery time and processing time of task T_g^P for machine M_{xk}
Variables for all AGVs	
$RTING_y^A$	Remaining time of the in-transport task for AGV V_y
T_{ye}^{LT}	Time of the e-th logistics task in the list for AGV V_y, $e = 1, \dots, N_y$, where N_y is the number of logistics tasks in the AGV's list
CT_y^A	Shortest time for completing the in-transport task and all tasks in the list for AGV V_y
PUT_{yg}	Pickup time of AGV V_y for task T_g^P

TABLE II
SIX KINDS OF STATE FEATURES

State	Content
State features for all jobs	
SF_1	the completion rate of the order; the mean/std of completion rates for all jobs.
State features for all machines	
SF_2	the mean/std of utilization rates for all machines; the mean/std of CT_{xk}^M for all machines; the proportion of faulty machines among all machines.
State features for all AGVs	
SF_3	the mean/std of utilization rates for all AGVs; the mean/std of CT_y^A for all AGVs.
State features for task pool	
SF_4	the number of tasks; the mean/std of processing times for all tasks; the mean/std of completion rates for all jobs; the mean/std of RT_g^P for all jobs; the mean/std/min/max of EAT_g^P for all jobs; the mean/std/min/max of EWT_g^P for all jobs.
State features for all machine candidates of the selected job	
SF_5	the mean/std of utilization rates; the mean/std of CT_{xk}^M; the mean of DPT_{gxk}; the proportion of faulty machines among all machine candidates; the EAT_g^P of the selected job; the EWT_g^P of the selected job.
State features for all AGV candidates of the selected job	
SF_6	the $CT_y^A + PUT_{yg}$ of each AGV for the selected job; the EAT_g^P of the selected job; the EWT_g^P of the selected job; the CT_{xk}^M of the assigned machine.

Method Design

Action Space

$$a^{\mathrm{TS}}(t) = [w_{\mathrm{BEWT}},\ w_{\mathrm{LWKR}},\ w_{\mathrm{CR}},\ w_{\mathrm{EDD}},\ w_{S/RT}]. \quad (12)$$

$$a^{\mathrm{MS}}(t) = [w_{\mathrm{SURM}},\ w_{\mathrm{SDPT}},\ w_{\mathrm{SCTM}}]. \quad (13)$$

$$a^{\mathrm{AS}}(t) = [w_{\mathrm{SPUT}},\ w_{\mathrm{SCTA}},\ w_{\mathrm{SCPT}}]. \quad (14)$$

1) Define PDR $\rho \in \mathcal{P}$, where the PDR set $\mathcal{P} = \{\mathrm{BEWT},\ \mathrm{LWKR},\ CR,\ \mathrm{EDD},\ S/RT\}$.
2) Calculate the priority vector of PDR ρ: $\mathrm{PV}_\rho \in \mathbb{R}^{1\times \mathrm{NTP}}$. First, define the production attribute vector of PDR ρ as $[\mathrm{SV}_{\rho,g},\ g = 1,\ \ldots,\ \mathrm{NTP}]$. For example, the $\mathrm{SV}_{\rho,g}$ of BEWT or LWKR is EWT_g^P or $-\mathrm{RT}_g^P$. Then, PV_ρ using Min-Max normalization is as follows:

$$\mathrm{PV}_\rho = \left[\frac{\mathrm{SV}_{\rho,g} - \mathrm{SV}_\rho^{\min}}{\mathrm{SV}_\rho^{\max} - \mathrm{SV}_\rho^{\min}},\ g = 1,\ \ldots,\ \mathrm{NTP}\right]. \quad (15)$$

3) Calculate $\mathrm{Sigmoid}(a^{\mathrm{TS}}(t)) \in \mathbb{R}^{1\times 5}$ based on $a^{\mathrm{TS}}(t)$

$$\mathrm{Sigmoid}\left(a^{\mathrm{TS}}(t)\right) = \left[\frac{1}{1+e^{-w_\rho}},\ w_\rho \in a^{\mathrm{TS}}(t)\right]. \quad (16)$$

Algorithm 1 Action Decoding

Task selection agent receives S_{TS}, and output $a^{JS}(t)$
Calculate $PDR_{TS} = [PV_{BEWT},\ PV_{LWKR}, PV_{CR},\ PV_{EDD},\ PV_{S/RT}]$
Calculate $PV_{TS} = Norm\left(Sigmoid\left(a^{TS}(t)\right) \cdot PDR_{TS}\right) + w^{TS} \cdot PV_{SEAT}$
Consider machine breakdown and remove unavailable tasks
Select the task with highest priority from the task pool
Machine selection agent receives S_{MS}, and output $a^{MS}(t)$
if the selected task $T_g^P \in T_1^{Pool}$ **then**
    Calculate $PDR_{MS} = [PV_{SURM},\ PV_{SDPT},\ PV_{SCTM}]$
    Calculate $PV_{MS} = Norm\left(a^{MS}(t) \cdot PDR_{MS}\right) + w^{MS} \cdot PV_{SCTM}$
    Remove failed machines
    select the machine with highest priority from all machine candidates
else
    Set $a^{MS}(t) = \delta_0$ ($\delta_0 = [0,\ 0,\ 0]$), and represents the do-nothing action
AGV selection agent receives S_{AS} and output $a^{AS}(t)$
Calculate $PDR_{AS} = [PV_{SPUT},\ PV_{SCTA},\ PV_{SCPT}]$
Calculate $PV_{AS} = Norm\left(a^{AS}(t) \cdot PDR_{AS}\right) + w^{AS} \cdot PV_{SCTA}$
Select the AGV with highest priority from all AGV candidates

Method Design

4) Define $X = [x_g,\ g = 1,\ \ldots,\ NTP] = \text{Sigmoid}(a^{\text{TS}}(t)) \cdot \text{PDR}_{\text{TS}}$. Its matrix shape is $\mathbb{R}^{1\times 5} \cdot \mathbb{R}^{5\times NTP} = \mathbb{R}^{1\times NTP}$

$$x_g = \sum_{p\in\mathcal{P}} \left(\frac{1}{1+e^{-w_p}} \cdot \frac{\text{SV}_{p,g} - \text{SV}_p^{\min}}{\text{SV}_p^{\max} - \text{SV}_p^{\min}} \right). \tag{17}$$

5) Based on Min-Max normalization, the half of PV_{TS}, i.e., $Y = \text{Norm}(\text{Sigmoid}(a^{\text{TS}}(t)) \cdot \text{PDR}_{\text{TS}}) = \text{Norm}(X) \in \mathbb{R}^{1\times NTP}$, is as follows:

$$Y = \left[\frac{x_g - x_g^{\min}}{x_g^{\max} - x_g^{\min}},\ g = 1,\ \ldots,\ NTP \right]. \tag{18}$$

6) Another half of PV_{TS} is $Z = w^{\text{TS}} \cdot \text{PV}_{\text{SEAT}} \in \mathbb{R}^{1\times NTP}$. w^{TS} is the adjustment weight. Rule SEAT represents that the task with smallest EAT_g^P is selected first, and the $\text{SV}_{p,g}$ of SEAT is EAT_g^P. So Z is as follows:

$$Z = \left[w^{\text{TS}} \cdot \frac{\text{SV}_{p,g} - \text{SV}_p^{\min}}{\text{SV}_p^{\max} - \text{SV}_p^{\min}},\ g = 1, \ldots, NTP,\ p = \text{SEAT} \right]. \tag{19}$$

7) Finally, the decision basis PV_{TS} of task selection agent is equal to $Y+Z$, and its shape is $\mathbb{R}^{1\times NTP}$. Each element P_g in PV_{TS} is expressed by (20), and it represents the priority of task T_g^P in task pool

$$P_g = \frac{x_g - x_g^{\min}}{x_g^{\max} - x_g^{\min}} + w^{\text{TS}} \cdot \frac{\text{SV}_{p,g} - \text{SV}_p^{\min}}{\text{SV}_p^{\max} - \text{SV}_p^{\min}}. \tag{20}$$

Algorithm 1 Action Decoding

Task selection agent receives S_{TS}, and output $a^{JS}(t)$
Calculate $PDR_{TS} = [PV_{BEWT},\ PV_{LWKR}, PV_{CR},\ PV_{EDD}, PV_{S/RT}]$
Calculate $PV_{TS} = Norm\big(Sigmoid\big(a^{TS}(t)\big) \cdot PDR_{TS}\big) + w^{TS} \cdot PV_{SEAT}$
Consider machine breakdown and remove unavailable tasks
Select the task with highest priority from the task pool
Machine selection agent receives S_{MS}, and output $a^{MS}(t)$
if the selected task $T_g^P \in T_1^{Pool}$ **then**
    Calculate $PDR_{MS} = [PV_{SURM},\ PV_{SDPT},\ PV_{SCTM}]$
    Calculate $PV_{MS} = Norm\big(a^{MS}(t) \cdot PDR_{MS}\big) + w^{MS} \cdot PV_{SCTM}$
    Remove failed machines
    select the machine with highest priority from all machine candidates
else
    Set $a^{MS}(t) = \delta_0$ ($\delta_0 = [0,\ 0,\ 0]$), and represents the do-nothing action
AGV selection agent receives S_{AS} and output $a^{AS}(t)$
Calculate $PDR_{AS} = [PV_{SPUT},\ PV_{SCTA},\ PV_{SCPT}]$
Calculate $PV_{AS} = Norm\big(a^{AS}(t) \cdot PDR_{AS}\big) + w^{AS} \cdot PV_{SCTA}$
Select the AGV with highest priority from all AGV candidates

Method Design

Reward

Algorithm 2 Reward Calculation

for job $i = 1$ **to** n **do**
  if job J_i has been finished **then**
    Calculate $EWT_i = \max(0,\ C_i - D_i) \cdot w_i$
  else
    Calculate $EWT_i = \max(0,\ t + RT_i - D_i) \cdot w_i$
  end if
next for
Calculate $r_t = \sum_{i=1}^{n} EWT_i(t) - \sum_{i=1}^{n} EWT_i(t+1)$
Calculate $r_t = r_t - \alpha \cdot \left(\sum_{x=1}^{m} \sum_{k=1}^{N_x} ITM_{xk}\right) / \sum_{x=1}^{m} N_x$

Method Design

Algorithm 3 MAPPO-Based Training Algorithm

Initialize the actor networks of three agents $\pi_{TS}(\theta_{TS})$, $\pi_{MS}(\theta_{MS})$, $\pi_{AS}(\theta_{AS})$; the critic networks of three agents $v_{TS}(\phi_{TS})$, $v_{MS}(\phi_{MS})$, $v_{AS}(\phi_{AS})$; three memory buffers MB_{TS}, MB_{MS}, MB_{AS}
Initialize all hyperparameters of MAPPO, memory number $MN = 0$
for *episode* $= 1: L$ **do**
  Initialize the shop floor environment using problem *PROB*
  while all jobs have not returned to the finished product area **do**
    Implement Algorithm 1, and assign resources to the selected task
    Execute three actions, and machines and AGVs keep running
    Update task pool in action execution process
    Observe the new state $\{SF_1,\ SF_2,\ SF_3,\ SF_4\}_{t+1}$
    Calculate the reward r_t based on Algorithm 2
    if the current state is the terminal state **then**
      Capture the observations $\{SF_5,\ SF_6\}_{t+1}$
    end if
    Put $\{S_{TS}(t),\ a^{TS}(t),\ r_t,\ S_{TS}(t+1)\}$ into MB_{TS}
    Put $\{S_{MS}(t),\ a^{MS}(t),\ r_t,\ S_{MS}(t+1)\}$ into MB_{MS}
    Put $\{S_{AS}(t),\ a^{AS}(t),\ r_t,\ S_{AS}(t+1)\}$ into MB_{AS}
    Update the memory number $MN = MN + 1$
    if one disturbance event occurs **then**
      Execute the corresponding strategy to handle it
    end if
  end while
  Form trajectory τ using the transitions of current episode
  Compute advantage estimate $\widehat{A}$ via GAE using PopArt
  Compute reward-to-go $\widehat{R}$ on τ and normalize with PopArt
  if $MN \geq$ memory update capacity MUC **then**
    Adam update $\{\pi_{TS}(\theta_{TS}),\ \pi_{MS}(\theta_{MS}),\ \pi_{AS}(\theta_{AS})\}$ with (21)
    Adam update $\{v_{TS}(\phi_{TS}),\ v_{MS}(\phi_{MS}),\ v_{AS}(\phi_{AS})\}$ with (23)
    Regenerate a new training problem *PROB*
    Clear memory buffers $\{MB_{TS}, MB_{MS}, MB_{AS}\}$ and set $MN = 0$
  end if
next for

Method Design

Strategy for Handling Disturbance Events

1) New Job Arrivals: When a new job arrives at the workshop, the decision system puts its first task into the task pool, so that the agents can assign machine and AGV to it.

2) Machine Breakdowns: When a machine fails, determine the corresponding disrupted tasks and put them into the task pool. These tasks include: 1) tasks being processed by the faulty machine; 2) tasks in the input buffer of the faulty machine; and 3) tasks of the above jobs that are assigned in advance. The agents will reallocate the disrupted tasks based on the workshop state and job urgency degree, which prevents these jobs from having a large tardiness due to machine failure.

When the machine has finished repairing, determine the corresponding disrupted tasks and put them into the task pool. These tasks include: 1) tasks in the input buffers of same-kind machines; 2) tasks of the above jobs that are assigned in advance; (note that exclude tasks that are being delivered). The agents will reallocate the disrupted tasks based on the workshop state and job urgency degree, which can prevent the repaired machine from being idle for a long time.

3) Job Rework: When a job rework event occurs, put the task corresponding to the rework operation into the task pool, and the agents can reassign machine and AGV to it.

4) Fuzzy Transportation Time: The DRL-based agents can learn to allocate manufacturing resources reasonably under ızzy transportation time through the relevant training.

Contents

Experiment Results

Performance Comparison Index

$$\mathrm{SP}_Y^X = (\mathrm{TTC}_Y - \mathrm{TTC}_X)/\mathrm{TTC}_X \cdot 100\% \qquad (26)$$

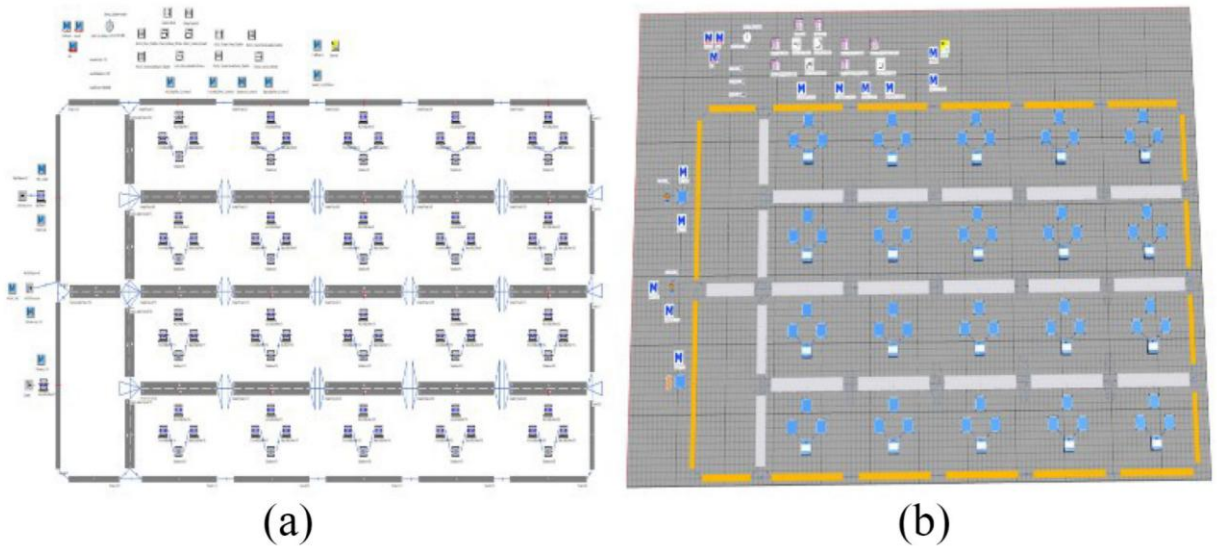

Fig. 4. Plant simulation model. (a) 2-D model. (b) 3-D model.

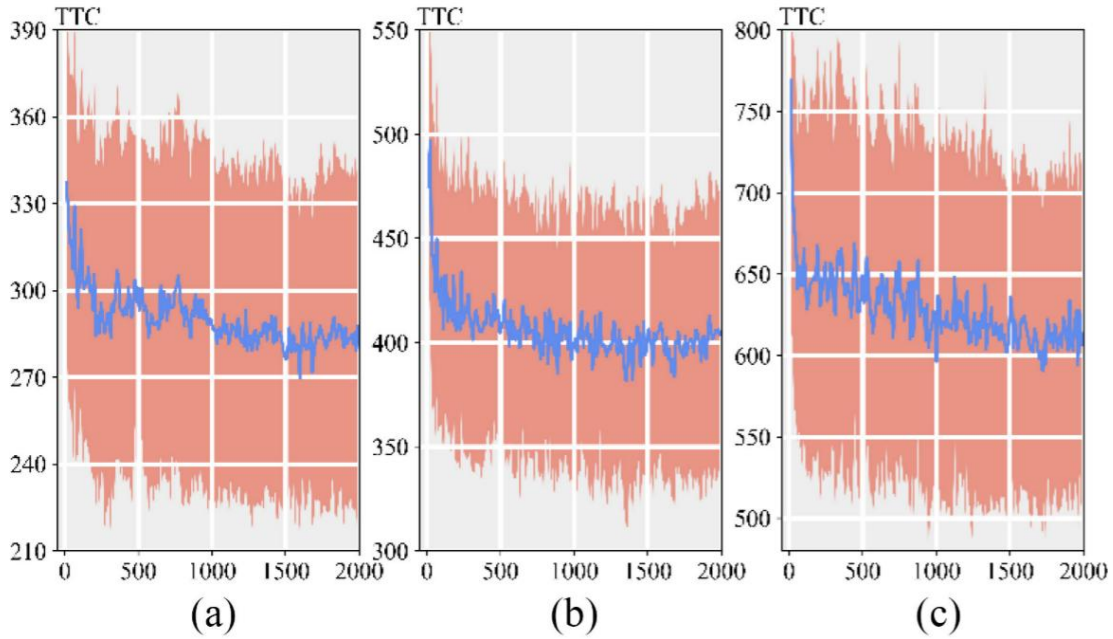

Fig. 5. Evaluation results under different problem settings. (a) Problem setting 1. (b) Problem setting 2. (c) Problem setting 3.

Experiment Results

TABLE III
ABLATION OF FOUR STRATEGIES IN ACTION DECODING

MAPPO Model	Sigmoid	TS adjustment	MS adjustment	AS adjustment
1	-0.4/7.5	1125.4/593.1	63.6/35.5	8468.6/5485.6
2	3.2/5.2	1164.3/589.8	51.2/36.8	7076/4353.8
3	4.5/9.9	1173.2/619.8	39.1/23.8	6067.6/3392.7
4	2.7/8.5	1245.9/686.6	30.1/15.6	6617.2/6130.3
5	3.8/9.4	1236.9/675.9	32.7/24.4	7362.8/5591.9
6	0.2/6.5	1256.4/660.9	31.4/22.4	9361.1/4663.3
7	4.5/10.6	1262.2/728.2	27.6/25.4	8379.5/5697.5
8	0.9/6.2	1338.1/728.9	23.7/14.8	7215.2/5819.3
9	1.6/6.8	1382.4/776.6	23.6/15.7	8949.3/6736.3
10	2.5/7.7	1498.7/714	14.9/12.3	7503.7/5408.3

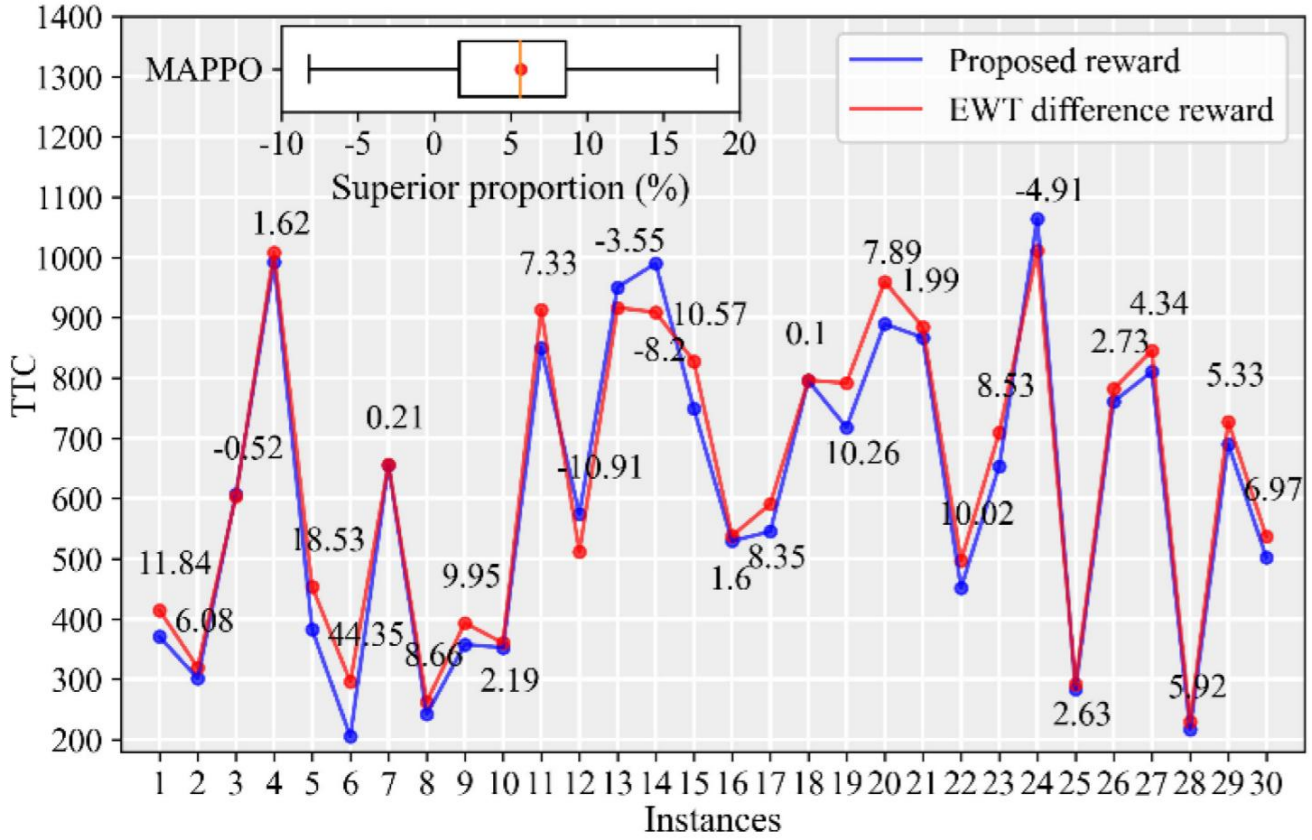

Fig. 6. Ablation of machine idle time in reward function.

Experiment Results

TABLE IV
COMPARISON WITH COMPOSITE PDRS CONSIDERING NEW JOB ARRIVALS

J_{new}	DDT	U	R_1	R_2	R_3	R_4	R_5	R_6	R_7	R_8	R_9	R_{10}
100	1.5	0.9	37	59	40	33	55	33	58	39	49	79
		0.95	15	28	25	16	29	17	27	26	30	55
	2	0.9	38	57	44	25	41	23	41	34	46	71
		0.95	31	58	47	19	45	25	48	34	41	61
150	1.5	0.9	36	63	46	29	51	27	66	40	52	83
		0.95	23	43	26	21	33	19	32	24	35	56
	2	0.9	50	96	78	43	74	41	76	59	68	118
		0.95	46	77	70	32	66	30	62	72	55	113
200	1.5	0.9	45	71	43	30	64	34	70	52	57	103
		0.95	33	50	39	29	48	29	50	39	46	69
	2	0.9	19	46	38	20	46	17	46	36	34	72
		0.95	32	63	40	28	55	25	49	38	49	79

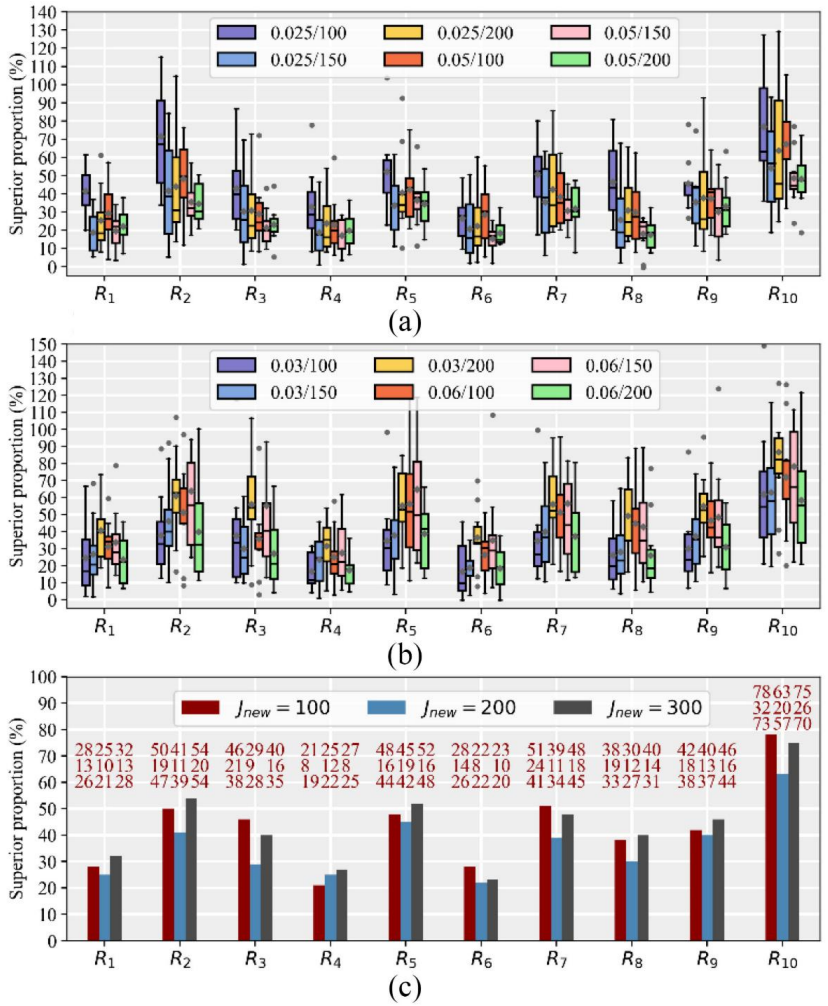

Fig. 7. Comparison with composite PDRs under various disturbance. (a) Robustness comparison under new job arrivals and machine breakdowns. (b) Robustness comparison under new job arrivals and job reworks. (c) Robustness comparison under new job arrivals and fuzzy transportation time.

Experiment Results

TABLE V
COMPARISON WITH GP AND DRL CONSIDERING NEW JOB ARRIVALS

J_{new}	DDT_H	U	GR_1	GR_2	GR_3	GR_4	Luo	Park	Li	Lei
100	1.5	0.9	21	28	21	24	41	6	18	-4
		0.95	12	9	10	15	19	7	14	4
	2	0.9	22	27	25	23	42	18	19	9
		0.95	20	26	20	19	27	14	14	3
150	1.5	0.9	26	27	21	21	39	14	19	4
		0.95	18	16	13	11	26	6	12	8
	2	0.9	36	48	36	39	66	20	34	6
		0.95	28	28	21	34	50	11	29	8
200	1.5	0.9	28	29	29	27	47	11	23	3
		0.95	23	21	18	20	33	14	25	4
	2	0.9	17	20	14	17	31	8	15	0
		0.95	22	33	20	16	28	13	23	0

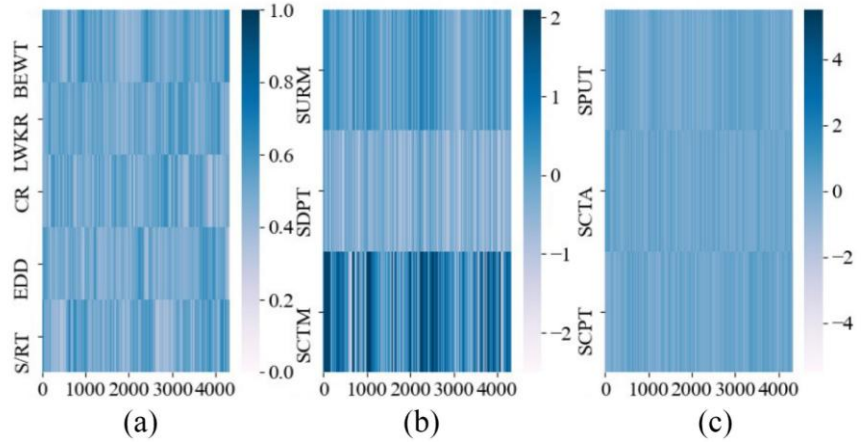

Fig. 9. Heatmap of actions on three instances. (a) Task selection agent. (b) Machine selection agent. (c) AGV selection agent.

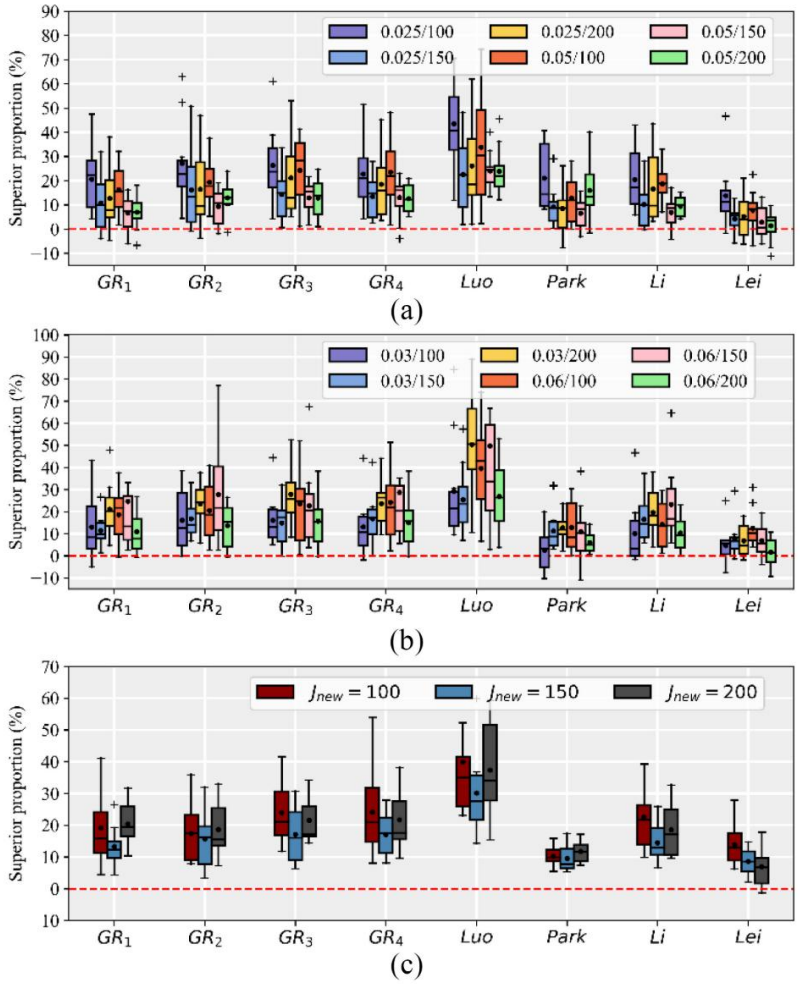

Fig. 8. Comparison with GP and DRL under various disturbance events. (a) Robustness comparison under new job arrivals and machine breakdowns. (b) Robustness comparison under new job arrivals and job reworks. (c) Robustness comparison under new job arrivals and fuzzy transportation time.

Contents

Future Work

Contributions

This paper proposes a real-time scheduling method for DFJSP AGVs based on MARL, which optimizes action decoding through PDR weights and adjustment mechanisms, improves learning efficiency, and designs a generalized state space, improved reward function, and disturbance handling strategy to enhance performance and robustness. The experimental results show that this method is superior to composite PDRs, GP, and four DRL methods, and can achieve efficient and stable workshop scheduling under various disturbance conditions.

Future Work

Further research can combine domain knowledge to optimize action decoding, introduce advanced deep learning models, and improve the reward function based on inverse reinforcement learning to enhance the stability and optimality of the algorithm.

Paper 5

北京工業大學
BEIJING UNIVERSITY OF TECHNOLOGY

A deep multi-agent reinforcement learning approach to solve dynamic job shop scheduling problem

Renke Liu, Rajesh Piplani, Carlos Toro

Publish Journal: Computers and Operations Research (2023)

Contents

Contents

Problem Description

- **Background:** The manufacturing industry is undergoing a data-driven transformation, necessitating real-time production scheduling techniques to manage the increasing complexity and volatility of modern shop floors.

- **Challenge:** Existing dynamic scheduling methods struggle with invariable problem sizes and non-stationary environments, limiting their effectiveness in real-world applications.

- **Method:** A deep multi-agent reinforcement learning-based approach with double deep Q-networks, centralized training with decentralized execution, and enhanced state-action representations is proposed to achieve efficient and scalable dynamic job shop scheduling.

Problem Description

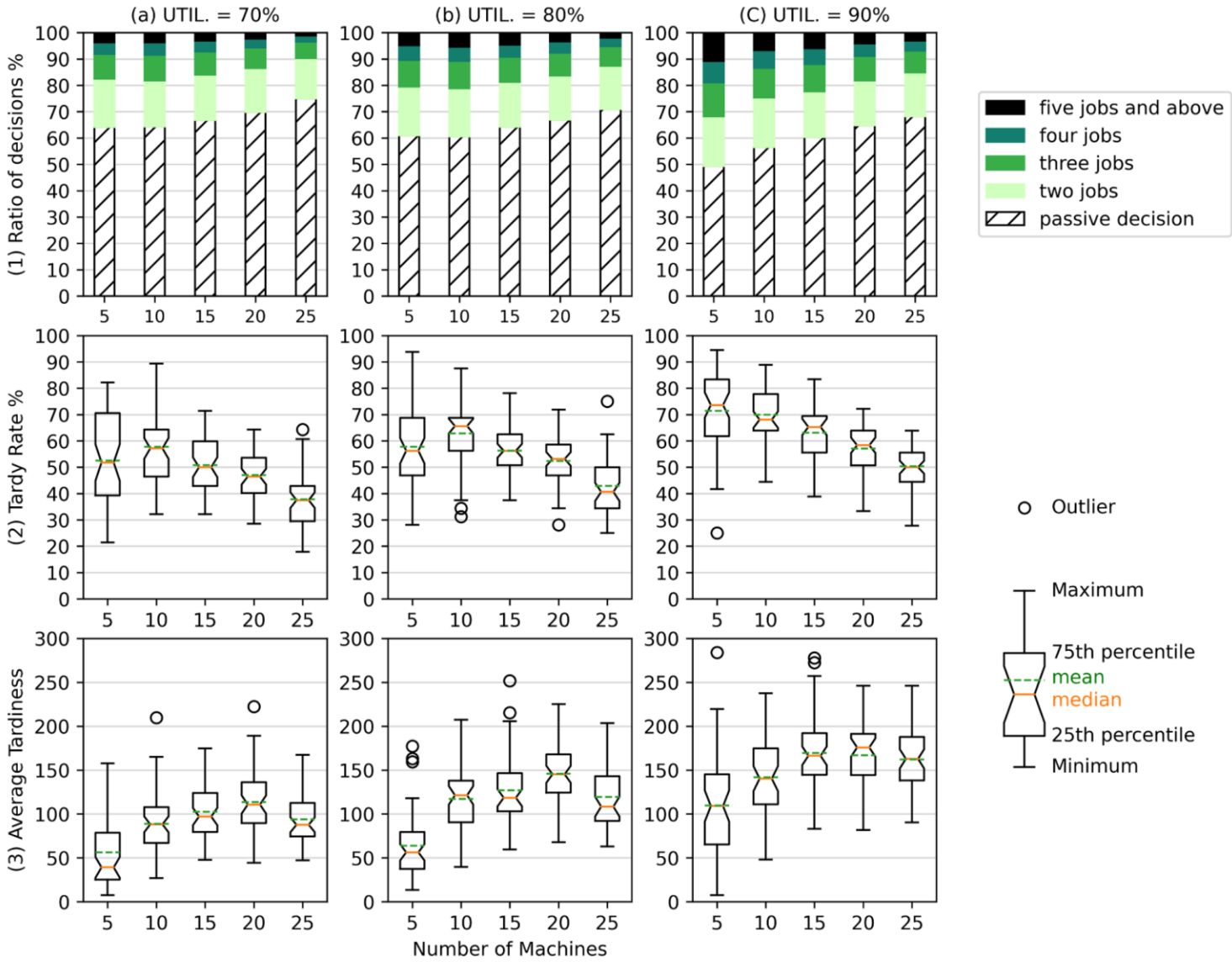

Fig. 1. Patterns of production under three levels of utilization rate.

Contents

Method Design

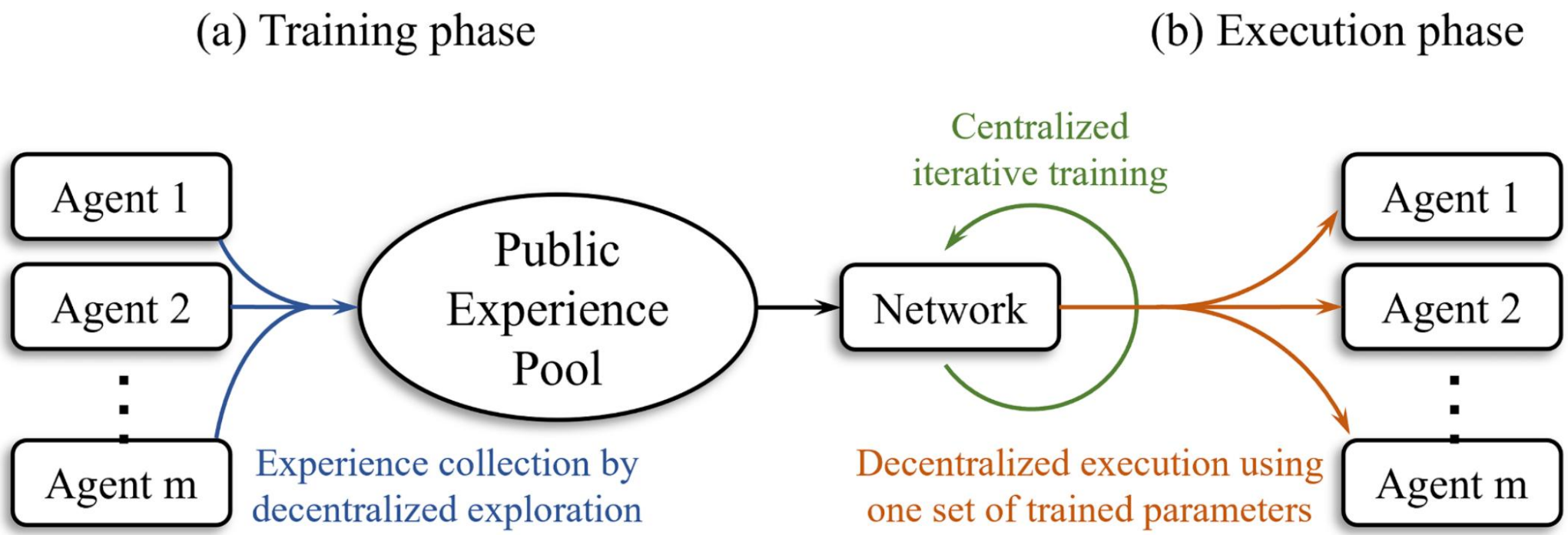

Fig. 2. Centralized training and decentralized execution scheme.

Method Design

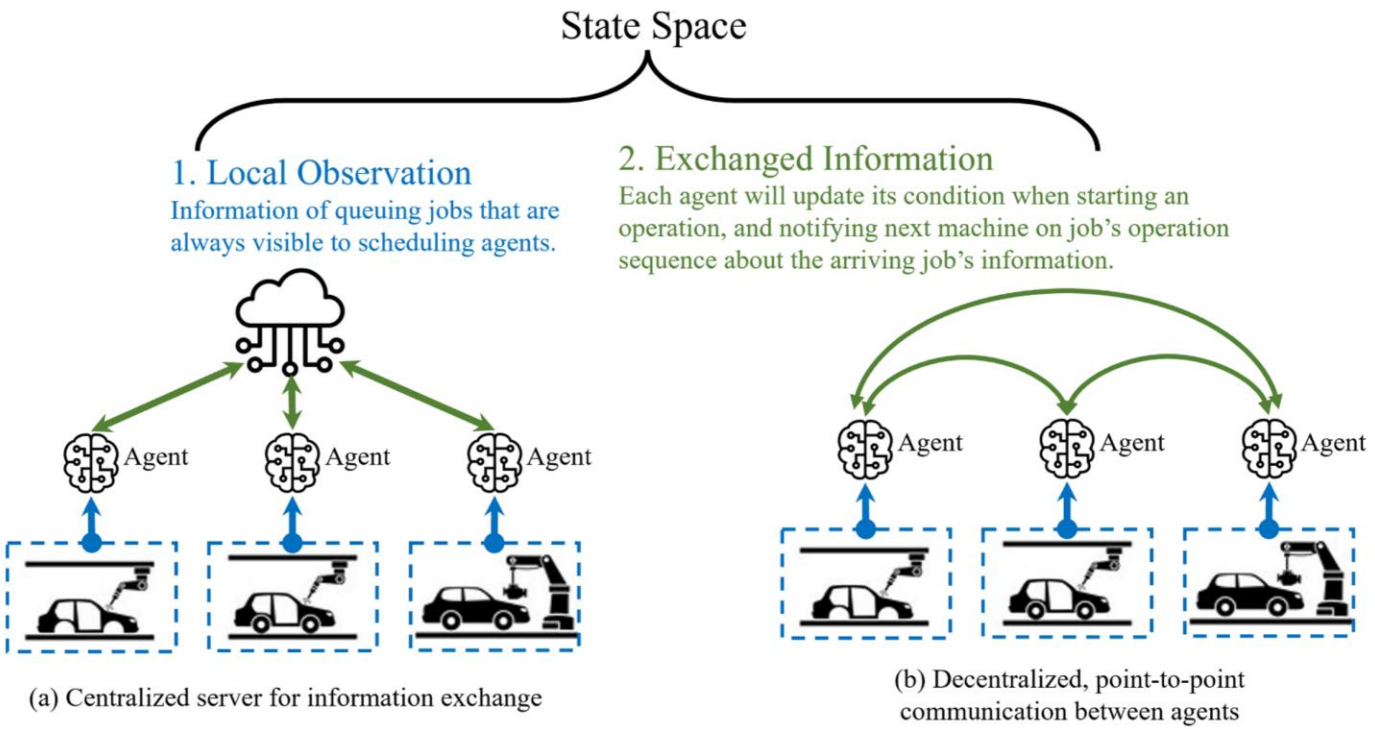

Fig. 3. Hypothetical information flow on the shop floor.

(1) **Shortest processing time (SPT)**: selects the job that can be processed in the shortest time, to minimize the slack time consumption for other queuing jobs.
(2) **Least work remaining (LWKR)**: selects the job that could exit system in the shortest time (estimated), to reduce the overall congestion level.
(3) **Minimal slack (MS)**: selects the most urgent job to protect it from being tardy or incurring too much tardiness.
(4) **Work in queue (WINQ)**: selects the job that exposes its succeeding operation to least congestion, to balance the workload of machines and avoid wasting machine idle time.

Some extra variables are introduced to facilitate the information exchange in system: (1) for job J_i, let the available time of its succeeding machine be denoted as SAM_i; (2) the time J_i have waited in the current queue, be denoted as CQ_i; and (3) the time till next arrival of job to machine M_k, be denoted as NA_k.

Five features are extracted for each candidate job: (1) $t_{i,k}$: the time expense of processing the candidate job, also the prolonged queuing time for other jobs (if selected); (2) WR_i: the minimal time before the completion of a job, showing how likely the congestion in the system can be reduced; (3) S_i: slack time, measurement of the urgency of a job; (4) SAM_i: a surrogate measurement of the queuing time of job's next operation; (5) CQ_i: the time that the agent has detained the job, indicating the accountability of agent in job's tardiness (if any).

Method Design

Algorithm 1 Minimal-repetition approach to build the state space for M_k

Require: J^k

Initialize empty state tensor: $s_t \leftarrow [\ ]$
Initialize the buffer job set: $J^{buffer} \leftarrow J^k$
Initialize the rule set: $Rules \leftarrow [SPT, LWKR, MS, WINQ]$
Initialize the rule count: $x \leftarrow 1, y \leftarrow 1$
while $J^{buffer} \neq empty$ **and** $x \leq 4$ **do**
    Select J_a from J^{buffer} by x^{th} rule in *Rules*
    Append feature vector $\left[t_{a,k}, WR_a, S_a, SAM_a, CQ_a\right]$ to s_t
    x $\leftarrow$ x + 1
    Delete J_a from J^{buffer}
end while
while $x \leq 4$ **do**
    Select J_b from J^k by y^{th} rule in *Rules*
    Append feature vector $\left[t_{b,k}, WR_b, S_b, SAM_b, CQ_b\right]$ to s_t
    x $\leftarrow$ x + 1, y $\leftarrow$ y + 1
end while
if a job that will arrive at M_k is being processed elsewhere **then**
    Identify the job J_c that will arrive
    Append the feature vector $\left[t_{c,k}, WR_c, S_c, AM_k, NA_k\right]$ to s_t
else
    Append the dummy feature vector $[0, 0, 0, AM_k, 0]$ to s_t
end if
return s_t

Method Design

Chronology joint action and knowledge-based reward shaping

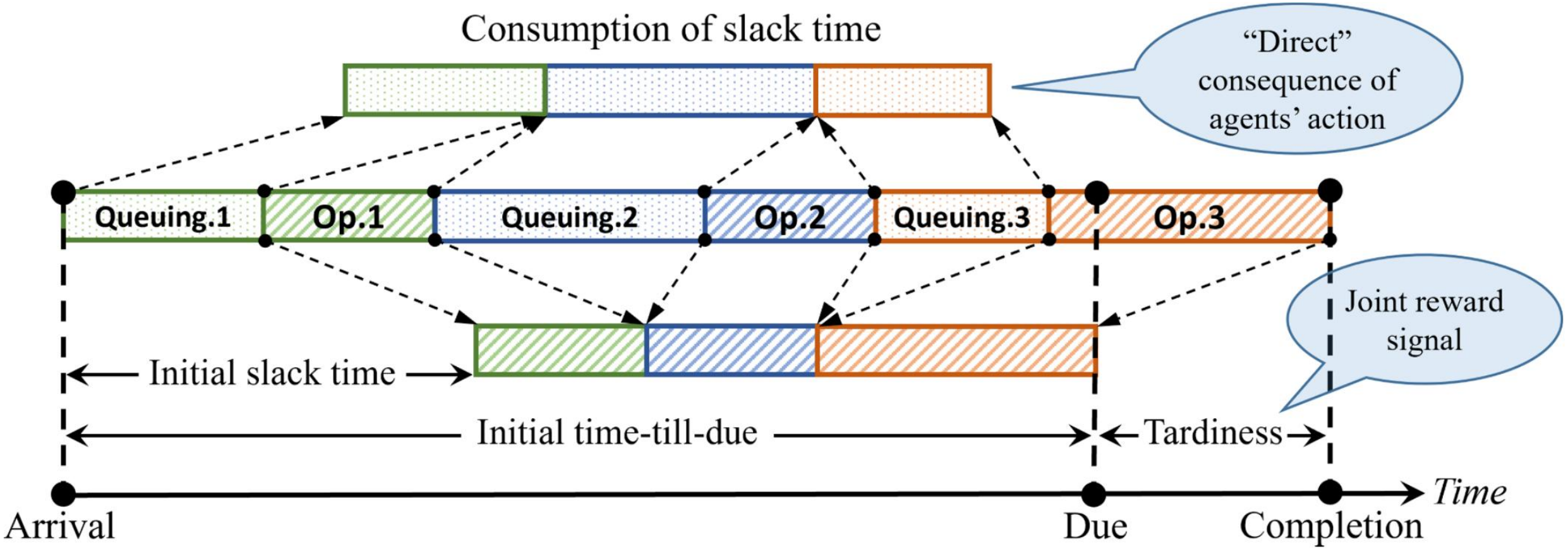

Fig. 4. Example production history.

Method Design

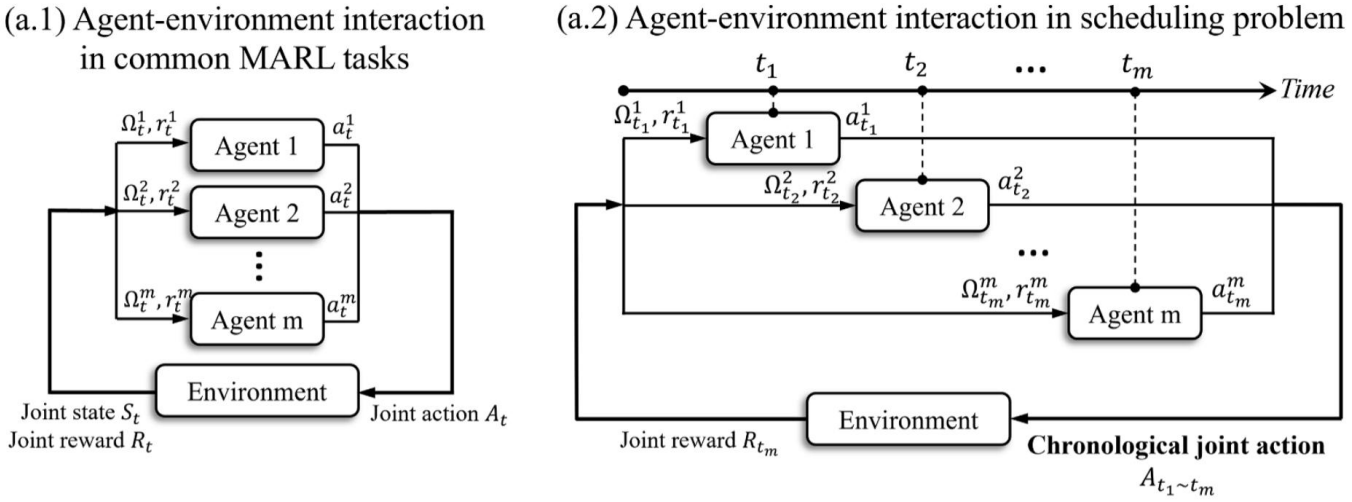

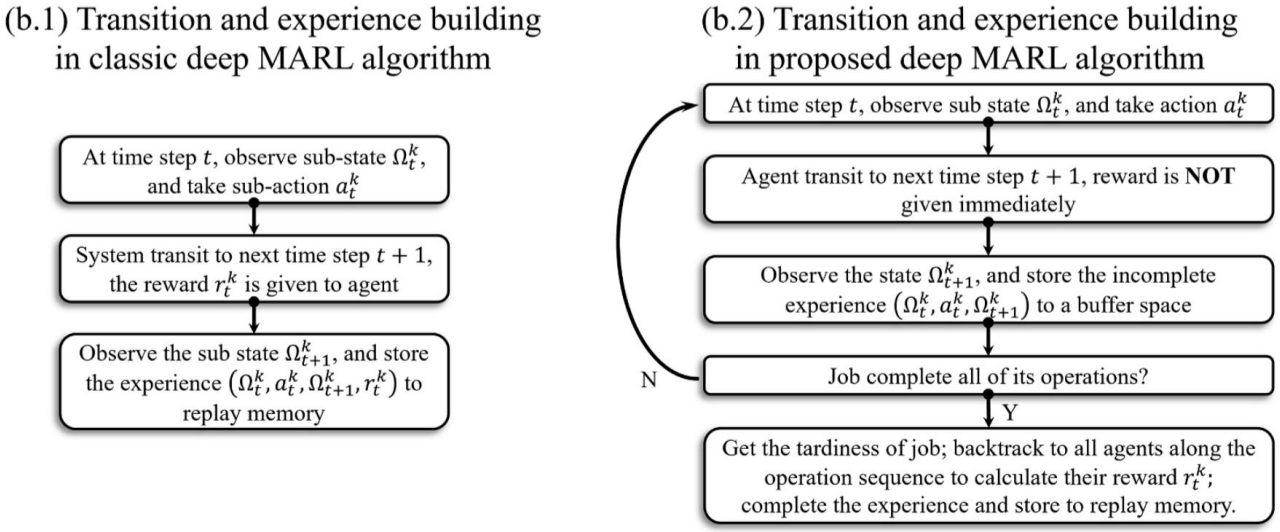

Fig. 5. Comparison between common MARL tasks and scheduling problem.

- Queue time before each operation $Q_i = \left[Q_i^1, \cdots, Q_i^{O_i}\right]$
- Slack time upon the job's arrival at each machine $SA_i = \left[S_i^1, \cdots, S_i^{O_i}\right]$
- The reward vector for each agent in the trajectory $R_i = \left[R_i^1, \cdots, R_i^{O_i}\right]$

Algorithm 2 Calculation of reward upon the completion of job J_i

Require: T_i, Q_i and SA_i
Initialize empty reward vector $R_i \leftarrow [\,]$
if $T_i == 0$ **then**
  Fill reward vector with 0s:$R_i \leftarrow [0, \cdots, 0], |R_i| = O_i$
else
  for $j \leftarrow 1$ *to* O_i **do**
    Re-construct the queue time: $RQ_i^j = (1-\alpha) \times Q_i^j + \alpha \times Q_i^{j+1}$
    Calculate the criticality factor: $\beta = 1 - \left(S_i^j / \left(\left|S_i^j\right| + \delta\right)\right)$
    Get the reward: $R_i^t = -\left(\beta \times RQ_i^j / \varphi\right)^2$
    Clip the R_i^t to $[-1, 0]$
    Append R_i^t to R_i
  end for
end if
return R_i

Contents

Experiment Results

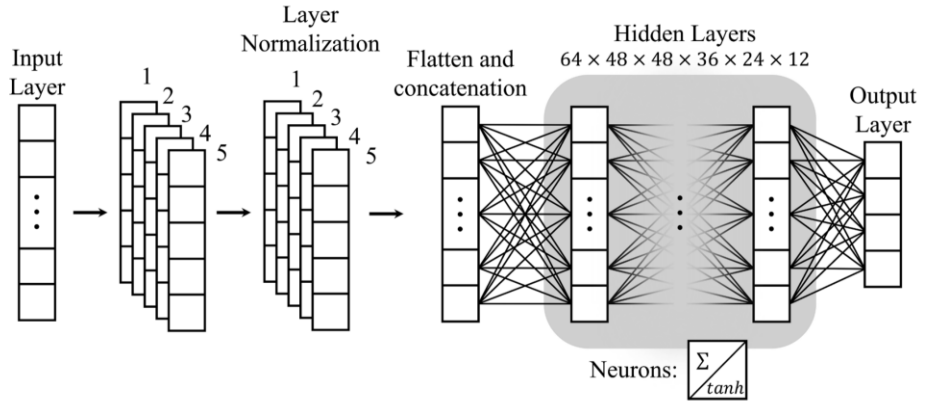

Fig. 6. Architecture of MLP.

Table 1
Parameters of training and hyperparameters of MLP.

Category	Parameter	Value
deep MARL	Discount factor (γ)	0.95
	Exploration rate (ε)	40% decay to 10%
	Minibatch size	64
	Replay memory size	1024
MLP	Activation function	tanh
	Loss function	Huber loss
	Optimizer	SGD, momentum = 0.9
	Learning rate	5×10^{-3} decay to 10^{-3}
	Hidden layers	$64 \times 48 \times 48 \times 36 \times 24 \times 12$

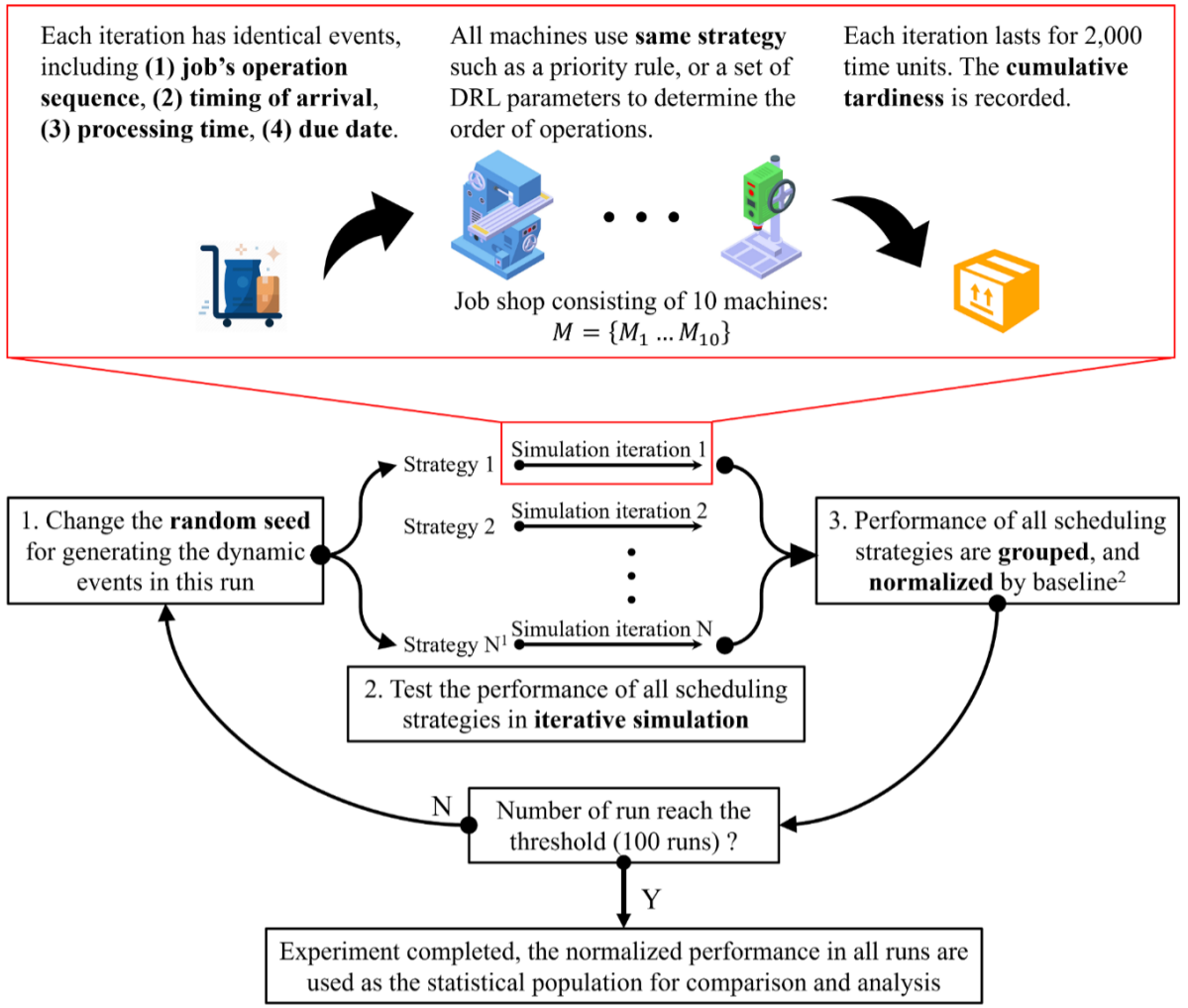

[1] The number of strategies and respective number of iterations in a simulation run subject to the size of benchmark set. In Section 5.1, N = 8; while in Section 5.2, N = 21.
[2] Baseline is the performance of algorithm with minimal enhancements (I-DDQN algorithm in Section 5.1), or the priority rule that manages the job sequence in a most passive way (FIFO rule in Section 5.2).

Fig. 8. Experiment in dynamic environments (in one scenario).

Experiment Results

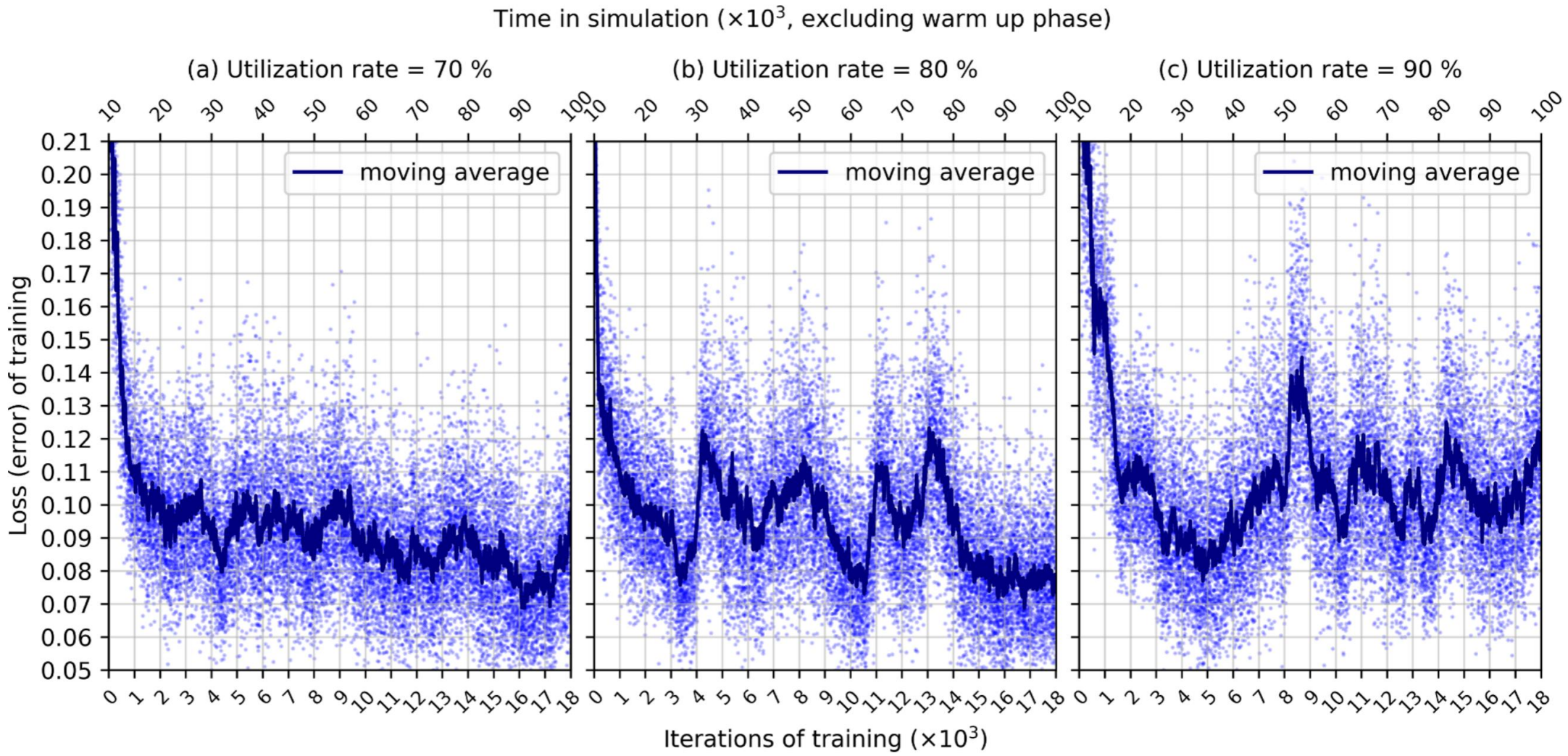

Fig. 7. Training loss.

Experiment Results

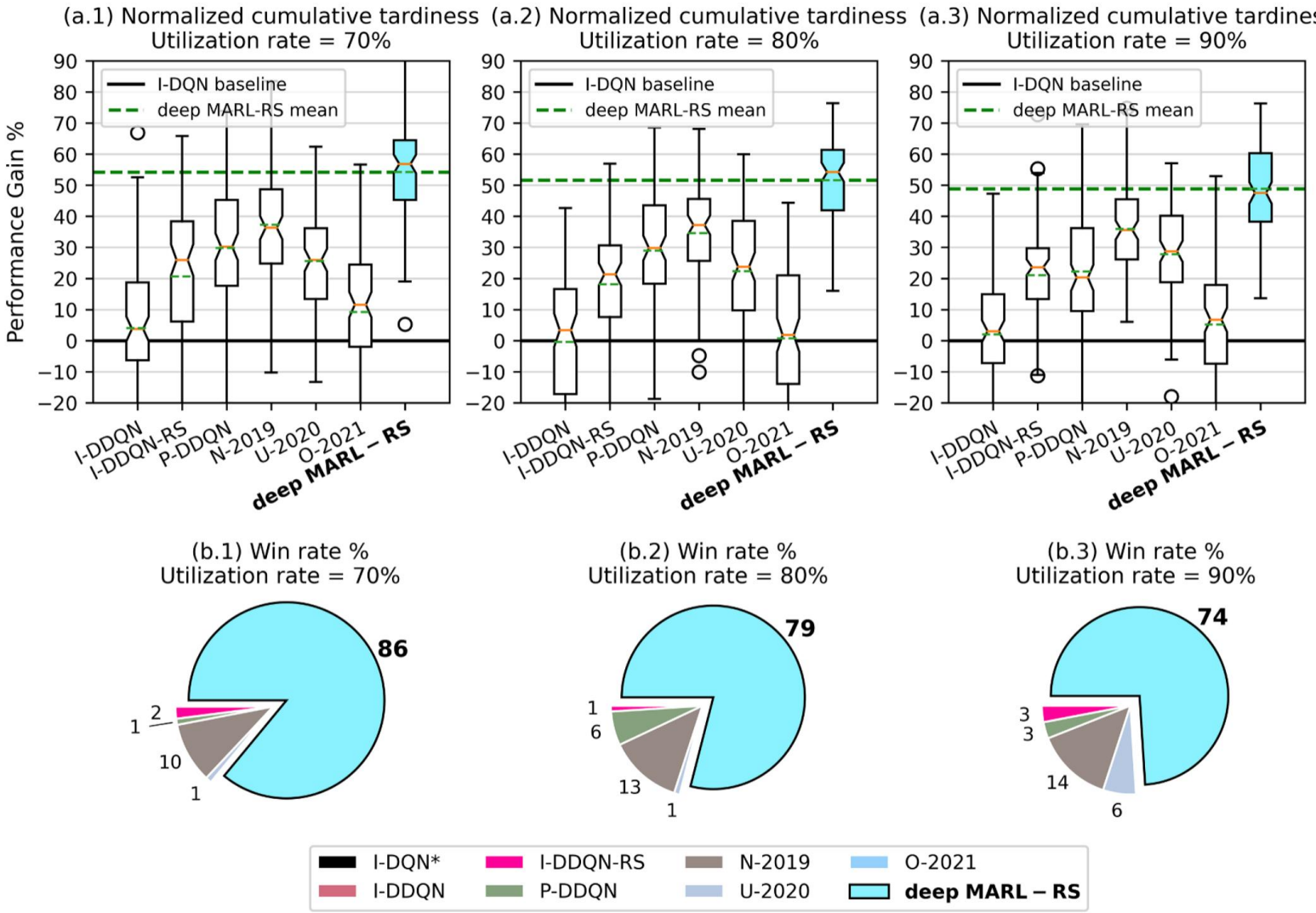

Fig. 9. Result of ablation study and peer comparison in dynamic environment.

Table 4
Quantified contribution of components (by percentage).

Category	Calculation	Contribution (by percentage) under three utilization rate levels		
		70%	80%	90%
Training scheme + Parameter sharing	$\frac{T_{sum}^{I-DDQN} - T_{sum}^{P-DDQN}}{T_{sum}^{I-DDQN}}$	24.44	27.73	19.00
	$\frac{T_{sum}^{I-DDQN-RS} - T_{sum}^{deepMARL-RS}}{T_{sum}^{I-DDQN-RS}}$	40.46	38.96	33.83
Reward-shaping	$\frac{T_{sum}^{I-DDQN} - T_{sum}^{I-DDQN-RS}}{T_{sum}^{I-DDQN}}$	15.00	16.75	17.97
	$\frac{T_{sum}^{P-DDQN} - T_{sum}^{deepMARL-RS}}{T_{sum}^{P-DDQN}}$	32.86	29.81	32.10

Experiment Results

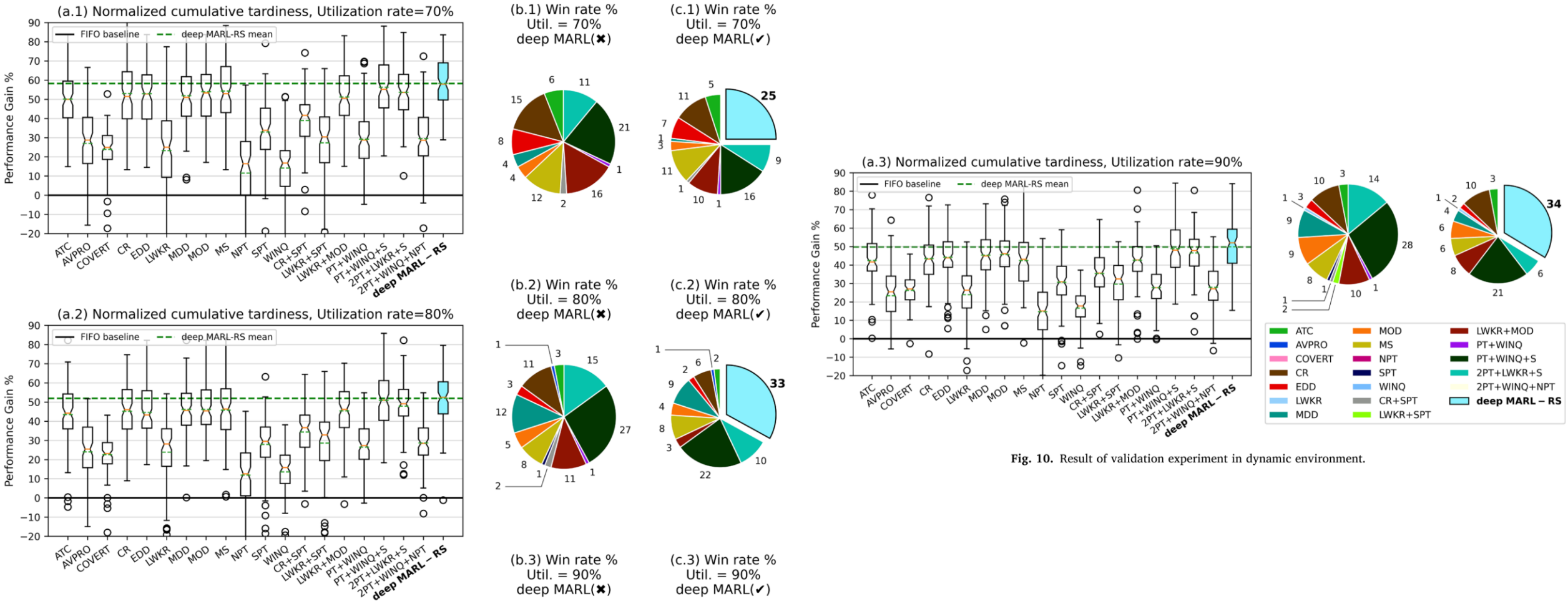

Fig. 10. Result of validation experiment in dynamic environment.

Experiment Results

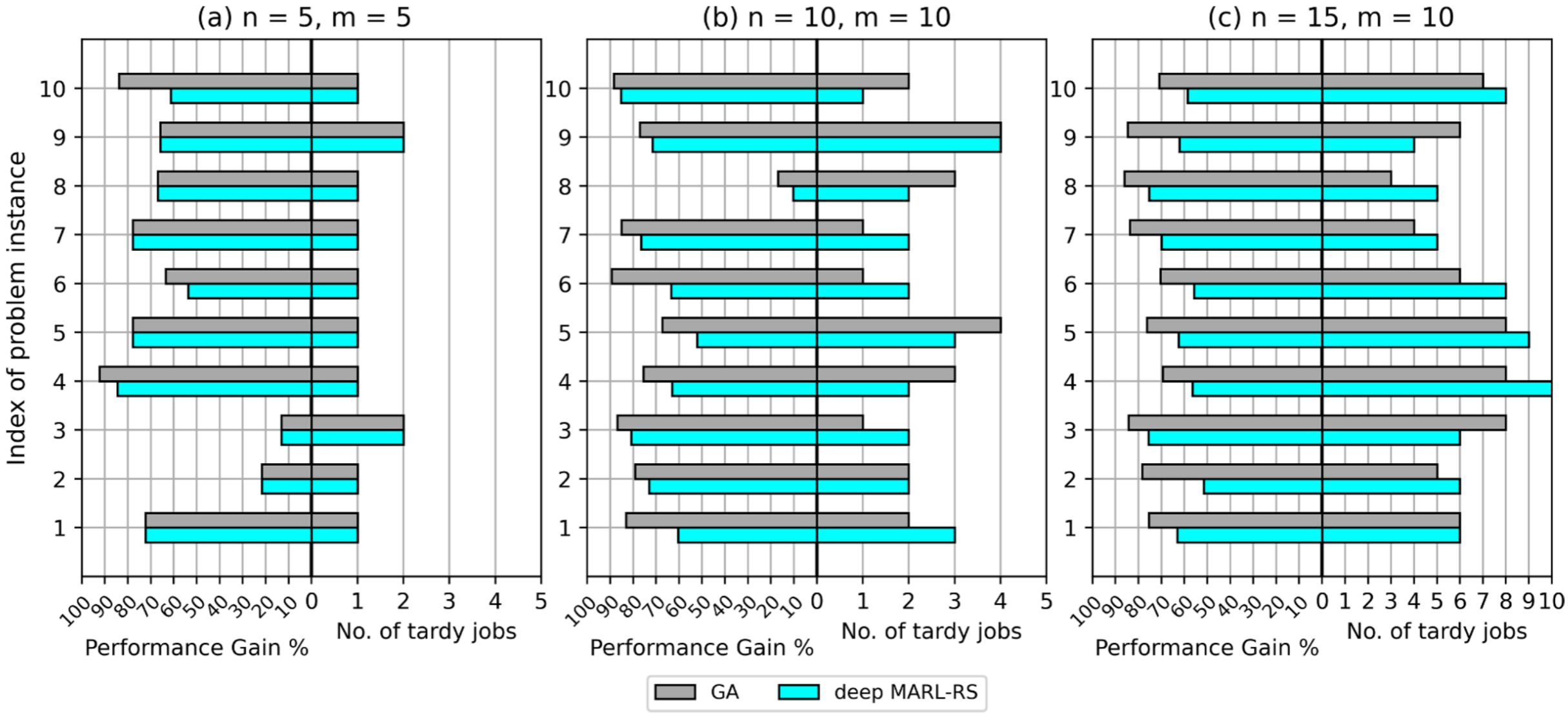

Fig. 11. Performance on static problem instances.

Experiment Results

Table 7
Average CPU time for scheduling decision.

Problem Size ($n \times m$)	Category	Priority rule (FIFO)	Deep MARL-RS	Genetic Algorithm
5×5	Single decision	$9.46 \times 10^{-7}s$	$2.11 \times 10^{-4}s$	3.26*s*
	All decisions	$2.37 \times 10^{-5}s$	$5.28 \times 10^{-3}s$	
10×10	Single decision	$9.87 \times 10^{-7}s$	$2.12 \times 10^{-4}s$	31.43*s*
	All decisions	$9.87 \times 10^{-5}s$	$2.12 \times 10^{-2}s$	
15×10	Single decision	$9.96 \times 10^{-7}s$	$2.14 \times 10^{-4}s$	62.80*s*
	All decisions	$1.49 \times 10^{-4}s$	$3.21 \times 10^{-2}s$	

Contents

Future Work

Contributions

1. Proposed a deep MARL approach for dynamic job scheduling, enabling low-latency and high-quality decision-making.
2. Introduced novel state and action representations to overcome fixed-size constraints in traditional scheduling.
3. Developed knowledge-based reward shaping to enhance agent learning.
4. Validated the approach through ablation studies, outperforming existing methods and priority rules.

Future Work

1. Establish benchmark problems for dynamic scheduling.
2. Improve model performance with deeper networks.
3. Develop automated industrial data processing.
4. Optimize RL training problem design.

北京工業大學
BEIJING UNIVERSITY OF TECHNOLOGY

Thank you for listening